Augmented Reality Approach for Marker-based Human Posture Measurement on Smartphones

Shahin Basiratzadeh

Thesis submitted to the Faculty of Engineering
in partial fulfillment of requirements for the degree of

Master of Applied Science

in

Biomedical Engineering

uOttawa

Ottawa Carleton Institute for Biomedical Engineering
University of Ottawa
Ottawa, Ontario

September 2019

Abstract

Quantifying human posture and range of motion remains challenging due to the need for specific technologies, time for data collection and analysis, and space requirements. The demand for affordable and accessible human body position measurement requires alternative methods that cost less, are portable, and provide similar accuracy to expensive multi-camera systems.

This thesis developed and evaluated a novel augmented reality mobile app for human posture measurement to bring marker-based body segment measurement to the point of patient contact. The augmented reality app provides live video of the person being measured, AprilTag2 fiducial markers locations in the video, processes marker data, and calculates angles and distances between markers.

Results demonstrated that the mobile app can identify, track, and measure angles and distances between AprilTag2 markers attached to a human body in real-time with millimetre accuracy, thereby allowing researchers and clinicians to quantify posture measurements anywhere, at anytime.

Table of Contents

Abstract ..... **ii**

Table of Contents ..... **iii**

List of Figures ..... **vi**

List of Tables ..... **viii**

Abbreviations and Definitions ..... **ix**

Acknowledgments ..... **x**

1 Introduction **1**

1.1 Introduction 1
1.2 Rationale 1
1.3 Thesis objectives 2
1.4 Thesis contributions 2
1.5 Thesis outline 3

2 Literature Review **4**

2.1 Overview 4
2.2 Human posture measurement 4
2.3 Inertial measurement unit 4
2.4 Markerless systems 5
2.5 Marker-based optical systems 9
2.5.1 Passive marker systems 9
2.5.2 Active marker systems 9
2.5.3 Magnetic systems 10
2.6 Fiducial markers system 10
2.6.1 AprilTag 11
2.6.2 ArUco 13
2.6.3 ARToolKit 13
2.6.4 ArUco, ARToolKit, and AprilTag2 advantages 14
2.6.5 ArUco, ARToolKit, and AprilTag2 disadvantages 16
2.7 Summary 17

3 Fiducial Marker Approach for Biomechanical Smartphone-Based Measurements... 18

3.1 Overview ... 18
3.2 Abstract ... 18
3.3 Introduction ... 18
3.4 Selection criteria and background ... 21
3.4.1 Design criteria ... 21
3.4.2 Selected fiducial systems ... 21
3.5 Test and results ... 22
3.5.1 Methodology ... 22
3.5.2 Results ... 23
3.6 Conclusion ... 23
3.7 Future work ... 25

4 Augmented Reality Approach for Marker-based Measurement on Smartphones 26

4.1 Overview ... 26
4.2 Abstract ... 26
4.3 Introduction ... 27
4.4 Methodology ... 29
4.4.1 Design criteria ... 29
4.4.2 Design ... 29
4.5 Evaluation ... 31
4.6 Results ... 32
4.7 Discussion ... 35
4.8 Conclusion ... 36

5 Evaluation of a Biomechanical Augmented Reality Mobile-based Application 37

5.1 Overview ... 37
5.2 Abstract ... 37
5.3 Introduction ... 38
5.4 Methodology ... 39
5.4.1 Body opponent bag ... 40
5.4.2 Human Testing ... 42
5.5 Results ... 43
5.5.1 Arm-abduction insight ... 44
5.6 Discussion ... 47

5.6.1 Pelvis and shoulder measurement 47
5.6.2 Arm-abduction measurement 48
5.7 Conclusion 50
6 Thesis Conclusions and Future Work 51
6.1 Conclusions 51
6.2 Future work 51
References 53
Appendix A 61

List of Figures

Figure 2-1 Padded elastic straps secured on the thigh and shank (adapted from [17]). **5**

Figure 2-2 Posture Print output with sagittal (A) and coronal (B) views. Anatomical landmarks are seen as white dots. Gray vertical line represents gravity-based plumb line. Arrows denote directions of postural deviations (adapted from [1]). **6**

Figure 2-3 Reach posture measurement (adapted from [22]) **7**

Figure 2-4 Image acquisition system (adapted from [28]). **8**

Figure 2-5 AprilTag applications. Clockwise from top left: robot-to-robot localization and identification on MAGIC robots, object localization for Boston Dynamics Atlas robot, virtual reality headset testing at Valve, and tracking individual ants to study their social organization (adapted from [51]). **12**

Figure 2-6 AprilTag fiducial system (adapted from [49]) **15**

Figure 3-1 Examples of fiducial marker systems. **20**

Figure 3-2 AprilTag2 marker detection using BAR-M with Samsung Galaxy S5. ..... **24**

Figure 4-1 Tracking module flowchart. **30**

Figure 4-2 BAR-M augmented reality screen output. **31**

Figure 4-3 Setup environment, a) phone parallel to markers, b) yaw rotation, c) tilt rotation **32**

Figure 4-4 Back and front camera angles from two markers. **33**

Figure 4-5 Back and front camera distances between two markers **34**

Figure 4-6 Yaw and tilt angle results **34**

Figure 4-7 Yaw and tilt distance results **35**

Figure 5-1 AprilTags adapters, a) flat mount, b) post-adapter, c) velcro-adapter **41**

Figure 5-2 BOB measurements, a) pelvis, b) shoulder, c) arm abduction **41**

Figure 5-3 Participant measurement: a) hip, b) shoulder, c) arm abduction **43**

Figure 5-4 Absolute mean differences between Vicon angle and app saved data and standard deviations, for all participants for the arm abduction trials: a) torso to horizontal line, b) arm to horizontal line, c) arm to torso. **45**

Figure 5-5 Vicon angle and app saved data for participant 4: a) torso to horizontal line, b) arm to horizontal line, c) arm to torso**. 46**

Figure 5-6 Arm-abduction error and solution, a) locating tags using a stick b) measurement methodology error visualization**. 49**

List of Tables

Table 3-1 AprilTag2 results **24**

Table 4-1 Angle and distance results **33**

Table 5-1 Participant test app AR angle and stored data results **44**

Abbreviations and Definitions

2-D	Two Dimension
3-D	Three Dimension
IMU	Inertial Measurement Units
AR	Augmented Reality
ROM	Range of Motion
IR	Infrared
LED	Light-Emitting Diode
SPGA	Posture Evaluation Rotating Platform System
ODAU	Optotrak Data Acquisition Unit
EMG	Electromyography
MAL	Movement Analysis Laboratory
DOF	Degree of Freedom
QR	Quick Response
FoV	Field-of-View
GPS	Global Positioning Systems
BOB	Body Opponent Bag
BAR-M	Biomechanics Augmented Reality Tag
JNI	Java Native Interface
OpenGL	Open Graphics Library
SD	Standard Deviation
HCI	Human Computer Interface

Acknowledgments

My joy knows no bounds in expressing my greatest appreciation to my supervisors; Prof. Natalie Baddour and Prof. Edward Lemaire. I have been extremely lucky to have supervisors who trusted in my abilities and cared so much about my work. During the last two years, I benefited from their guidance, great support, fruitful discussions and kind pieces of advice that encouraged me to do my best. It was a real privilege and an honor for me to be supervised with their exceptional scientific knowledge and extraordinary human qualities. They have always been responsive to my questions with patience and enthusiastically guided me towards the best solutions. They have taught me how to think and perform as an academic researcher. I am deeply thankful for the thorough revisions and feedback provided to me on the research papers and thesis, which enabled me to take my work to completion in the most professional manner.

I am truly grateful to my mom for her immeasurable love, care and patience. She has always encouraged me to believe in my potential and pursue my dreams. Her presence and support through thick and thin has motivated me to perform my best.

My gratitude extends to three gentlemen who have significantly contributed in more than one way to bring this project to reality. Mr. Masoud Dorrikhteh for programming support, Dr. Hossein Gholizadeh for helping me collecting relevant data, and Mr. Theja Ram Pingali for support in 3D-printing. I would also like to thank all of my friends and lab colleagues for their valuable cooperation, when needed.

Last but not the least, I feel privileged to be part of CREATE-BEST program and receive funding from NSERC. The journey has been immensely rewarding and I truly cherish the time spent at uOttawa and The Ottawa Hospital.

1 Introduction

1.1 Introduction

Posture measurement aids have been used to detect poor posture among school-aged children, adolescents, college students, and adults [1]. Accurate and reliable posture measurements can also be used for treatment planning. Quantitative posture measurements, alongside a clinical assessment, may provide the insight needed to properly evaluate sensory issues related to exteroception, proprioception, stereognosis, two-point discrimination, and motor impairments that affect muscle strength, range of motion, and spasticity. This is particularly important among individuals with disabilities [2], [3]. Currently, human posture quantification can involve various motion analysis systems (i.e., inertial, optical). These multi-camera labs are necessary to determine anatomical points, body segments, and biomechanical models. However, these systems can have high purchase and installation costs, and require a permanent, large footprint.

In an effort to reduce costs and eliminate permanent large equipment footprints, researchers have implemented posture measurement using IMU sensors or coloured markers [4], [5]. However, computing positions from IMU sensors requires double integration, which is affected by system noise and sensor drift [5], [6]. Tracking coloured marker in the video field has problems associated with background "confusion" and difficulties with multi-marker tracking, which can adversely affect accuracy. A fiducial marker system is a 2D landmark (i.e., QR barcode) that could be a viable approach to uniquely identifiable features. These markers can be easily recognizable without being affected by background noise or confusion between multiple markers [7]. Therefore, this research develops and evaluates a novel marker-based mobile application for real-time human posture and range of motion (ROM) measurements using fiducial markers. The goal is for this application to be used anywhere and at anytime with high accuracy.

1.2 Rationale

Posture measurements are routinely required by clinicians, but current methods of measuring angles such as pelvic obliquity require specialized equipment or take an unacceptable amount of clinic time. A conventional approach is to make these measurements manually, with a goniometer, tape, etc. However, visual observation can be affected by human error [8]. This may lead to a risk for patients, since improper pelvis alignment can cause long-term damage. Additionally, advanced

technologies such as x-ray and marker-based motion analysis systems (Vicon, etc.) are time consuming, costly, and may be hard to access. Considering the drawbacks of these methods, we propose an innovative solution using smartphone Augmented Reality (AR) technology in a real-time application. We will demonstrate that the developed system fills the gap between cost, accessibility, and system accuracy. An AR system allows both patients and medical experts to save costs and time, and also provides a standardized quantitative measurement in real-time, an important feature that does not exist in clinical practice.

Based on our preliminary research, the AprilTag [7] (visual fiducial system) was selected as the best marker option for this application, thereby removing colour or reflective marker errors when working in a clinical environment (i.e., markers conflicting with background, lighting changes, etc.). Fiducial markers are objects located in the smartphone camera's field of view, to be used as reference points for measurement. AprilTag is "2D barcode style" marker (similar to QR codes) that can be printed on paper. The AprilTag software library computes precise 2D position, tag orientation, and also identifies the tag relative to the smartphone camera.

1.3 Thesis objectives

The objective of this thesis is to develop and evaluate an Augmented Reality (AR) mobile application that measures range of motion and human posture between anatomical landmarks and between body segments in real-time, with an accuracy comparable to other systems currently used in practice.

1.4 Thesis contributions

This thesis developed and evaluated a novel Android mobile phone application (BAR-M, Biomechanics Augmented Reality - Marker) for real time human posture measurement using fiducial markers (AprilTag2) [7], [9]. Specific contribution include:

- BAR-M is the first smartphone-based tool to successfully identify, track, and store 2D positions and orientations of AprilTag2 markers.
- Marker-based outcome measures were displayed in realtime, over video, to provide an AR tool that enables clinicians to actively measure posture and other relevant angles and distances immediately during a patient encounter.

- Accuracy was comparable to industry standard motion capture systems (error less than 1° for angle, 4 mm for distance). Anthropometric dummy test errors were less than 0.15° (pelvis), 0.14° (shoulder), 0.7° (arm abduction). Human test errors were less than 2° (pelvis), 1.5° (shoulder), 11.5° (arm abduction).
- AR (real-time) interface provided equivalent results to stored post-processed results
- Easy and accurate to apply
- Novel marker mounting hardware was developed and was effective for easily positioning markers on the body

1.5 Thesis outline

This thesis is divided into six chapters and one appendix:

Chapter 2 is a literature review and discusses the importance of human posture measurement. This chapter summarizes relevant technologies currently being used for human body postural measurement and reviews different types of fiducial marker systems.

Chapter 3 contains a modified IEEE manuscript published in the 3rd International Conference on Bio-engineering for Smart Technologies (BioSMART), Paris, France, April 2019 that compares and evaluates different types of fiducial marker systems and validates the selection of AprilTag2 as a viable fiducial marker system for further android mobile application development.

Chapter 4 discusses the development and evaluation of the Biomechanics Augmented Reality Tag (BAR-M) mobile application that measures angles and distances between two markers using a Samsung Galaxy S6 phone.

Chapter 5 evaluates and reports BAR-M app performance on a Body Opponent Bag (BOB) and a group of 15 healthy participants. The results are compared to those obtained with a Vicon system as a gold standard comparator.

Chapter 6 summarizes thesis findings, and suggestions for future work.

Appendix A presents details of the data collected from each participant and the comparison between Vicon and mobile app outcomes.

2 Literature Review

2.1 Overview

This chapter discusses the importance of human posture measurement and reviews related technologies for posture measurements to determine the requirements for a mobile-based posture-measurement app. Moreover, the chapter introduces several fiducial marker systems to gain insights for choosing the most compatible solution for Android mobile app development.

2.2 Human posture measurement

Human posture is "the alignment of body segments at a particular time [10]." Posture measurement is widespread within biomechanics, ergonomics, and orthopedics [11]–[15]. As a key indicator of health, posture-related abnormalities are correlated with disorders and medical conditions inclusive of pain-related syndromes, musculoskeletal disorders, respiratory functions, and amputations [1], [10], [16]. Posture assessment enables clinicians to identify potential problems and develop a care plan. These assessments may focus on postural realignment, range of motion, and corrective practices to promote good posture and correct posture abnormalities. Large variations from ideal posture can initiate stress on spinal tissues that triggers back fatigue, headaches, intervertebral discs degradation, neck pain, spinal ligaments, and spinal structural deformities [1]. Posture measurement and range of motion methods include inertial measurement unit (IMU) sensors, marker-based systems, and markerless systems.

2.3 Inertial measurement unit

An IMU typically includes a gyroscope, accerometer, and sometimes magnetometer. Data from these sensors (rotational velocities, accelerations, heading by tracking magnetic-north) can be combined to determine the device's orientation [4], [5]. IMU has shown good accuracy in monitoring normal activities, such as gait or sports performance, and outcomes of a rehabilitative process in patients. For instance, in knee joint angle measurement the IMU can be attached in a sensor alignment tool (Figure 2-1) that is manually aligned to the person's anatomy. This orientation is recorded as the reference orientation. The person then removes the IMU from the alignment tool and places them in the sensor cases secured to their thigh and shank. The difference between the orientation on the thigh and shank relative to the reference orientation are calculated

and utilized to transform the data into an anatomical coordinate system. Moreover, IMU sensors are available in the majority of smart phone devices for multiple purposes, including orientation and movement acceleration detection.

Figure 2-1 Padded elastic straps secured on the thigh and shank (adapted from [17]).

Although having vast uses in biomechanics, IMU can produce errors for position determination since double integration is required, thereby enhancing drift and noise in the system [5]. Furthermore, maintaining a durable interconnection between sensors and joints remains challenging, especially for dynamic measurement trials.

2.4 Markerless systems

Motion analysis systems that do not require markers could be used in movement analysis to reduce participants preparation time and encourage natural movement. Posture can be qualitatively and quantitatively assessed by interpreting photographs. For example, Posture Print software [10] can be used to measure postural deviations using images, generate a report on anatomical points displacement, and prescribe corrective exercises (Figure 2-2). Posture Print had a chest measurement error of 1.2 degrees for rotation and 1.6 mm for translation, and head measurement error of 1.38 degrees for rotation and 1.1 mm for translation [10]. Since these errors are within a clinically acceptable range, this postural assessment software tool was a viable instrument for measuring body angles [10].

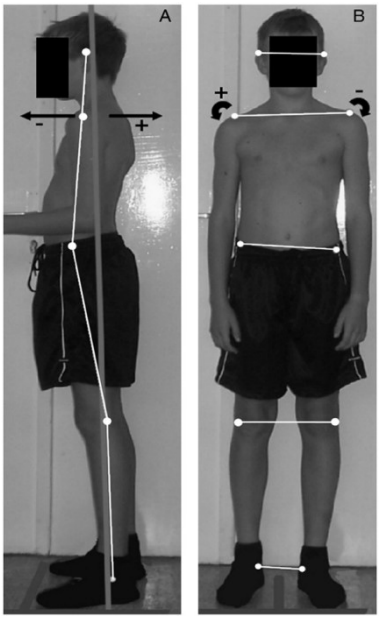

Figure 2-2 Posture Print output with sagittal (A) and coronal (B) views. Anatomical landmarks are seen as white dots. Gray vertical line represents gravity-based plumb line. Arrows denote directions of postural deviations (adapted from [1]).

Establishing relationships between body parts via measurements in software is both easy and quick [18]; however, key methodological steps are needed to minimize image errors and extract optimal results [18], [19]. This includes selection of the environment, camera position, image resolution, and anatomical landmarks to be identified in the picture [18]–[20]. Parallax may occur when the image is not in the anatomical plane being analyzed, thereby producing measurement errors [18].

Multiple 2D images of an object (typically 3-6 images) can be used to convert 2D marker locations into 3D data [18], [21]. Another approach uses artificial neural networks to define limb 3D orientation [22]. A neural network learned arm reach posture from 3D motion trajectories of the shoulder, elbow, and wrist (Expert Vision Motion Analysis System generated 3D coordinates from two images (Figure 2-3). No significant differences were found between neural network and Expert Vision Motion Analysis System joint coordinates when reaching [22]. The neural network approach demonstrated potential in simulating and measuring human reach; however, training an accurate model requires large data sets and markers can be confused with backgrounds or other people in the video field. Moreover, specific landmarks not included in the neural network model cannot be identified. Therefore, a marker based approach is more beneficial.

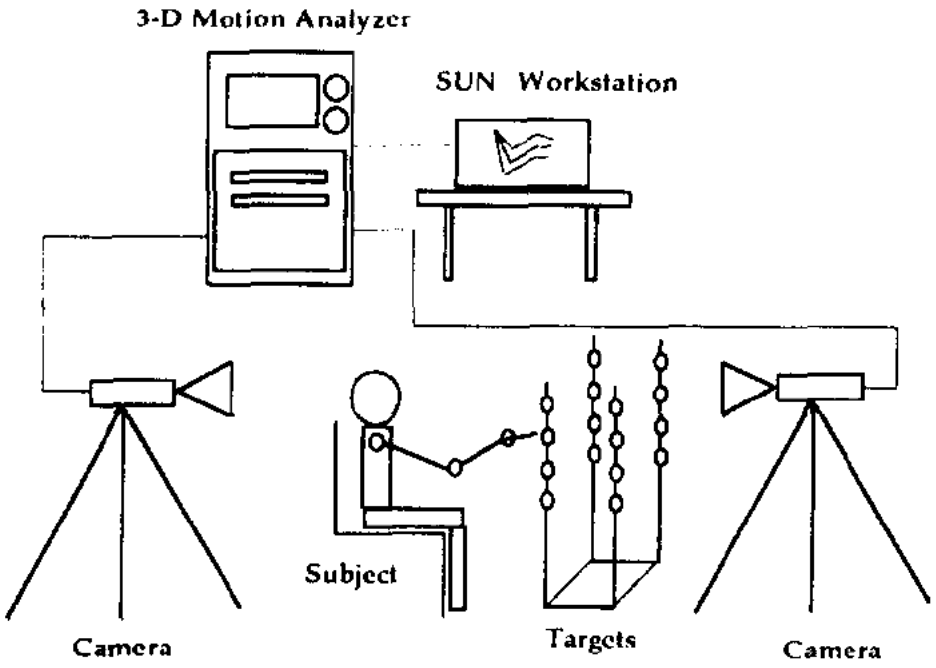

Figure 2-3 Reach posture measurement (adapted from [22]).

Another markerless system, laser acquisition, is used by 3D scanners to measure surface geometry. A laser is fixed in the equipment, projects a laser light pattern on the surface, and a video camera moves step by step to scan the individual's body [18]. Although laser acquisition is precise and can detect small differences, it requires skilled operation that might not be practical in a clinical environment. Laser scanning precision has contributed to its adoption for scanning static objects, but systems such can be expensive, bulky [18], and individuals must be completely still during measurement. This precludes this laser technology for clinical posture and range of motion measurement.

Depth-cameras can be used to measure the distance from the camera to a given person or object, using a pattern of lights (IR or white light) [18], [19]. Systems such as Microsoft Kinect were developed by the gaming industry to track player movements while they interact with a game [23]. This gaming device can be used to assess gait kinematics, as well as spatiotemporal gait variables [23]–[25]; however, Kinect fails to accurately record body kinematic data [23]. Kinect

could measure some spatiotemporal parameters associated with gait [23], [24], [26], [27], but measurement accuracy can be affected by sensor position and tracking methodology.

SPGAP (Posture evaluation rotating platform system) is an instrument for quantitative analysis of body posture with applicability for clinical use. As a noninvasive body posture evaluation system, SPGAP is easy to handle and transport for posture evaluation within clinical practices [28]. SPGAP eliminates parallax errors associated with photographic methods [28] by using a rotating platform, known as PGA, to rotate the individual during the filming procedure. Therefore, a sequence of images of the individual was developed and calibrated using a digital video camera, image processor, computer, and analysis software [28]. The PGA is responsible for rotating the individual under evaluation during the filming procedure. Because of this movement, a sequence of images of the individual were saved in a file and can be selected, thus enabling statistical analysis post process (averaging values, probabilistic density, standard deviation). In this way the adverse effect of the parallax obtained from the analysis of a single image will be reduced (Figure 2-4).

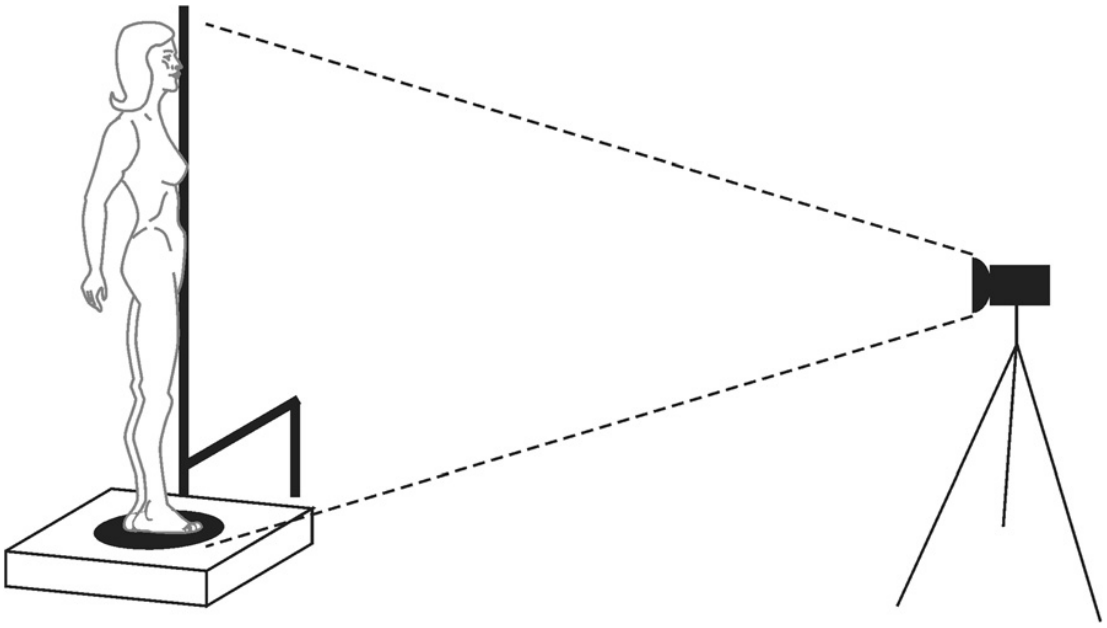

Figure 2-4 Image acquisition system (adapted from [28]).

Findings from this study revealed that SPGAP-generated values were relatively close to real measurements. During the retest, SPGAP had an error of approximately 1% for height-related dimensions alongside an error of about 0.3% for dimensions of width [28]. Such findings prove that this marker-less system is both reliable and valid as a method to measure body posture within clinical practice settings [28].

2.5 Marker-based optical systems

2.5.1 Passive marker systems

Passive marker-based systems typically use retro-reflective balls that are illuminated using infrare (IR) lights mounted on the cameras.Systems include Motion Analysis Corporation (Santa Rosa, CA), Qualisys (Göteborg, Sweden), Vicon (Oxford, England),. Song & Godøy [29] claimed that passive marker-based motion tracking systems that attach independent retro-reflective markers to clothing or skin are convenient but passive markers exacerbate challenges in post-processing 3D data for markers close to each other [29]. This may require manual editing to relabel markers [30], [31]. Reflective surfaces in the background may also be mistaken for markers, requiring manual background masking or relabelling [32]. Distances between markers have been used to evaluate both precision (0.015 mm) and accuracy (0.15mm) of motion caption systems [31], [33]. The closer the camera is to the dynamic object, the better the motion capture performance due to greater resolution [32], [34].

While passive marker systems are accurate, using them in clinical practice is limited due to motion lab space requirementes, system cost, and time requirements for patient setup and data processing [35], [36].

2.5.2 Active marker systems

Active systems use light-emitting diodes (LED) as markers, with each marker having a predefined frequency to assist in marker differentiation [4]. However, individuals need to carry several cables and other components that may affect their movements. Active markers systems include Codamotion (Rothley, England), Optotrak (Northern Digital, Inc., Waterloo, Ontario, Canada), Qualysis (Göteborg, Sweden), Selcon (Selspot Systems, Ltd., Southfield, Michigan), [37]. Active markers can eliminate errors due to marker misidentification and therefore marker sorting time during postprocessing [38].

Neelesh, Nissa, Amod, and Sohi's [39] evaluated an active marker system using LED-based markers to compute spatiotemporal and kinematic parameters through LabVIEW. A study of 19 healthy participants and 39 patients with lower back pain revealed that patients with lower back pain demonstrated a rigid (less flexible) pelvis-thorax coordination compared to healthy participants [40]. Lamoth [41] noted that active markers enhance distractibility and reduce gait alteration since the cable system responsible for powering and controlling the LED lags behind the participant as they walk. New Optotrak markers have in-line batteries that eliminate the need for a tether following the person, but wires are still needed for limb markers on the body.

The Selspot system taped active markers to the participant's limbs [42]. Drawbacks of the Selspot system included errores due to reflections, the need to carry apparatus and cables, and a trade-off between the number of markers and sampling rate [42]. Since distance influences image resolution, as LEDs are moved away from Selspot cameras the amount of light intercepted per light pulse decreases [43], and increasing the aperture to capture more IR light can distort image.

In next decade, future developments of active marker systems will employ radio-frequency active emitters as gait analysis hardware [42]. Radio-frequency signals are applied in the military. Due to their lightweight nature and low cost, implementation of a similar approach in clinical practice settings requires further research and development [42]. However, research and development of hardware and software entail costs that are significantly below the costs attributed to passive marker systems [42].

2.5.3 Magnetic systems

Low frequency quasi-static magnetic field techniques can be used to determine position and orientation of a sensor relative to a source [44]. While these 3D measurement systems are portable, they are more cumbersome to employ due to the system's power, size, and weight [44] and are susceptible to metal within the capture volume.

2.6 Fiducial markers system

Fiducial marker systems are characterized by "patterns that are mounted in the environment and automatically detected in digital camera images using an accompanying detection algorithm [45]." Fiducial markers are most applicable in augmented reality applications, robotics, and other applications where accurate, real-time camera-object pose is required and tracked [45]–[49]. Since

virtual information in augmented reality is shared with the real world, this illusion requires good registration of both the virtual and real worlds [47], [48]. To the best of the author's knowledge, no research literature has yet to examine fiducial markers in posture measurement.

Fiducial marker systems performance is typically measured by the false negative rate, false positive rate, and inter-marker confusion rate. False negative rate is when a fiducial marker is present within the image yet never reported [45]. Falsely reporting the existence of a given marker despite its absence is a false positive, while inter-marker confusion occurs when a fiducial marker is detected yet incorrect identification is provided [45]. Research literature also includes the importance of minimal marker size in reliable detection, detection jitter, and immunity to lighting [45], [46]. Errors increase as the markers move farther from the camera [46], [47]. Minimal marker size is measured using $TD_{Min} = MS \text{ x } 2$ metres [46], where TD_{Min} represents the minimum tracking distance and *MS* represents the marker size in meters. In addition to jitter, challenges have been found with this marker-based approach related to blurredness, movement of markers or camera along x or y-axis, occlusion, robustness, and tracking stability [46].

2.6.1 AprilTag

Based on earlier fiducial markers such as ARToolkit and ARTag, Edwin Olson developed the AprilTag system (Figure 2-5), a black and white square tag encoded with a binary payload [7]. The detection process includes seeking linear segments, detecting tags, computing tag position and orientation, and decoding the barcode [50].

The marker detection system calculates a marker's identity, orientation, and position to the camera [7], [9], [47]. According to Walters and Magna [49], AprilTag was developed to

- Maximize the number of distinguishable codes
- Maximize correctable bit errors
- Minimize false positive confusion rate
- Minimize the number of bits per tag (minimizing tag size) [7]

Figure 2-5 AprilTag applications. Clockwise from top left: robot-to-robot localization and identification on MAGIC robots, object localization for Boston Dynamics Atlas robot, virtual reality headset testing at Valve, and tracking individual ants to study their social organization (adapted from [51]).

AprilTag works robustly in environments with lens distortion, occlusion, and warping [47]. AprilTag markers revealed increased sensitivity to edge occlusions [50]. AprilTag markers performed at satisfactory levels when the internal portion of a tag was occluded, yielding a detection rate of 50-100% depending on the tag ID [50]. AprilTag marks showed strong resistance to lateral and normal rotations because markers were detected and recognized at 0°, 10°, 20°, 30°, 45°, 55°, and 65° relative to clockwise and counterclockwise directions [50]. Occlusion and rotation around the longitudinal axis were successful at 0°, yet unsuccessful at 22°, 45°, 67°, and 90° [50].

2.6.2 ArUco

ArUco is an opensource system that uses black and white square markers to estimate camera pose. ArUco detection involves:

- Image segmentation: yields good results for an array of values and parameters (ω_t)
- Discard small contours
- Contour extraction and filtering: the remaining contours are approximated by the most similar polygon based on the Douglas and Peucker algorithm [52]
- Marker code extraction: assess innermost region of the remaining contours to determine marker validity
- Subpixel corner refinement: locate corners with subpixel accuracy

ArUco applies an adaptive threshold in a gray image, then seeks to find potential marker candidates by eliminating all contours that are not approximated by a rectangle [53]. Relative to contour extracting and filtering, a perimeter smaller than $P(\tau_c) = 4 \times \tau_c$ pixels will be rejected [54], where $P(\tau_c)$ is the canonical image perimeter and τ_c is the side length. Considering a detected contour $v \in I^r$, and denoted by $P(v)^j j$, then its perimeter is in the image, $I^j \in$ I. The best image $I^h \in$ I for code extraction and identification is computed by

$$I^h \mid h = argmin \mid P(v)^j - P(\tau c) \mid \quad (2.1)$$
$$j \epsilon \{0,1, \ldots n\}$$

and precedes error correction within ArUco's detection and identification process [54]. A variation of ArUco (Chilitags) utilizes a similar decoding method for marker binary codes [54].

2.6.3 ARToolKit

ARToolKit was initially used in scientific and industrial research [45], [51], [55]. This 2D planar marker system identifies markers in a given image and is widely employed in interactive and augmented reality applications due to source availability [56], [57].

According to Fiala [45], inter-marker confusion is computed by

$$P(\neq A) = \sum_{n=1}^{36} H D(n) \cdot p(n) q(n) \quad (2.2)$$

$$P(\neq A) = \sum_{n=1}^{36} H D(n) \cdot p^n (1-p)^{36-n} \quad (2.3)$$

where $P(\neq A)$ is the probability that a marker A can be mistaken for another marker in the set used in a system; $p(n)$ and $q(n)$ are the probability of n bits being falsely and correctly detected, respectively; and $HD(n)$ represents Hamming distance histogram [45].

2.6.4 ArUco, ARToolKit, and AprilTag2 advantages

All three marker systems are black-and-white squared-based fiducial markers [58] that have reliable decoding schemes and can be identified efficiently. ArUco may be the most popular and reliable marker detection system due to its adaptability to non-uniform illumination [54]. ArUco is inherently robust and is capable of detecting and correcting binary code errors [54]. Detection is based an adaptive threshold within a gray image followed by identification of marker candidates only after eliminating and discarding contours that cannot be approximated by a rectangle [53], [54]. Thereafter, codes are extracted, markers are identified, and errors are corrected accordingly [53]. ArUco is also characterized by a good performance at a range of marker orientations, bit error detection and correction, reduced inter-maker confusion, ability to use smaller tag sizes, and decreased total bits in a tag [51].

ARToolKit was the earliest marker detection system to be widely used in augmented reality. ARToolKit executes faster than ARTag and ARToolKitPlus [45], [55]. Such tags are appropriate and highly applicable within robotic applications, since robotics requires a highly robust system [58].

AprilTag is robust to lighting variations and accuracy relative to tag orientation (Figure 2-6). AprilTag2 improved over AprilTag [9], [53], yielding shorter detection computation time and fewer false positives due to tag covering, color-related errors, and lighting [49] in natural environments [7]. The tag's lexicode-based generation process reduces the false positive rate without hindering location accuracy [7], [9]. With special algorithms to detect markers, the

AprilTag2 redesigned tag detector enhanced the efficiency and robustness when compared to its predecessor [9]. AprilTag2 also has enhanced performance on smaller images, in particular decimated input images, yielding significant improvements in detection speed [9]. Unlike other marker systems, AprilTag encodes only 4-36 bits of data, enabling quicker tag detection [7]. Improved robustness and efficiency reveal the advancements in AprilTag2 compared to ArUco and ARToolKit [9]. Thus, AprilTag2 is an appropriate tool for cases where computational power is a challenge. AprilTag2 tag detection via smartphones could improve real-time tag tracking on mobile devices.

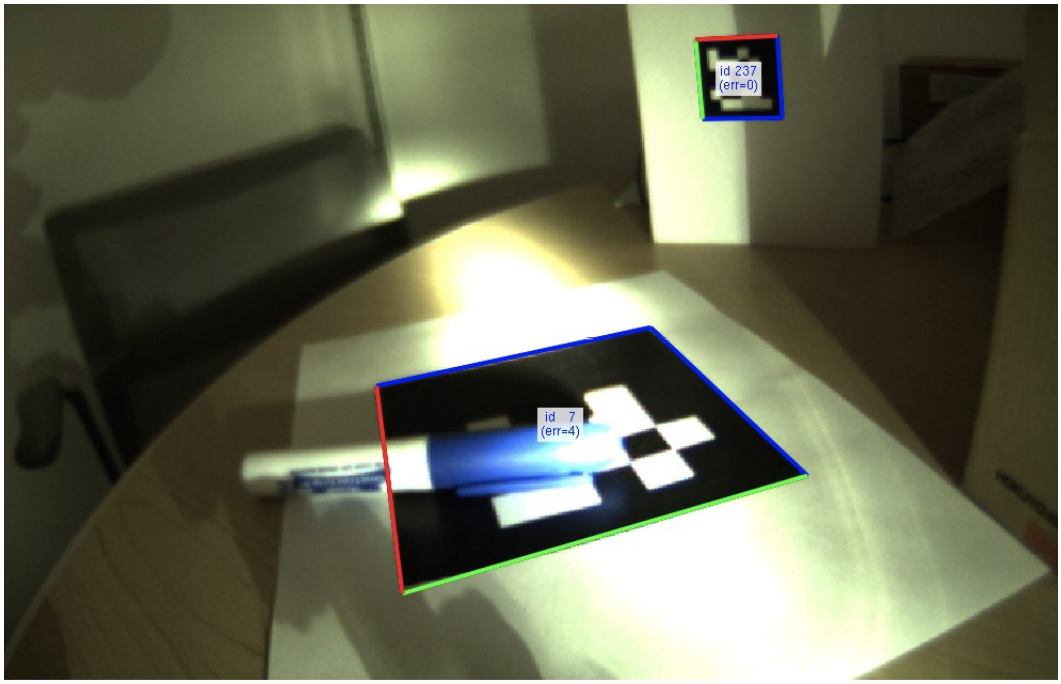

Figure 2-6 AprilTag fiducial system (adapted from [49]).

Future studies on AprilTag2 should focus on experiments related to occlusion resilience, such as rotating around three principal axes [50], [51], [59], and resistance to inter-marker confusion and illumination changes [59]. To deal with inter-marker confusion, ArUco maximizes inter-marker differences and bit transitions, both of which reduce the prevalence of inter-marker confusion rates and false positive rates while enhancing ArUco system robustness [45]. Classifying markers patterns have proven to reduce inter-marker confusion rates. Badeche and Benmohammed [60] used Latin characters to classify ARToolKit markers pattern in an effort to lower inter-marker confusion. AprilTag2 uses a similar method to minimize confusion rates.

2.6.5 ArUco, ARToolKit, and AprilTag2 disadvantages

ArUco and ARToolKit have disadvantages compared with AprilTag2. This section outlines these disadvantages.

ARToolKit has several drawbacks [45]. While ARToolKit is faster than ArUco and AprilTag2 for marker recognition, ARToolKit is challenged by slow pattern recognition processing [55]. In ARToolKit, a global threshold is used to produce a binary image. This image is correlatdd with images in a predefined database [53], which increases processing effort since the database grows with each picture processing instance and for each individual tag in the picture [47], [50], [51]. To improve ARToolKit performance, taking pictures of the markers from different angles and with varying lighting will improve the database for accurate marker detection, but make marker detection and identificaton time longer since more correlations are required. Moreover, ARToolKit applies a greyscale threshold to each image before processing, and this threshold setting will adversely affect either false negative rate or false positive rate (i.e., if false negative rate increases, false positive rate decreases).

ARToolKit uses basic error correction methods, resulting in poorer performance compared with edge based detection approaches [45]. However, ARToolKit error correction does provide a low false positive rate and is robust when the marker rotates [9], [53].

Differing opinions have been presented on the effect of ARToolKit library size on marker uniqueness. A study by Xiao, Owen, and Middlin [61] proposed an ARToolKit library with components of spatial frequency to widen and expand the library, thereby improving marker detection with increased library size. In contrast, A study by Khan, Ullah, and Rabbi indicated that the new library size did not improve inter-marker confusion rates [45] despite ARToolKit's ability to reduce inter-marker confusion rates, a generalized classification algorithm was not proposed for ARToolKit [55], [60].

ArUco has relatively poorer behavior than ARToolKit and AprilTag2, regardless of the resolution [54]. ArUco detection reliability is affected by uncalibrated cameras with small focal length because they usually exhibit high distortion [54].

AprilTag2 performance advantages over ArUco and ARToolKit are partly due to image segmentation based on a graph with local gradients to approximate edge lines [7], [58]. Occlusion is handled with a quad detection method (attempting to find four-sided regions facilitate by black

and white border of a tag)[53], [62]. After initial detection of lines, AprilTag2 uses black and white pixels to aid in decoding the image payload within a spatially-varying threshold [53], [62].

A common disadvantages of all fiducial marker systems is the tradeoff between marker detection distance and accuracy. The rate of the successful marker detection decreases as distance from the camera (Hamming distance: the sum of the differences between two digital sequences) increases. In AprilTag2, false positive rates are dependent on Hamming distance [7], with false positive rates increasing as Hamming distance increases.

2.7 Summary

Based on the literature, these items can be considered:

- Human posture measurement is required routinely by researchers and clinicians. Accurate and real time posture measurement at the point of patient contact has been a challenge for decades.
- Accelerometer, gyroscope, and often magnetometers can be combined to compute position; however, accuracy (noise amplification due to double integration from acceleration) remain a challenge.
- Markerless posture measurement using videos or pictures can be used to manually determine anatomical points by selecting points on-screen. The manual anatomical selecting process might result in errors, and real time evaluation is not possible.
- Marker-based approaches use markers on person to provide accurate measurements. However, a dedicated location for the motion analysis cameras and other hardware are required, and systems can be costly.
- Fiducial marker systems are uniquely identifiable objects in the field of view that can provide location and orientation (i.e., marker angle in the 2D image). AprilTag2 is a viable fiducial system since low computational cost and high accuracy should allow human posture measurement in real time on smartphones (i.e., anywhere at any time).

3 Fiducial Marker Approach for Biomechanical Smartphone-Based Measurements

3.1 Overview

This chapter introduces fiducial marker systems for potential use in a mobile app that measures human posture using anatomical and body segments. The chapter compares and evaluates the performance of different fiducial markers system on a Samsung Galaxy S5. The chapter contains a modified IEEE manuscript published in 3rd International Conference on Bio-engineering for Smart Technologies (BioSMART), Paris, France, April 2019.

3.2 Abstract

Marker-based measurement has been used to assess human body positioning, but human marker tracking has yet to make the transition from the laboratory to personal computing devices, such as smartphones. A novel smartphone-based approach could use a fiducial marker system. Fiducial markers are applicable to augmented reality, robotics, and other applications where a camera-object pose is required and tracked. However, few fiducial systems can be implemented on a mobile phone because of the processing requirements for identifying and tracking the tags in real-time. In augmented reality, virtual information is shared with the real world to further enhance a person's view of the environment; therefore, this illusion is directly associated with good registration of both virtual and real worlds. Measurement applications also require accurate and fast registration so that real objects are in alignment with virtual objects in real-time. Our research reviewed and evaluated various fiducial marker systems by developing an Android mobile application for real-time biomechanical measurement. A test was designed for two nominated fiducial systems to compare their speed and robustness on the mobile phone. AprilTag2 was selected as the best fiducial marker option for this application.

3.3 Introduction

Posture measurements are routinely required by clinicians, but current methods of measuring joint and pose require specialized equipment or unacceptable clinic time. These angle measurements are typically taken manually, using a protractor or goniometer, since visual observation introduces human error. Advanced technologies such as x-ray and marker-based

motion analysis systems (Vicon, etc.) are time consuming, costly, and may be hard to access. We proposed an innovative solution using smartphone augmented reality (AR) technology. With smartphone-based AR in a real-time application, the gap can be filled for cost, accessibility, and accuracy. An AR system could provide standardized quantitative measurements in realtime, an important feature that does not exist in clinical practice, providing clinicians with instant feedback on human body orientations and distances.

Based on our preliminary research, visual fiducial marker systems were selected as the best option for this application, since other colour or light-based markers were susceptible to background noise, lighting conditions, and confusion between markers when working in a clinic environment. Fiducial markers are uniquely identifiable objects placed in the field of view that can provide a location and orientation (i.e., marker angle in the 2D image). By placing fiducial markers on body segments, the segment position and orientation can be tracked in realtime. However, fiducial systems for this application have yet to be appropriately implemented on mobile phones.

Fiducial marker systems are characterized by "patterns that are mounted in the environment and automatically detected in digital camera images using an accompanying detection algorithm" [45]. System performance can be measured by the false negative rate, false positive rate, and inter-marker confusion rate. Of these metrics, the false negative rate is deemed the least serious since a fiducial marker is present within the image yet never reported [45]. Inter-marker confusion rate occurs when a fiducial marker is detected yet incorrectly identified [45]. Other evaluation metrics include minimal marker size for reliable detection, detection jitter, and immunity to lighting [45], [47]. Blurredness, movement of markers or camera along x or y-axis, occlusion, robustness, and tracking stability have also been analyzed [47]. The fiducial system's decoding algorithm has a profound impact on computational cost and time in various conditions, including occlusion and lighting. One method (ARToolKit) uses arbitrary image patterns embedded inside a square, which are matched to a database of known patterns for identification [45], [57]. AprilTag, ARTag, ArUco, and AprilTag2 use 2D binary code patterns to improve tag detection by detecting tag edges, which is an improvement over the ARToolkit thresholding method [50], [54].

ARToolKit is one of the earliest visual fiducial systems, introduced in 1999 at SIGGRAPH. ARToolKit was initially used in scientific and industrial research [45], [51], [55]. The 2D planar marker system includes planar patterns and computer vision algorithms to identify markers in a

given image [56], [57]. Due to ARToolKit's source availability, it has been widely employed in interactive and augmented reality applications.

Based on earlier fiducial markers such as ARToolkit and ARTag, Edwin Olson developed a new system called AprilTags, a black and white square tag encoded with a binary payload [7]. The AprilTag detection process involves seeking linear segments, detecting squares (tags), computing the tag's position and orientation, and decoding the barcode.

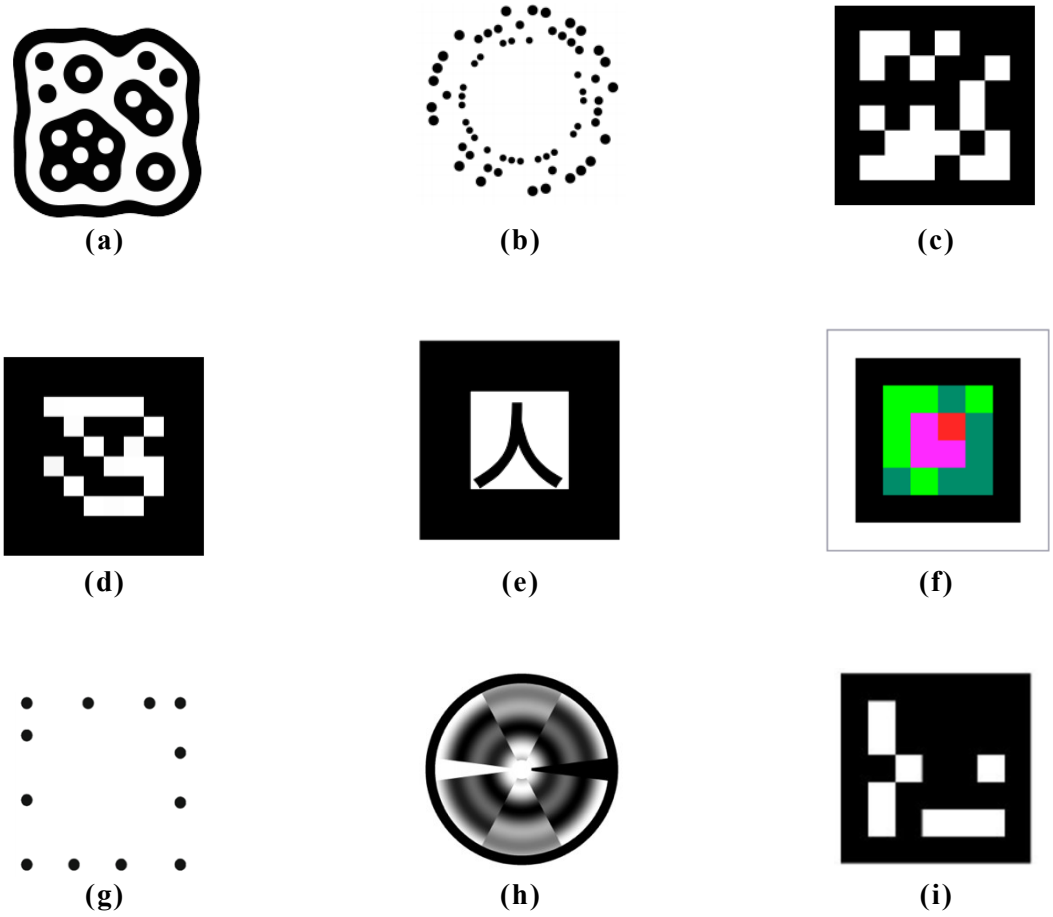

Figure 3-1 Examples of fiducial marker systems**.**

In addition to existing square black and white tags, researchers have proposed other encoding methods, such as reacTVision [63] that uses a recognition model that was introduced by d-touch [64]. By degrading smoothly, FourierTags [65] can be detected at longer distances. For better localization accuracy, RUNE-Tags [66] uses circles of unconnected ellipses to shape the marker.

Although RUNE-Tags is more accurate and robust to blurring and occlusion, it requires more computation time. To overcome projective geometry, PI-Tag [67] uses crossratio to detect the tag. To enhance AprilTag, ChromeTags [49] use two bicolor blended tags in CIELAB color scheme to increase gradient magnitude and detection speed by reducing the number of edges. Figure 3-1 shows different fiducial marker systems patterns.

3.4 Selection criteria and background

3.4.1 Design criteria

For an AR-based mobile application, the fiducial system needs to meet the following criteria:

- Function in real-time (marker detection, marker tracking, display marker border and outcome measures on screen) on smartphones having these minimum specifications: 16MP rear camera, 2 MP front camera, 2 GB Ram, 2.5 GHz quad core CPU speed
- Detection and tracking with at least 1 meter between the phone and markers (i.e., full body in video frame)
- Save marker coordinates and BAR-M outcome measures in a data file

3.4.2 Selected fiducial systems

Only two fiducial systems met the criteria and were selected for further testing, AprilTag2 and ArUco. Both use black-and-white squared-based fiducial tags [58]. As fiducial marker systems, ArUco and AprilTag2 possess reliable decoding schemes and can be identified efficiently. Romero-Ramirez, Muñoz-Salinas, and Medina-Carnicer [53], [54] claimed that ArUco is the most popular and reliable marker detection system today. The system's adaptability to non-uniform illumination is key to its reliability.

AprilTag calculates a specific identity, orientation, and position of a marker relative to the camera [7], [9], [47]. AprilTag was developed to maximize the number of distinguishable codes, maximize correctable bit errors, minimize false positive confusion rate, and minimize the number of bits per tag (minimizing tag size) [49].

Maximizing the distance between tags (hamming distance) makes AprilTag highly distinguishable. AprilTag2 remained robust to false positives [9], [49]. AprilTags play a quintessential role in reducing false positives that occur due to tag covering, color-related errors, and lighting issues [49]. Olson claimed that AprilTags are resilient against false positive only in

natural environments [7]. Since tag coding is the same as AprilTag, AprilTag2 remains robust to false positives within the coding system. However, AprilTag2 improved performance detection, yielding fewer false positives and shorter computational time to ensure detection. Additional findings demonstrated that the tags' lexicode-based generation process reduces false positive rates without hindering location accuracy [7], [9]. Olson further claimed AprilTag works robustly with lens distortion, occlusion, and warping [47]. AprilTag markers revealed increased sensitivity to edge occlusions, limiting its effectiveness for cases where occlusion occurs [51]. Upon occlusion of the internal portion of the tags, AprilTag markers performed at satisfactory levels, yielding a detection rate of 50-100% depending on the tag ID [51]. AprilTag markers showed strong resistance to lateral and normal rotations since markers were detected and recognized at 0°, 10°, 20°, 30°, 45°, 55°, and 65° relative to both clockwise and counterclockwise rotations [51].

ArUco uses black and white square markers to calculate camera pose. The detection process involves:

- Image segmentation
- Contour extraction and filtering. After discarding small contours, the remaining contours are approximated by the most similar polygon using the Douglas and Peucker algorithm
- Marker code extraction. Assessment of the remaining contours' innermost region to determine marker validity
- Subpixel corner refinement. Corner locations are estimated with subpixel accuracy

ArUco applies an adaptive threshold in a gray image then seeks to find potential marker candidates by eliminating all contours that are not approximated by a rectangle [53]. ArUco maximizes inter-marker differences and bit transitions, both of which reduce the prevalence of inter-marker confusion rates and false positive rates while enhancing ArUco system robustness [45]. Classifying markers has proven to reduce inter-marker confusion rates in other studies.

3.5 Test and results

3.5.1 Methodology

An Android mobile phone application was developed to test tracking response of AprilTag2 and ArUco in real-time. Java language was implemented for both Apriltag (C language) and Aruco (C++) Libraries by calling Java Native Interface (JNI). The core image processing library of both

fiducial marker systems was not modified. As an initial test, observational analysis was used to evaluate the speed of tag detection and tracking of each tag system. A Samsung Galaxy S5 was used for testing. Two ArUco markers were placed on a wall in different locations and angles with respect to the phone (Figure 3-2). An examiner held the phone in front of tags and moved the phone to visually evaluate the marker tracking response. The test was repeated for AprilTag2.

For the second test, the mobile phone was set on a tripod with the parallel distance between the phone and the markers was 70 cm (Figure 3-2). 10 seconds of marker orientation and 2D position data in the camera frame were recorded (corner coordinates for each marker). The false positive rate and inter-marker confusion rate between two markers were calculated and the standard deviation (SD) of each corner was used to assess jitter rate (i.e., "shaking" in the marker image position).

3.5.2 Results

Appropriate marker detection and tracking response was required to avoid pauses while tracking. ArUco could not meet this first criteria, with perceivable marker tracking latency. AprilTag2 successfully tracked markers while the smartphone was in motion. Therefore, further testing was performed only on AprilTag2. For the second test set, AprilTag2 performance was acceptable (Table 3-1), with no inter-marker confusion, few false positives, and <0.2 SD for corner coordinates.

3.6 Conclusion

Ten fiducial systems were reviewed to select a suitable system for the intended biomechanical measurement mobile phone application. Among these systems, ArUco and AprilTag2 were selected for further testing on a Samsung Galaxy S5 smartphone. Both AprilTag2 and ArUco are open source and have an affordable computational process. However, only AprilTag2 met our tracking response requirement on the smartphone. The AprilTag2 system also demonstrated robust tag location accuracy. AprilTag2's boundary-based segmentation algorithm for reducing tag detection computing time for and increasing detection rate may have contributed to the acceptable performance on the smartphone. Unlike other marker systems, AprilTag2 encodes only 4-36 bits of data, thus enabling accurate and quick tag detection [9]. Improved robustness and efficiency revealed the advancements in AprilTag2 compared to ArUco. Therefore,

AprilTag2 is preferred over the other fiducial marker systems due to its improved performance relative to small images, thus providing improved detection speed on mobile devices.

Table 3-1 AprilTag2 results

	Marker 1	**Marker 2**
False positive rate	1%	1%
Inter-Marker confusion rate	0%	0%
SD of 1st corner location (pixel)	0.184	0.180
SD of 2nd corner location (pixel)	0.177	0.185
SD of 3rd corner location (pixel)	0.185	0.192
SD of 4th corner location (pixel)	0.179	0.188

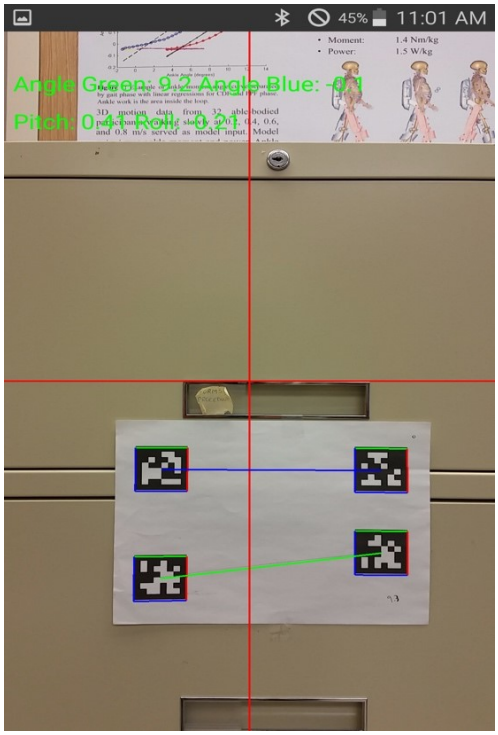

Figure 3-2 AprilTag2 marker detection using BAR-M with Samsung Galaxy S5**.**

3.7 Future work

Additional to detecting and tracking markers, the developed mobile application is capable of measuring angle and distance between markers (Figure 3-2). Angle and distance are often used to quantify human body segments for different applications; such as, diagnosing skeletal deformities (e.g., scoliosis, limb length discrepancy), range of motion measurement for sports science, and research. The next step is to evaluate angle and distance between markers with people, using a motion analysis system as a “gold standard”.

4 Augmented Reality Approach for Marker-based Measurement on Smartphones

4.1 Overview

This chapter discusses Biomechanics Augmented Reality Tag (BAR-M) development and reports app performance when measuring angle and distance between two markers using the front and back camera of a Samsung Galaxy S6 in different mobile holding positions.

4.2 Abstract

The use of marker tracking for postural and range of motion measurements with a mobile device transcends multiple disciplines including, healthcare, ergonomics, engineering, robotics, and training. While image analysis has been used to compute angles and distances, a viable real-time mobile application is currently lacking for measuring limb angles and body posture. To address this need, a novel Android smartphone augmented-reality-based application was developed using the AprilTag2 fiducial marker system. In augmented reality, virtual information is shared with the real world to improve a person's interaction with the environment. To evaluate the app, two markers were printed on paper and attached to a wall. A Samsung S6 (rear camera 16MP, front camera 5 MP, Ram 3 GB, CPU Octa core with 2.1GHz Quad + 1.5GHz Quad) mobile phone was fixed on a tripod, parallel to the wall. The smartphone app tracked and recorded marker orientation and 2D position data in the camera frame, from front and rear cameras, for different smartphone placements. The average error between mobile phone and measured angles was less than 1 degree for all test settings. The average error for the back camera was 0.29º, front camera was 0.33º, yaw rotation was 0.75 º and tilt rotation was 0.22 º. The average error between mobile phone and measured distance was less than 4 mm for all test settings. The average error for the back camera was 1.8 mm, front camera was 2.5 mm, yaw rotation was 3 mm, and tilt rotation was 3.8 mm. Overall, the app obtained valid and reliable angle and distance measurements with smartphone positions and cameras that would be expected in practice. Thus, it is concluded that this app has potential for use in clinical range of motion and posture assessments.

Keywords— measurement, markers, fiducial markers, range of motion, posture, augmented reality, healthcare, apriltag2, mobile application, smartphone

4.3 Introduction

Posture is commonly characterized as the alignment of body segments at a given time and serves as an important health indicator [68]. Posture and range of motion (ROM) measurements are used to identify abnormalities stemming from various disorders; including, scoliosis, musculoskeletal disorders, pain syndromes, and respiratory dysfunctions [1], [10], [69]. The fields of ergonomics, biometrics, orthopedics, and rehabilitation readily employ posture and ROM measurement in both able-bodied and clinical populations [1], [3], [10], [16], [70]. However, quantitative measurements are dependent on equipment availability and accessibility. A mobile technology approach could be considered to bring real-time measurement to the point of patient contact.

Mobile-based approaches have been employed to measure human posture and ROM. Mobile applications have become popular because of accessibility. There are two main approaches for smart-phone based applications. One approach involves capturing a still image with a smartphone or tablet camera and then annotating the image to calculate angles between body segments or segment to camera frame. The user will capture images and add anatomical landmarks on screen to define reference segments [71]. However, accurate measurements are challenging because the selected points might not be placed on the correct anatomical landmarks.

A second approach uses smartphone accelerometer and gyroscope sensors to quantify the posture measurement and ROM. Inertial Measurement Units (IMU) combine data from a gyroscope (rotational velocity), accelerometer (acceleration), and sometimes magnetometer (heading by tracking magnetic-north) to determine the sensor's orientation [5], [6]. Determining an IMU's position in space is difficult because computing position requires a double integration that is affected by sensor drift and system noise [5].

Another approach for markerless measurement of human pose involves depth cameras, such as Kinect [5], [72]. These markerless systems can have low accuracy and may not be applied in real-time [7], [49], [51]. The lack of real-time feedback reduces the likelihood of improving posture among workers during ergonomic interventions [73]. Depth camera systems such as Microsoft Kinect can quickly and reliably measure and compute joint angles within posture-related evaluations and assessment [73]. However, the depth of view is small and the system struggles with dark and shiny surfaces.

In desktop applications, Open CV and other libraries provide the ability to track coloured or active markers in a video field. However, there are problems with background “confusion”, difficulty with consistent multi-marker tracking, and confusion between markers. All of these negatively affect accuracy. On the other hand, real-time marker-based systems are of high accuracy and can be used for Augmented Reality (AR) mobile-based applications, where live video of the real world is augmented by virtual information. In AR marker-based systems, black-and-white pictures (fiducial markers) can be recognized by webcams prior to being superimposed by objects in real-time multimedia, without the problems associated with coloured or active marker tracking [51], [62].

Fiducial markers could be a viable approach for real-time mobile human body measurement. Fiducial marker systems are characterized by “patterns that are mounted in the environment and automatically detected in digital camera images using an accompanying detection algorithm” [45]. These uniquely identifiable objects are placed in the field of view as reference points to provide a location or orientation (i.e., marker angle in the 2D image) that the camera can measure. By placing fiducial markers on body segments, position and orientation can be tracked in real-time.

Fiducial systems are a viable option to meet these criteria because the computational cost is low with high accuracy [74]. Fiducial markers will be more easily recognizable than colour or light-based markers. Based on our preliminary research, colour or light-based markers were vulnerable to background noise, lighting conditions, and confusion between markers when working in a clinic environment.

AprilTag are "2D barcode style" fiducial markers, similar to QR codes, that can be printed on paper. The AprilTag software computes precise 2D position, tag orientation, and identifies the tag location relative to the camera [7]. AprilTag2 improved on the original AprilTag by providing greater reliability than other fiducial systems, featuring a smaller number of false positives and a decreased false positive rate compared to other fiducial systems [9]. False positive rate is deemed the most important since the fiducial marker would be missing within the image yet reported as present [45].

Based on a survey of the literature, current accurate posture measurement and ROM systems cannot be used anywhere and at any time since they depend on the experiment setup and location. Therefore, a need still remains for a system to measure location or orientation in real-time with inexpensive and accurate computational processes. The fast nature of the AprilTag2

marker-based system, along with its ease of use, makes this a potential approach for accessible human posture measurement in healthcare. Therefore, this research developed an AR mobile-app using AprilTag2 fiducial markers for posture and ROM measurement by determining marker 2D position and orientation and providing information to the user in real-time. Following successful evaluation, this mobile AR approach could bridge the gap for posture and range of motion measurement at the point of personal contact, thus making postural measurement widely accessible and usable [75].

4.4 Methodology

4.4.1 Design criteria

The design criteria for the AR-based posture and ROM measurement mobile application includes:

- Track markers smoothly without noticeable delay on a mobile phone screen (minimum 15Hz tracking rate)
- Real-time display of live video, angles, distance between markers, or marker orientation
- Appropriate performance with back and front cameras. The front camera is typically lower resolution but allows the user to see the screen during use (i.e., self-evaluate or hold marker on a person and see the outcome measure)
- Angle measurement accuracy to 1 degree and distance accuracy to 5mm
- Convenient to access anywhere, at any time (i.e., mobile application without network connectivity requirements)

4.4.2 Design

The Biomechanics Augmented Reality Tag (BAR-M) app was developed for Android and AprilTag2 fiducial markers, as an extension of the original BAR app that used smartphone sensors and orientation for measurement [76]. This novel Android application was developed to track AprilTag2 orientation and 2D position in a real-time. Java language was implemented for the AprilTag2 Library by calling the Java Native Interface (JNI). The core AprilTag2 image processing library (C language) was not modified.

Smart phone camera captured frames were sent to a background thread (Figure 4-1). This thread processed the frame data and sent this data to JNI so that the AprilTag2 library could detect

and process markers in the video frame. The AprilTag library returned (x,y) coordinates for marker corners and tag center to the processing thread through JNI. Marker angles and distance between markers were calculated using regional slope equations and a scale factor (determined from a ratio between marker real-world dimensions and marker coordinates in pixels) [77].

OpenGL was used to render the overlayed graphics in the correct viewpoint relative to the smartphone and marker, with marker coordinates transformed into a global affine coordinate frame. The graphical overlay included drawing a box around each marker and a line connecting marker centers. By drawing a box in real time around markers, the user knows which markers are detected (Figure 4-2). Additionally, the phone axis can be displayed on the screen for relative feedback of phone orientation to the environment. App output was saved in a .csv file and included frame times, marker corner coordinates, marker centre coordinates, and marker side lengths (all units in pixels).

The user can select the live AR view from two options, individual marker angle to horizontal, with horizontal defined by the camera sensor gravity vector; or angle between a line connecting the centres of two markers and the horizontal.

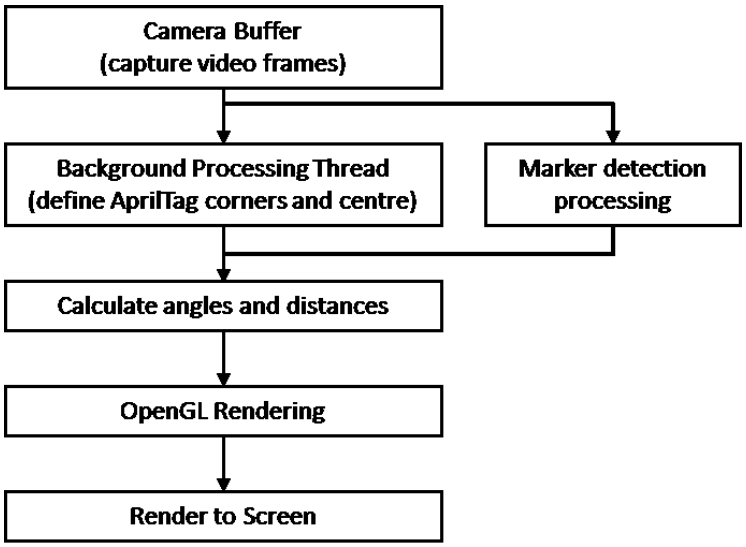

Figure 4-1 Tracking module flowchart.

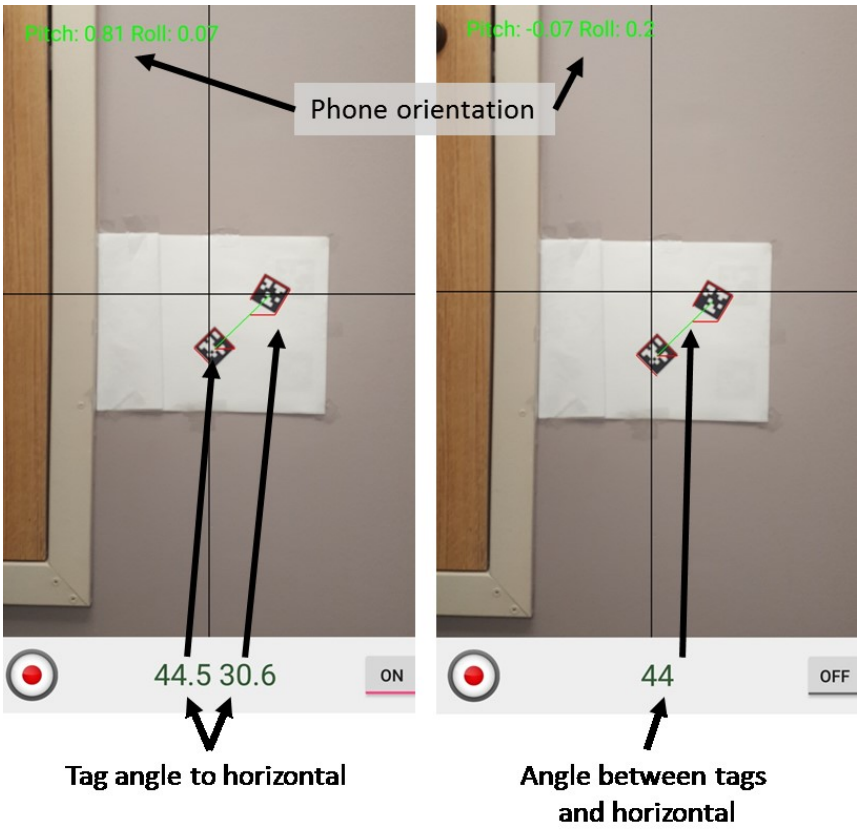

Figure 4-2 BAR-M augmented reality screen output.

4.5 Evaluation

To test the app, two 3.65 cm x 3.65 cm AprilTag2 markers were printed on rigid cardboard (i.e., no flexing during testing) and attached to a wall. Tag orienation and distance between tags were set in a Microsoft PowerPoint document. This marker size was chosen during pilot testing since this was the smallest dimension to enable marker identification within a camera field of view that included the entire human body. A bubble level was used to orient the paper to vertical.

The BAR-M app was installed on a Samsung Galaxy S6 (rear camera 16MP, front camera 5 MP, Ram 3 GB, CPU Octa core with 2.1GHz Quad + 1.5GHz Quad) phone and then affixed to a tripod (Figure 4-3). All tests were performed with both front (1440p) and back (2160p) cameras to evaluate differences between video image resolutions. 10 seconds of video data were captured for each trial. The effect of distance between the smartphone and the markers was evaluated by placing the tripod from 60 cm to 150 cm parallel distance from the tags, in 10 cm intervals. The effect of camera rotation was evaluated by placing the tripod 90 cm from the markers (i.e., distance with best results from the front camera) and rotating the tripod mount in yaw and then tilt

directions. Trials were completed at 0, 5, 10, 15, 20, 25 degrees clockwise and then with the same angles counter-clockwise. The angle between a line connecting the 2 markers and the horizontal, and the distance between marker centres, were calculated for every output frame and then compared to the measured values. The scale factor for distance conversion from pixels to cm was calculated using the ratio between marker real-world dimensions and marker coordinates in pixels.

a **b** **c**

Figure 4-3 Setup environment, a) phone parallel to markers, b) yaw rotation, c) tilt rotation

4.6 Results

The angle and distance results are presented in Table 4-1. The measured angle was 44.1 degree and the measured distance was 9.55 cm.

For the parallel distance test, the front camera detected the markers from 60 cm to 115 cm, with an average frequency for providing marker data of 14 Hz. The back camera detected markers for the entire 150 cm range, at an average frequency of 22 Hz. Back and front camera results of angle and distance between a line connecting markers is shown in Figure 4-4 and Figure 4-5, respectively. For the front camera, 90 cm from the markers enabled measurement with the full body on the screen and the lowest errors (0.29° and 0.27 cm difference from the measured values).

Table 4-1 Angle and distance results

		Angle (deg)			Distance (cm)		
		Average Difference	**Max**	**Min**	**Average Difference**	**Max**	**Min**
Back camera	Parallel	0.29±0.16	44.58	43.58	0.18±0.07	9.84	9.44
Front camera	Parallel	0.33±0.15	44.41	43.48	0.25±0.07	9.93	9.70
	Yaw	0.75±0.40	45.90	43.20	0.29±0.23	10.15	9.50
	Tilt	0.23±0.14	44.02	43.59	0.38±0.05	10.05	9.85

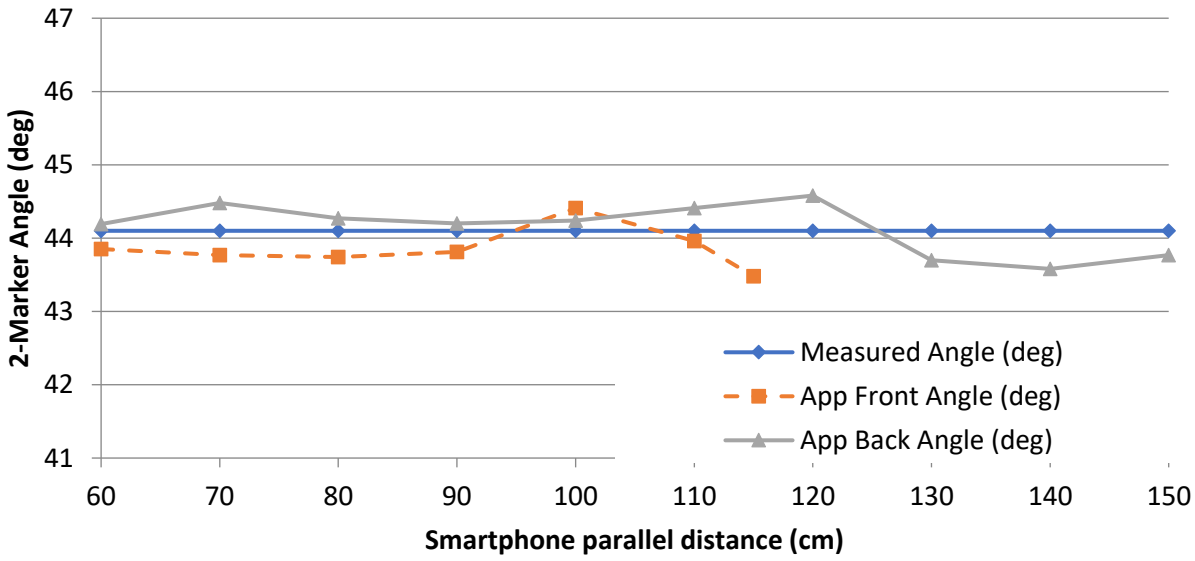

Figure 4-4 Back and front camera angles from two markers.

For the smartphone yaw and tilt tests, Figure 4-6 and Figure 4-7, there is a constant error which leads to underestimate the angle measured and overestimate the distance measured between markers. The inflection points of tilt and yaw tests occurred at 0 degree. The average, standard deviation, min, and max errors were shown in Table 4-1. There were errors greater than 1 degree and 5mm from -15 to -25 degrees and 15 to 25 degrees respectively in yaw test. The reason for tilt test offset is due to the smartphone built in sensors which data drifted.

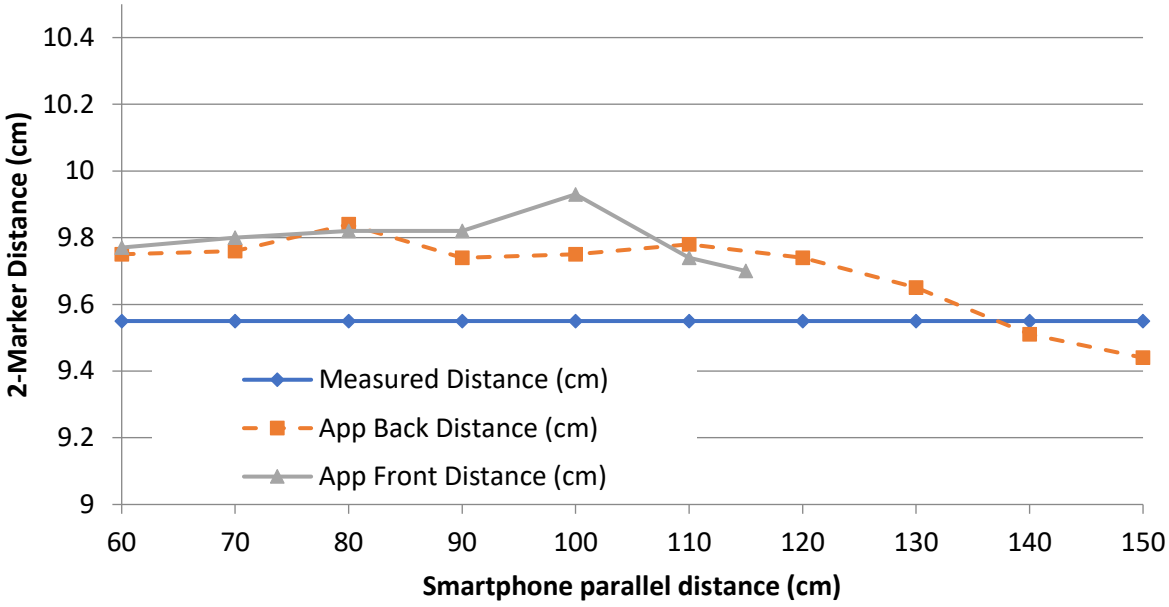

Figure 4-5 Back and front camera distances between two markers

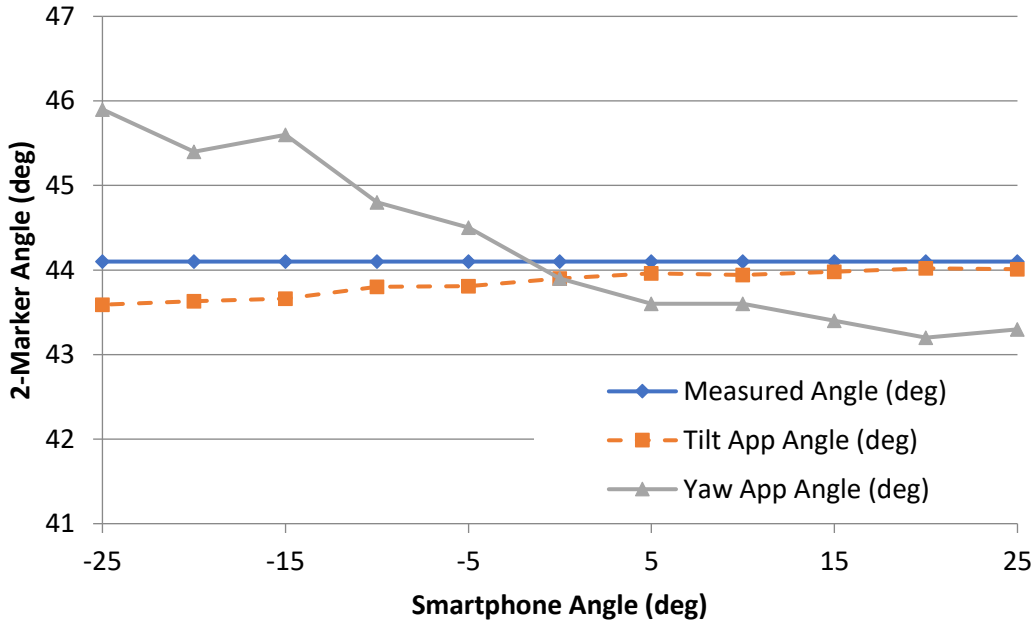

Figure 4-6 Yaw and tilt angle results

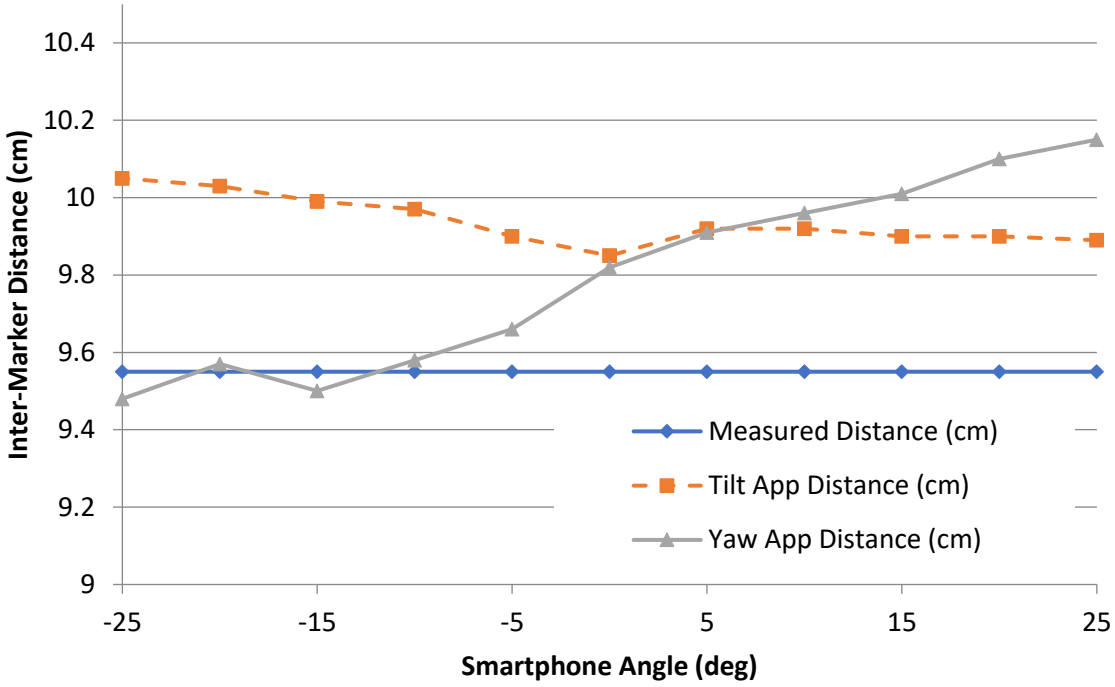

Figure 4-7 Yaw and tilt distance results

4.7 Discussion

The outcomes of this study support the use of AprilTag2 fiducial markers for an AR-based mobile application. Accuracy was found to be within the design criteria, with angle and distance average errors in all setups less than 1° and 4mm, respectively. These results would support the use of this app approach for augmented-reality-based measurement of human posture and range of motion.

All study evaluations were completed with a Samgung Galaxy S6 smartphone; therefore, any device with at least an Octa-core processor (4x2.1 GHz Cortex-A57, 4x1.5 GHz Cortex-A53) and 1440p camera resolution would be appropriate. Higher camera resolutions could improve marker identification accuracy and also would allow smaller tags to be used. Smaller tags could be easier to implement for some human movement tracking applications.

The rear camera had a higher video resolution than the front camera, therefore tags could be detected at a longer distance and the sampling rate was faster than the front camera. The maximum distance for tag identification was 115 cm for the front camera and 150 cm for the rear camera. The minimum number of pixels in 1 cm detected by the mobile phone was 10.23 and 9.33 pixels

for front and back camera respectively. The average marker sampling frequency was less than 22Hz and was influenced by orientation and 2D position computation. At 22Hz, the user preceives smooth marker tracking on the AR display. It is expected that this frequency will increase with more powerful smartphone processors. Markers exposed to too much light cannot be detected and tracked. Hence, having normal lighting (room light) has a profound impact on marker detection and the permissible distance between phone and markers.

AprilTag2 enables robust tag detection for viability on smartphones and other computation-limited systems, extending their significance for tag tracking in real-time applications. The markers showed strong resistance to camera yaw and tilt rotations since markers were detected and recognized at 0º, 5º, 10º, 15º, 20º, and 25º relative to both rotation directions (clockwise and counter clockwise). Hence, the application was also reliable for posture measurement by clinicians even if the tags are not perfectly parallel and the mobile device screen is not vertical to gravity. However, the recommendation app use would be to have the smartphone or tablet parallel to the tags when measuring. In future research, correction factors based on tag edge-coordinate differences from square could be used to better adapt to cases where markers are not parallel to the camera plane.

4.8 Conclusion

The Biomechanics Augmented Reality Tag app detected, tracked, and measured angles and distances between tags as a real-time augmented reality application, and also stored results in a csv file for more detailed evaluations. This AR smartphone app could be viable for posture, range of motion, and distance measurements that are routinely required by clinicians and researchers. Therefore, customizing the mobile application and tag related tools to capture human body posture and range of motion will be the next step in BAR-M development.

5 Evaluation of a Biomechanical Augmented Reality Mobile-based Application

5.1 Overview

This chapter evaluates the performance of the augmented reality (AR)-based mobile application that measures human posture using anatomical and body segments markers. Contents from this chapter will be submitted as a journal paper.

5.2 Abstract

Human posture measurements and range of motion (ROM) assessments are important for many fields; including, healthcare, ergonomics, and sport science. Currently, video analysis and motion capture systems are the most common techniques for quantifying postural measurement. However, for broad implementation in clinical practice measurement techniques should be real-time, accurate, and portable. To address these criteria, a novel smartphone and tablet-based approach was developed to enable marker-based (AprilTag2 fiducial marker) body segment measurement at the point of patient contact (Biomechanical Augmented Reality – Marker, BAR-M). This augmented reality app provides real-time angle measurements for use in clinical decision-making. This research evaluated mobile app performance for measurements on a body opponent bag (BOB) and a group of 15 healthy participants. App measurements were compared with Vicon motion analysis system measurements. BOB evaluations provided an optimal situation for smartphone measurement baseline accuracy, while evaluation on humans demonstrated system accuracy in practice. For both tests, a Samsung Galaxy S6 smartphone was set on a tripod, 1 meter parallel distance from the participant. The front camera recorded live video and the app calculated AprilTag orientations and the angle of "a line connecting the center of two tags" to the horizontal. The resulting angle was displayed in real time on the phone's screen. For Vicon, reflective markers were attached to the pelvis, shoulder, arm, and torso. Marker data were processed to calculate pelvic obliquity, shoulder, and arm abduction. For the app, a prosthetist held the AprilTag markers on the person's anatomical landmarks so that the angle could be read from the screen. A app streaming data file was also created to enable angle post-processing. Each measurement was repeated 10 times. For the BOB test, the absolute mean angle difference between Vicon and smartphone was 0.09° ±0.05° for hip, 0.09°±0.06° for shoulder, and 0.69° for arm abduction. For

the participant test, the absolute mean angle difference between Vicon and smartphone was 1.70°±0.23° for hip, 1.34°±0.27° for shoulder, and 11.18° ± 3.68° for arm abduction. Overall, the app obtained valid and reliable angle measurements in postural and ROM assessments on BOB and 15 participants using the front camera of the Samsung Galaxy S6 (rear camera 16MP, front camera 5 MP, Ram 3 GB, CPU Octa core with 2.1GHz Quad + 1.5GHz Quad). The poorer arm abduction results were due to systematic errors in a few participants (i.e., clothes movement during measurement caused Vicon markers to move differently from AprilTag markers). Thus, with appropriate measurement methods this app is a viable tool for posture and range of motion assessments.

5.3 Introduction

Posture is the body's position or bearing for a special purpose, and is considered a valuable health sign [1]. When also considering movement, joint range of motion (ROM) is often used in clinical assessments. However, quantitative measurement of posture and body segment positioning in clinical practice has remained a challenge due to the need for specific and typically expensive technology, time for data collection and analysis, and separate testing space requirements. An Augmented Reality (AR) mobile based application approach would be a convenient solution, enabling real-time measurement of human posture and ROM at the point of patient contact.

Biomechanics Augmented Reality (BAR) is an example of an AR-based smartphone app for real-time human angle measurement and result reporting [76]. BAR measures angles using the phone's orientation to the gravity line, defined using the smartphone accelerometer. For example, aligning the phone screen to the torso would measure the torso angle to vertical. The app also shows a constant grid and vertical line based on gravity. Real-time angle measurements on a smartphone could support clinicians for accurate and immediate decision making.

Video based body angle measurements can also be performed by post-processing each frame manually. Angle measurements on stored video have been implemented as mobile phone apps or a web-based application [71], [78], by selecting three points on the video frame (i.e., online goniometer). While angle measurement is accurate based on the selected points, these clinician-selected points on video might not be the exact anatomical points of measure. This approach takes additional time for capturing video, processing markers, and reporting results, but does allow the clinician to step through the stored video frames to aid in observational movement analysis.

Marker-based motion caption systems are currently considered to be the most accurate body segment angle measurement method, and are thus taken as the gold standard for comparing with different measurement systems [5]. However, these systems are costly, not portable, and need to be set up with calibration. Furthermore, some systems can be sensitive to bright light, restricting their use to controlled indoor areas.

Fiducial marker systems are defined objects mounted in an optical imaging device field of view, and can be dynamically detected in software. These markers are best applied in situations where a relative pose between the source and the object is needed; for example, robotics, Augmented Reality (AR), and Human-Computer Interactions (HCI) applications. To apply fiducial markers to human posture and angle measurement, a novel AR-based smart device application (Biomechanics Augmented Reality Tag – BAR-M) was implemented with AprilTag2 and evaluated in bench tests [74]. However, human trails were needed to verify app function in clinical situations.

A gap exists for technology to measure human posture and ROM at the point of patient contact in real-time, with high accuracy and easy accessibility. The fast nature of the AprilTag2 fiducial marker-based system, along with its ease of use, makes this a potential approach for real-time human posture measurement in healthcare. Therefore, this research evaluated BAR-M function for anthropometric evaluation. Following successful evaluation, this AR-based digital measurement tool could be used by clinicians to obtain real-time angle measurements to assist in clinical decision making at the point of patient contact.

5.4 Methodology

A novel Android app was developed to display live video of the person being measured, locate AprilTag2 fiducial markers in the video, process marker data, and calculate angles between markers. This research investigated two measurements approaches for pelvis obliquity, shoulder position, and arm-abduction: evaluation on a body opponent bag (BOB) and evaluation with 15 healthy adults. The front camera was so clinicians can measure the person and see the result live on the screen, allowing clinicians work independantly.

5.4.1 Body opponent bag

A BOB mannequin was used as a static human surrogate for initial evaluation, since anatomical-based measurements could be made without human movement and tissue variability. As shown in Figure 5-2, reflective markers were attached to the BOB pelvis (superior iliac spines), shoulder (acromioclavicular joint), arm, and torso (zyphoid process). A 10 camera Vicon motion analysis system recorded reflective marker 3D locations. Angles between the reflective markers were calculated as a gold standard comparator.

For the mobile phone application, a Samsung S6 smartphone (rear camera 16MP, front camera 5 MP, Ram 3 GB, CPU Octa core consist of 2.1GHz Quad + 1.5GHz Quad) was set up on a tripod such that the screen was 1m in front and parallel to the BOB frontal plane. The application tracked AprilTag2 coordinates (tag centre); calculated the angle formed by the tags and displayed the angle onscreen in realtime (i.e., angle between a line connecting two tags and the phone orientation to gravity, reported as an angle from the horizontal); and stored tag coordinates, angles, and time for further analysis. Realtime measuremnt provides live feedback to clinicians, allowing them to position markers on the body see the outcome measures instantly.

Vicon and app data were collected simultaneously for all trials. The app and Vicon system were synchronized by voice (i.e., voice count of "1, 2, 3, Go" to start data collection on both systems). Since static measures were compared, precise synchronization was not required. Vicon data were collected at 100 Hz and the app data collection rate was approximately 19 Hz (app rate varied from 18 to 21 Hz, depending on settings). One second of steady state data (i.e., lowest standard deviation) was averaged for each comparative measure.

AprilTag2 markers were mounted on custom 3D printed adapters to enable positioning at anatomical locations:

- Flat mount: Plastic mount with AprilTag on one side and various mounting options on the other side (post-adapter, Velcro, or caliper, Figure 5-1a). The plastic mount can be held in square or diamond orientations, with the diamond approach enabling point contact between the mount and the anatomical location (Figure 5-2b).
- Post-adapter: Orients the AprilTag normal to a pointed post (Figure 5-1b) that can be placed on an anatomical landmark, especially for landmarks such as the superior iliac spine that can be obscured from the camera.

- Velcro-adapter: A Velcro band can be passed through the flat mount, to secure the mount to the body or limb (i.e., upper arm, chest, etc.) (Figure 5-1c).

a **b** **c**

Figure 5-1 AprilTags adapters, a) flat mount, b) post-adapter, c) velcro-adapter

AprilTag markers were co-located beside reflective markers. As shown in Figure 5-2, two post-adapters were used for pelvic obliquity measurements (Figure 5-2a).

a **b** **c**

Figure 5-2 BOB measurements, a) pelvis, b) shoulder, c) arm abduction

Flat mounts were held in a diamond position (i.e., corner vertical) for shoulder angle measurement (Figure 5-2b). Since tags are square, a diamond position allows precise corner positioning on the anatomical landmark. Velcro adapter markers were secured to the upper arm and torso for arm abduction angle measurement (i.e., angle between torso and arm) (Figure 5-2c).

All measurements were made by the same person, who stood behind BOB and held adapters next to the reflective markers. Since BOB arm abduction was constant, 1 trial was recorded. Pelvis and shoulder angles were measured 10 times.

5.4.2 Human Testing

A convenience sample of 15 health adults were recruited (14 male, 1 female). All measurements were made by the same prosthetist. All participants provided information consent and signed a consent form (approval from uOttawa Research Ethics Board). All participants could safely stand for at least 40 minutes. Exclusion criteria were balance problems that affect safe standing and cognitive problems that make following instructions difficult.

An 8 marker set was affixed to each participant, with reflective markers at acromia, anterior superior iliac crests, superior iliac crests, torso and arms. The participant was positioned 1 meter in front of the phone, such that the body frontal plane was parallel to the phone screen. Three measurements were evaluated: pelvis obliquity, shoulder angle, arm-abduction angle.

For pelvis obliquity measurements, the participant stood still with the right leg on a 2mm thick plate, simulating hip misalignment, with their arms at their sides. The prosthetist stood behind the participant and held post-adapters on the left and right posterior superior iliac crests for at least 3 seconds (Figure 5-3a). In addition to the same saved data as the BOB test, the prosthetist recorded the most consistent angle from the app's real-time display (i.e., small angle changes could occur due to changes in the handheld Apriltag position, so this represented the angle that a clinician would select in practice). This procedure was repeated 10 times (i.e., 10 pelvis angle measurements). Angles from anterior superior iliac crests reflective markers locations were used as comparators.

For shoulder angle measurements, the participant stood with their arms at their side. The evaluator stood behind the participant and held two marker adaptors in a diamond orientation on top of the reflective markers on the acromioclavicular joints, for at least 3 seconds (Figure 5-3b). Saved data and evaluator recorded angle were logged. This procedure was repeated 10 times.

For arm abduction angle measurement, the participant stood with their arms at their sides and facing the camera. Velcro straps secured the Apriltags to the participant's torso and upper arm. The evaluator positioned the torso Apriltag vertically at the center of the participant's front. Two reflective markers were positioned on the chest at top and bottom of the adaptor. The upper arm adaptor was aligned to the arm's long axis and two reflective markers were positioned beside the adaptor along the arm's long axis. The participant abducted their arm to their comfortable range and held the position for 3 seconds (Figure 5-3c). Angles of each AprilTag orientation with respect to the horizontal were displayed on the app screen and saved on the phone.

a **b** **c**

Figure 5-3 Participant measurement: a) hip, b) shoulder, c) arm abduction

The evaluation criteria was 3 degrees maximum difference between Vicon and BAR-M angles [79]. This criteria is below other measurment systems such as IMU sensors (maximum 8° error for shoulder angle measurement [80]), inclinometer (average knee angle error above 6°) and phone applications (minimum 12° error [81]).

5.5 Results

For the BOB, the absolute mean angle difference between Vicon and app results were 0.09° ±0.05° for pelvis (maximum of 0.2°, minimum of 0.02°), 0.09°±0.06° for shoulder (maximum of 0.18°, minimum of 0 °), and 0.69° for arm abduction (one constant arm-abduction angle).

For the participant test (Table 5-1), the absolute mean difference between Vicon and app angle 1.70°±0.23° for pelvis (maximum 3.37°, minimum 0.59°), 1.34°±0.27° for shoulder angle

(maximum 3.70°, minimum 0.35°), and 11.18°±3.68° for arm abduction (maximum 28.46°, minimum 1.93°). After removing outliers, the new absolute mean difference was reduced to 7.68°±3.62° and new maximum difference to 11.60°.

The average angle difference between the value read from the app AR display and data stored on the phone is shown in Table 5-1. The absolute mean difference was 0.19°±0.09° for pelvis measurement (maximum 0.29°, minimum 0.10°) and 0.12°±0.09° for shoulder angle (maximum 0.23°, minimum 0.03°).

Table 5-1 Participant test app AR angle and stored data results

Participant	Average Difference Between Vicon Angle and App Saved Data			Average Difference Between App AR Angle and App Saved Data	
	Pelvis	Shoulder	Arm	Pelvis	Shoulder
P1	1.97 ° ± 0.60°	0.42° ± 0.49°	3.51° ± 1.59°	0.12° ± 0.14°	0.07° ± 0.06°
P2	1.09° ± 0.50°	0.82° ± 0.21°	19.08° ± 5.08°	0.31° ± 0.24°	0.07 ° ± 0.10°
P3	2.65° ± 0.80°	2.77° ± 0.30°	27.92° ± 1.98°	0.13° ± 0.09°	0.06 ° ± 0.04°
P4	2.73° ± 1.15°	0.61° ± 0.18°	8.37° ± 4.98°	0.21° ± 0.18°	0.23° ± 0.34°
P5	0.64° ± 0.56°	0.89° ± 0.68°	6.80° ± 3.51°	0.20° ± 0.29°	0.18° ± 0.18°
P6	0.78° ± 0.88°	0.42° ± 0.31°	28.46° ± 4.67°	0.18° ± 0.19°	0.09° ± 0.06°
P7	1.42° ± 0.98°	2.85° ± 0.98°	7.74° ± 5.40°	0.16° ± 0.10°	0.03° ± 0.02°
P8	1.78° ± 0.92°	2.28° ± 0.61°	7.37° ± 2.95°	0.12° ± 0.11°	0.08° ± 0.06°
P9	0.62° ± 0.46°	0.68° ± 0.42°	11.19° ± 5.41°	0.16° ± 0.14°	0.07° ± 0.07°
P10	1.68° ± 0.83°	3.70° ± 0.53°	13.33° ± 4.59°	0.18° ± 0.13°	0.12° ± 0.10°
P11	1.98° ± 0.89°	0.35° ± 0.21°	11.16° ± 1.49°	0.29° ± 0.33°	0.20° ± 0.25°
P12	0.59° ± 0.36°	2.38° ± 1.05°	2.71° ± 3.59°	0.27° ± 0.26°	0.15° ± 0.10°
P13	3.37° ± 0.72°	0.72° ± 0.39°	13.07° ± 6.58°	0.21° ± 0.31°	0.15° ± 0.14°
P14	1.72° ± 0.86°	0.84° ± 0.69°	1.93° ± 1.17°	0.17° ± 0.13°	0.07° ± 0.05°
P15	2.52° ± 0.52°	0.44° ± 0.33°	4.99° ± 2.22°	0.10° ± 0.07°	0.19° ± 0.13°
Average	1.70° ± 0.23°	1.34° ± 0.27°	11.18° ± 3.68°	0.19° ± 0.09°	0.12° ± 0.09°

5.5.1 Arm-abduction insight

The results for pelvis and shoulder measurement were satisfactory however, the arm-abduction measurements were not satisfactory, hence it was decided to investigate further. The arm-abduction angle measurement was split into a) angle between torso and horizontal line, b) angle between arm and horizontal line, c) angle between arm and torso, in order to find the cause of the error. Figure 5-4 shows mean differences for all participants, highlighting differences between participants and between mean and standard deviation. Torso standard deviations were

consistent but Standard Deviation (SD) varied for arm angle measurements. Therefore, the average angle between arm and torso was greater.

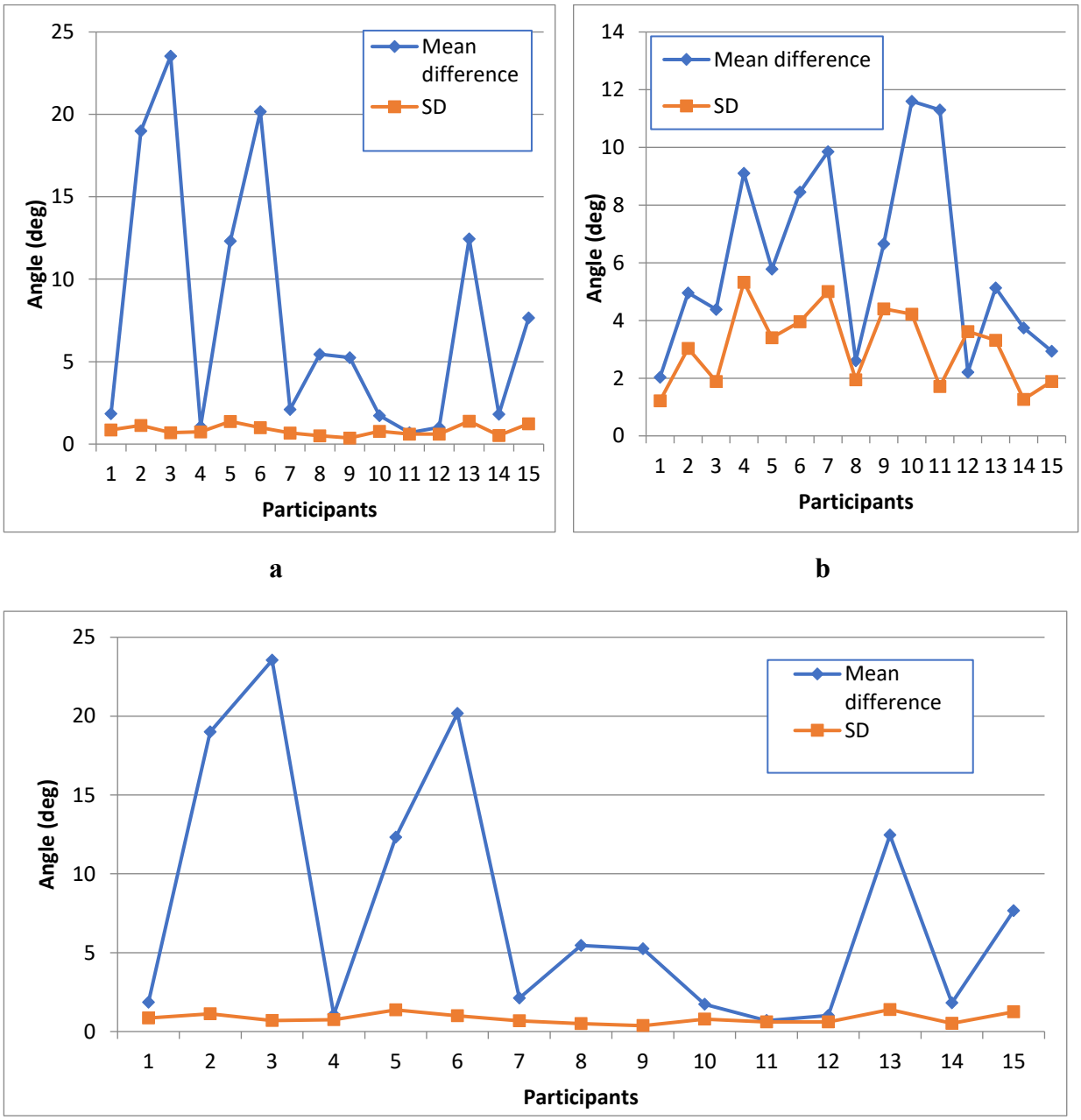

Figure 5-4 Absolute mean differences between Vicon angle and app saved data and standard deviations, for all participants for the arm abduction trials: a) torso to horizontal line, b) arm to horizontal line, c) arm to torso.

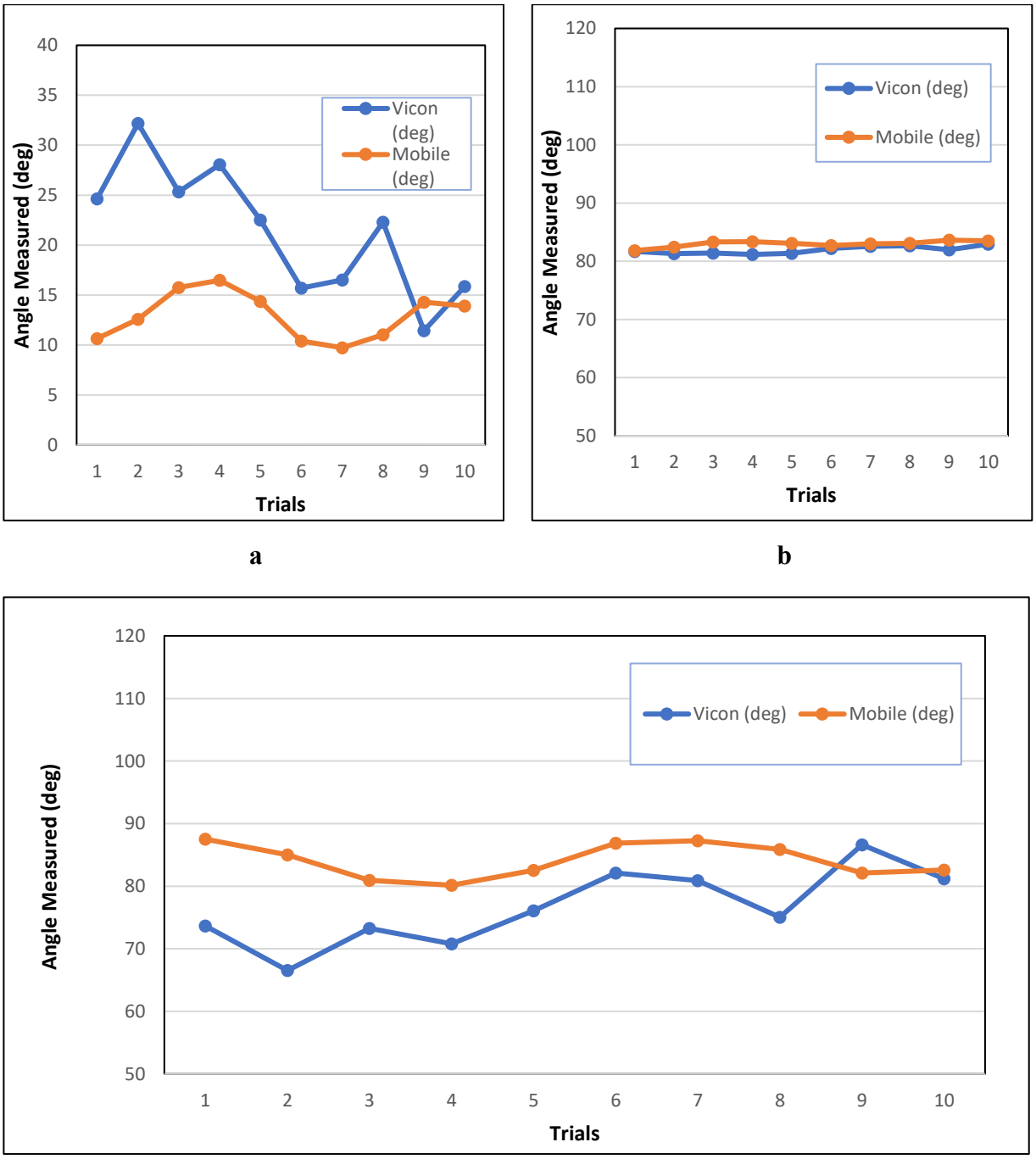

Figure 5-5 Vicon angle and app saved data for participant 4: a) torso to horizontal line, b) arm to horizontal line, c) arm to torso.

5.6 Discussion

The smartphone biomechanics augmented reality app successfully tracked and displayed accurate angles, based on evaluation with a Body Opponent Bag where anthropometric measures were not affected by clothing or participant movement. This demonstrated that the app provides viable angle measurements that can be used for point-of-contact assessments. Evaluations with humans also demonstrated viability for posture and ROM assessment, but results were not as good as the BOB analyses, indicating that measurement method improvements could be made to enable optimal patient encounters.

Various sources of marker-based measurement error have been reported for human movement analysis. These include skin movement over bone, clothing movement, and difficulty locating anatomical landmarks in areas with excessive tissue [82]–[84].

5.6.1 Pelvis and shoulder measurement

For shoulder and pelvis measurement, measurements with most subjects displayed differences between the Vicon and the app of less than 2°. However, two subjects had differences of more than 3°. The greater differences could be due to difficulties of positioning both markers sets (AprilTag and reflective markers) on the anatomical landmarks. For shoulder measurements, not holding the AprilTag's flat mount in a perfect diamond shape on top of the reflective markers would cause an error. For pelvis measurement, the greater differences could be due to the Vicon markers being positioned over clothing since using the post-adapter to locate anatomical landmarks could move clothing and thereby affect reflective markers locations. Vicon measurement SD was greater than the mobile app, especially for people with more fat on pelvis area because body mass would move when the prosthetist located the landmarks with the post adapter. Therefore, this research highlights the practical issues for using marker-based analysis at the point of patient contact. Since the AprilTag mount is held at the appropriate location, regardless of clothing, this approach may be more appropriate that markers that are stuck onto the person for other data collection-based approaches. Since BOB testing provided accurate results, attaching a reflective marker to the AprilTag mount would have also provided accurate results.

5.6.2 Arm-abduction measurement

Arm abduction differences between Vicon and app measurements were greater than the shoulder and pelvis measurements. In some cases, these differences were more than 10°, with the maximum of 28.46°. This error involved both the arm and chest, hence error summation was greater than the other two previous measurements (i.e., pelvis and shoulder). All errors were systematic and chest area errors could be resolved by an appropriate Velcro straps and locating tags on the participant's back rather than chest (i.e., flatter surface). Moreover, securing the mount with tape could help since strap movement due to breathing or torso movement could be reduced.

For the arm, errors occurred by lack of consistent alignment between the reflective markers an the AprilTag (i.e., marker slipped while a participant moved their arm because of clothing and marker locations on arm, which may not be a rigid body segment due to skin movement). This error could be reduced by positioning markers on a line adaptor (green stick) to avoid shirt movement (Figure 5-6a). In (Figure 5-6b) the line created from reflective markers (green line) has a different angle from a line passing through the AprilTag's center (orange line). The difference is small between a line created by torso reflective markers (yellow line) and a line passing through the AprilTag marker (light blue line). Therefore, the difference in arm-abduction measurement between phone and Vicon was due to their positioning on a shirt, which is a known measurement error. In some situations where participants are not comfortable removing their clothes (i.e., cultural reason or measurement in public), measurement errors caused by clothing is likely to happen for adhesive-based approaches. An appropriate strap and AprilTag marker approach could minimize clothing-based errors, As well as holding the marker in the appropriate orientation.

Reading the most consistent angle from the mobile screen provided accurate results, supporting the AR approach for pose measurement. The average difference between reading the most consistent number and calculating the average angle form saved data was less than a 0.2°. Therefore, reading instant measurements from the mobile screen is appropriate.

a

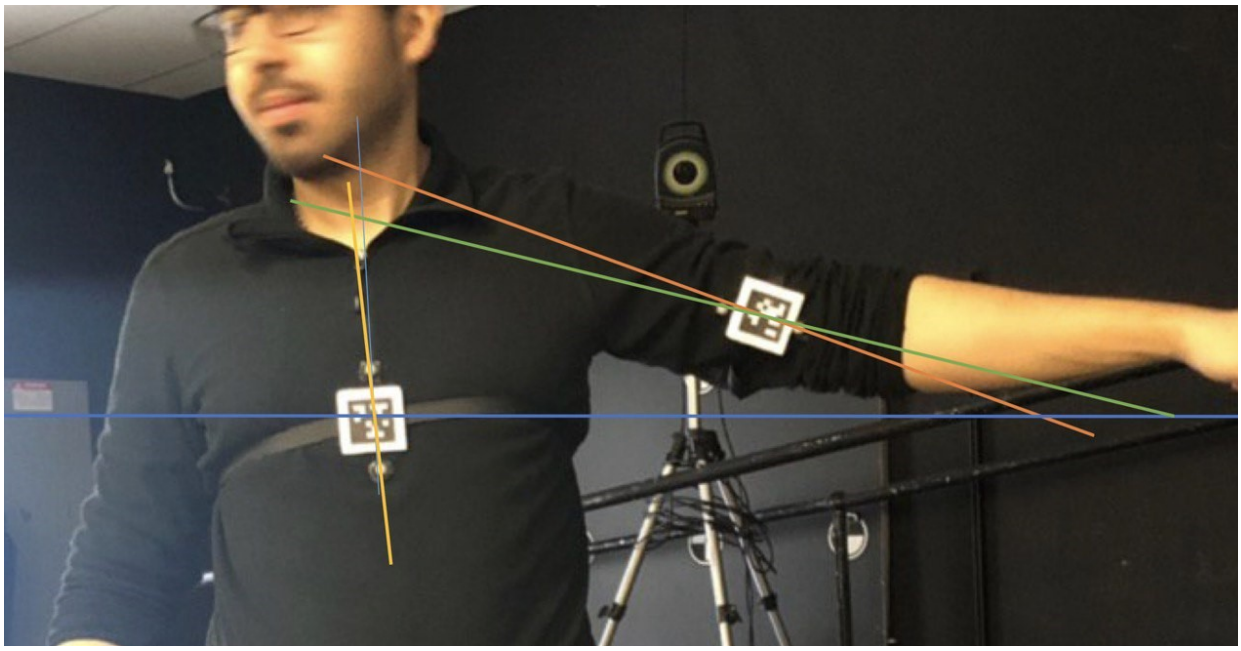

b

Figure 5-6 Arm-abduction error and solution, a) locating tags using a stick b) measurement methodology error visualization.

Fiducial markers were essential to avoid marker loss in environments with complex backgrounds and to avoid confusion between markers (each fiducial marker is unique). Another

benefit from AprilTag fiducial markers is that the marker corner coordinates are provided, which can be used to calculate a linear scale factor for distance measurements. With a smartphone, a trade-off exists between image resolution and AprilTag sample rate, with sample rate decreasing for higher resolutions. The current configuration enabled pose measurement with the entire body in the field of view. Newer mobile devices with faster processors will enable faster sample rates or higher video resolutions, which would allow enable the camera to be farther back or smaller AprilTags to be used. The BAR-M app has a setup option to configure the software for appropriate resolution for a functional frame rate.

The BAR-M approach is viable but systematic measurement method errors could negatively affect measurements. Future research can address and solve these errors, providing a quantitative measurement tool at the point of patient contact and the bench.

5.7 Conclusion

The Biomechanics Augmented Reality-Tag application detected, tracked, and calculated angles between anatomical landmarks, in real time. The angle was displayed on-screen and detailed data were stored on the mobile device. The AR smartphone app was viable for range of motion and postural measurements that are required by clinicians and researchers, both from recording the realtime angle and post processing saved data. The measurement methodology could be improved to compensate for measurement over clothes and other factors that can introduce measurement error. This includes developing straps that can be quickly applied to the body and provide a consistent fiducial marker location and expanding on the current set of adapters to make human measurement efficient for the clinician and the person being measured.

6 Thesis Conclusions and Future Work

6.1 Conclusions

This thesis developed and evaluated the first AR mobile phone based human posture measurement app using fiducial markers (AprilTag2) to measure angles between anatomical landmarks and between body segments. The algorithm identified, tracked, and recorded fiducial marker orientation and 2D position data in the camera frame (corner coordinates for each marker), and then stored the data as a CSV file in the mobile phone. This accomplished the thesis objecive, develop and evaluate an Augmented Reality (AR) mobile application that measures range of motion and human posture between anatomical landmarks and between body segments in real-time, with an accuracy comparable to other systems currently used in practice.

Initial bench tests with a Samsung Galaxy S6 smarphtone proved that the app can measure angles with an average error less than a 1º and distances with an average error of 4 mm. Even with the phone set in different positions and orientations from the markers (parallel distance, yaw and tilt rotation), the system responded with acceptable accuracy.

The average error between BAR-M and Vicon measurements on the BOB were less that 0.7°, which was within the evaluation criteria. The shoudler and hip results were exceptional, with only 0.09° average difference.

The app had larger differences from Vicon with human participants, with 1.70°±0.23° for pelvis obliquity, 1.34°±0.27° for shoulder angle, and 11.18° ± 3.68° for arm-abduction angle. Measuring on people presented various sources of human movement measurement error; such as, difficulty locating anatomical landmarks in areas with excessive tissue, which is a known source of bias for human body measurement. [82]–[84], skin and clothing movement, and relative movement between markers.

Overall, the results demonstrated that the BAR-M app provides accurate marker outcomes measures in realtime, but that clinicians should be aware of typical human marker-based meaurement factors when positioning markers on the body.

6.2 Future work

The research presented in this thesis is a novel human body segment measurement tool using an AR mobile-based approach that can demonstrate results in real-time, with the ability to be used

anywhere at any time. Contributions of this thesis include a cost-effective, easy-to-access, viable, and high accuracy solution to quantify human posture measurement using fiducial markers (AprilTag2 paper-based) and an Android mobile phone.

The successful BAR-M app opens the door for many new research opportunities. AprilTag3 was recently introduced and could improve 3D and dynamic postural measurements [85]. AprilTag3 should reduce tag detection and proceesing algorithm time, so Z direction can be computed live without a delay [85]. Z axis can be used in following scenarios:

- Provide 3D coordinates for each marker to enable better correction for out-of-plane marker positions or movements
- Enable movements unconstrained to the camera plane (i.e., person can move out of plane)
- Explore dynamic movements, with camera being moved to keep a person in the video field (e.g., walking or running)
- In industry or public where smartphone-based markerless measurements are difficult and error-prone (measuring furniture, living spaces, etc.)

Robust tag holders are required to avoid artifact caused by skin and clothing. New tag holders should consider different posture measurements requirements (i.e., curve, square, foldable).

Clinical research is needed to determine the best way to use BAR-M to perform common posture and ROM related measurements. BAR-M could be used for tuning prosthetic and orthotic devices, where realtime orthosis or prosthesis angle measures can be used during the live tuning process.

References

[1] J. Paušić, Ž. Pedišić, and D. Dizdar, “Reliability of a photographic method for assessing standing posture of elementary school students,” *J. Manipulative Physiol. Ther.*, vol. 33, no. 6, pp. 425–431, 2010.

[2] E. Jaspers, K. Desloovere, H. Bruyninckx, G. Molenaers, K. Klingels, and H. Feys, “Review of quantitative measurements of upper limb movements in hemiplegic cerebral palsy,” *Gait and Posture*, vol. 30, no. 4. pp. 395–404, 2009.

[3] A. L. Harrison, T. Barry-Greb, and G. Wojtowicz, “Clinical Measurement of Head and Shoulder Posture Variables,” *J. Orthop. Sport. Phys. Ther.*, vol. 23, no. 6, pp. 353–361, Jun. 2013.

[4] C. Prakash, A. Mittal, R. Kumar, and N. Mittal, “Identification of spatio-temporal and kinematics parameters for 2-D optical gait analysis system using passive markers,” in *2015 International Conference on Advances in Computer Engineering and Applications*, 2015, pp. 143–149.

[5] E. van der Kruk and M. M. Reijne, “Accuracy of human motion capture systems for sport applications; state-of-the-art review,” *Eur. J. Sport Sci.*, vol. 18, no. 6, pp. 806–819, 2018.

[6] M. A. Brodie, A. Walmsley, and W. Page, “Dynamic accuracy of inertial measurement units during simple pendulum motion,” *Comput. Methods Biomech. Biomed. Engin.*, vol. 11, no. 3, pp. 235–242, Jun. 2008.

[7] E. Olson, “AprilTag: A robust and flexible visual fiducial system." Robotics and Automation,” in *IEEE International Conference on Robotics and Automation*, 2011, pp. 3400–3407.

[8] M. Saleh and G. Murdoch, “In defence of gait analysis. Observation and measurement in gait assessment.,” *J. Bone Joint Surg. Br.*, vol. 67, no. 2, pp. 237–41, Mar. 1985.

[9] J. Wang and E. Olson, “AprilTag 2: Efficient and robust fiducial detection,” in *IEEE International Conference on Intelligent Robots and Systems*, 2016, vol. 2016-Novem, pp. 4193–4198.

[10] E. P. Maldonado, A. P. Marques, E. A. G. Ferreira, M. Duarte, and T. N. Burke, “Postural assessment software (PAS/SAPO): validation and reliabiliy,” *Clinics*, vol. 65, no. 7, pp. 675–681, 2010.

[11] B. Missaoui, P. Portero, S. Bendaya, O. Hanktie, and P. Thoumie, “Posture and equilibrium in orthopedic and rheumatologic diseases,” *Neurophysiologie Clinique*, vol. 38, no. 6. Elsevier Masson, pp. 447–457, 01-Dec-2008.

[12] E. N. Corlett and I. Manenica, “The effects and measurement of working postures,” *Appl. Ergon.*, vol. 11, no. 1, pp. 7–16, Mar. 1980.

[13] G. C. David, “Ergonomic methods for assessing exposure to risk factors for work-related musculoskeletal disorders,” *Occupational Medicine*, vol. 55, no. 3. Narnia, pp. 190–199, 01-May-2005.

[14] W. Y. Wong, M. S. Wong, and K. H. Lo, “Clinical applications of sensors for human posture and movement analysis: A review,” *Prosthet. Orthot. Int.*, vol. 31, no. 1, pp. 62–75, Mar. 2007.

[15] D. D. Harrison, S. O. Harrison, A. C. Croft, D. E. Harrison, and S. J. Troyanovich, “Sitting biomechanics part I: Review of the literature,” *J. Manipulative Physiol. Ther.*, vol. 22, no. 9, pp. 594–609, Nov. 1999.

[16] S. Tanaka, K. Yamakoshi, and P. Rolfe, “New portable instrument for long-term ambulatory monitoring of posture change using miniature electro-magnetic inclinometers,” *Med. Biol. Eng. Comput.*, vol. 32, no. 3, pp. 357–360, 1994.

[17] J. Huang, W. Xu, S. Mohammed, and Z. Shu, “Posture estimation and human support using wearable sensors and walking-aid robot,” in *Robotics and Autonomous Systems*, 2015, vol. 73, pp. 24–43.

[18] D. S. Schwertner, R. Oliveira, G. Z. Mazo, F. R. Gioda, C. R. Kelber, and A. Swarowsky, “Body surface posture evaluation: Construction, validation and protocol of the SPGAP system (Posture evaluation rotating platform system),” *BMC Musculoskelet. Disord.*, vol. 17, no. 1, p. 204, Dec. 2016.

[19] C. Fortin, D. Ehrmann Feldman, F. Cheriet, and H. Labelle, “Clinical methods for quantifying body segment posture: A literature review,” *Disability and Rehabilitation*, vol. 33, no. 5. pp. 367–383, 2011.

[20] S. H. Iunes DH, Bevilaqua-Grossi D, Oliveira AS, Castro FA, “Comparative analysis between visual and computerized photogrammetry postural assessment,” *Rev Bras Fisioter*, vol. 13, no. 4, pp. 308–15, 2009.

[21] Z. Sawacha *et al.*, "Biomechanical assessment of balance and posture in subjects with ankylosing spondylitis," *J. Neuroeng. Rehabil.*, vol. 9, no. 1, p. 63, Aug. 2012.

[22] E. S. Jung and S. Park, "Prediction of human reach posture using a neural network for ergonomic man models," *Comput. Ind. Eng.*, vol. 27, no. 1–4, pp. 369–372, 1994.

[23] S. Springer and G. Y. Seligmann, "Validity of the kinect for gait assessment: A focused review," *Sensors (Switzerland)*, vol. 16, no. 2, pp. 1–13, 2016.

[24] N. Ross A., Clark a, J. B. B, Kelly, F. M. A, Benjamin, P. A, Kade, and Y.-H. P. C, "Concurrent validity of the Microsoft Kinect for assessment of spatiotemporal gait variables," *J. Biomech.*, vol. 46, pp. 2722–2725, 2013.

[25] M. Gabel, R. Gilad-Bachrach, E. Renshaw, and A. Schuster, "Full body gait analysis with Kinect," in *Proceedings of the Annual International Conference of the IEEE Engineering in Medicine and Biology Society, EMBS*, 2012, pp. 1964–1967.

[26] S. Vernon *et al.*, "Quantifying individual components of the timed up and go using the kinect in people living with stroke," *Neurorehabil. Neural Repair*, vol. 29, no. 1, pp. 48–53, Jan. 2015.

[27] J. Behrens, C. Pfüller, S. Mansow-Model, K. Otte, F. Paul, and A. U. Brandt, "Using perceptive computing in multiple sclerosis - The Short Maximum Speed Walk test," *J. Neuroeng. Rehabil.*, vol. 11, no. 1, p. 89, 2014.

[28] D. S. Schwertner, R. Oliveira, G. Z. Mazo, F. R. Gioda, C. R. Kelber, and A. Swarowsky, "Body surface posture evaluation: Construction, validation and protocol of the SPGAP system (Posture evaluation rotating platform system)," *BMC Musculoskelet. Disord.*, vol. 17, no. 1, 2016.

[29] M.-H. Song and R. I. Godøy, "How fast is your body motion? Determining a sufficient frame rate for an optical motion tracking system using passive markers," *PLoS One*, vol. 11, no. 3, p. e0150993, Mar. 2016.

[30] L. Herda, P. Fua, R. Plänkers, R. Boulic, and D. Thalmann, "Using skeleton-based tracking to increase the reliability of optical motion capture," *Hum. Mov. Sci.*, vol. 20, no. 3, pp. 313–341, Jun. 2001.

[31] L. Chiari, U. Della Croce, A. Leardini, and A. Cappozzo, "Human movement analysis using stereophotogrammetry: Part 2: Instrumental errors," *Gait Posture*, vol. 21, no. 2, pp. 197–211, Feb. 2005.

[32] C. Ezeh, C. Holloway, and T. Carlson, “MoRe-T2 (mobility research trajectory tracker): validation and application,” *J. Rehabil. Assist. Technol. Eng.*, vol. 3, p. 205566831667055, Jun. 2016.

[33] P. Merriaux *et al.*, “A Study of Vicon System Positioning Performance,” *Sensors*, vol. 17, no. 7, p. 1591, Jul. 2017.

[34] C. Diaz Novo *et al.*, *The impact of technical parameters such as video sensor technology, system configuration, marker size and speed on the accuracy of motion analysis systems*, vol. 5, no. 1. Sociedad Mexicana de Ingeniería Mecánica, 2014.

[35] B. Carse, B. Meadows, R. Bowers, and P. Rowe, “Affordable clinical gait analysis: An assessment of the marker tracking accuracy of a new low-cost optical 3D motion analysis system,” *Physiother. (United Kingdom)*, vol. 99, no. 4, pp. 347–351, 2013.

[36] C. Fortin, D. E. Feldman, F. Cheriet, and H. Labelle, “Validity of a quantitative clinical measurement tool of trunk posture in idiopathic scoliosis,” *Spine (Phila. Pa. 1976).*, vol. 35, no. 19, pp. 988–994, 2010.

[37] Z. O. Abu-Faraj, *Handbook of Research on Biomedical Engineering Education and Advanced Bioengineering Learning*. 2013.

[38] “Measurement Sciences Aurora - Measurement Sciences.” [Online]. Available: https://www.ndigital.com/msci/applications/biomechanics/. [Accessed: 22-May-2019].

[39] N. Kumar, N. Kunju, A. Kumar, and B. S. Sohi, “Active marker based kinematic and spatio-temporal gait measurement system using LabVIEW vision,” *J. Sci. Ind. Res. (India).*, vol. 69, no. 8, pp. 600–605, 2010.

[40] C. J. C. Lamoth, O. G. Meijer, P. I. J. M. Wuisman, J. H. van Dieën, M. F. Levin, and P. J. Beek, “Pelvis-thorax coordination in the transverse plane during walking in persons with nonspecific low back pain.,” *Spine (Phila. Pa. 1976).*, vol. 27, no. 4, pp. E92-9, 2002.

[41] C. J. C. Lamoth, O. G. Meijer, A. Daffertshofer, P. I. J. M. Wuisman, and P. J. Beek, “Effects of chronic low back pain on trunk coordination and back muscle activity during walking: Changes in motor control,” *Eur. Spine J.*, vol. 15, no. 1, pp. 23–40, Feb. 2006.

[42] D. Sutherland, “The evolution of clinical gait analysis,” *Gait Posture*, vol. 16, no. 2, pp. 159–179, 2002.

[43] H. J. Woltring and E. B. Marsolais, “Optoelectric (Selspot) Gait Measurement in Two- and Three-Dimensional Space - a Preliminary Report,” *Bull. Prosthet. Res.*, vol. 17, no. 2, pp. 46–52, 1980.

[44] E. Lou, D. L. Hill, V. J. Raso, and N. G. Durdle, “A posture measurement system for the treatment of scoliosis,” in *IMTC/99. Proceedings of the 16th IEEE Instrumentation and Measurement Technology Conference (Cat. No.99CH36309)*, vol. 1, pp. 354–358.

[45] M. Fiala, “ARTag, a fiducial marker system using digital techniques,” *Proc. IEEE Comput. Soc. Conf. Comput. Vis. Pattern Recognit.*, vol. 2, pp. 590–596, 2005.

[46] I. Rabbi, S. Ullah, and D. Khan, “Automatic generation of layered marker for long range augmented reality applications,” *Kuwait J. Sci.*, vol. 44, no. 3, pp. 44–55, 2017.

[47] D. Khan *et al.*, “Robust tracking through the design of high quality fiducial markers: an optimization tool for ARToolKit,” *IEEE Access*, vol. 6, pp. 22421–22433, 2018.

[48] K. Pentenrieder, P. Meier, and G. Klinker, “Analysis of tracking accuracy for single-camera square-marker-based tracking,” *Proc. Dritter Work. Virtuelle und Erweiterte Realität der Gi-fachgr. VR/AR*, no. August 2016, p. 15, 2006.

[49] A. Walters and B. Manja, “ChromaTag-A Colored Fiducial Marker.”

[50] K. Shabalina, E. Magid, A. Sagitov, H. Li, and L. Sabirova, “ARTag, AprilTag and CALTag fiducial marker systems: comparison in a presence of partial marker occlusion and rotation,” 2017, pp. 182–191.

[51] A. Sagitov, K. Shabalina, R. Lavrenov, and E. Magid, “Comparing fiducial marker systems in the presence of occlusion,” *2017 Int. Conf. Mech. Syst. Control Eng. ICMSC 2017*, pp. 377–382, 2017.

[52] D. Douglas and T. Peucker, “Algorithms for the reduction of the number of points required to represent a line or its character.,” *The American Cartographer*, pp. 112–123, 1973.

[53] D. B. Dos Santos Cesar, C. Gaudig, M. Fritsche, M. A. Dos Reis, and F. Kirchner, “An evaluation of artificial fiducial markers in underwater environments,” in *MTS/IEEE OCEANS 2015 - Genova: Discovering Sustainable Ocean Energy for a New World*, 2015.

[54] F. J. Romero-Ramirez, R. Muñoz-Salinas, and R. Medina-Carnicer, “Speeded up detection of squared fiducial markers,” *Image Vis. Comput.*, vol. 76, pp. 38–47, 2018.

[55] D. Khan, S. Ullah, and I. Rabbi, “Computer standards & interfaces factors affecting the design and tracking of ARToolKit markers,” *Comput. Stand. Interfaces*, vol. 41, pp. 56–66, 2015.

[56] R. W. Hamming, “Error Detecting and Error Correcting Codes.pdf,” *Bell Syst. Tech. J.*, vol. 29, no. 2, pp. 147–160, 1950.

[57] H. Kato and M. Billinghurst, “Marker tracking and HMD calibration for a video-based augmented reality conferencing system,” in *Proceedings - 2nd IEEE and ACM International Workshop on Augmented Reality, IWAR 1999*, 1999, pp. 85–94.

[58] P. Jin, P. Matikainen, and S. S. Srinivasa, “Sensor fusion for fiducial tags: Highly robust pose estimation from single frame RGBD,” in *IEEE International Conference on Intelligent Robots and Systems*, 2017, vol. 2017-Septe, pp. 5770–5776.

[59] A. Sagitov, K. Shabalina, H. Li, and E. Magid, “Effects of rotation and systematic occlusion on fiducial marker recognition,” *MATEC Web Conf.*, vol. 113, p. 02006, 2017.

[60] M. Badeche and M. Benmohammed, “Classification of the Latin alphabet as Pattern on ARToolkit Markers for Augmented Reality Applications,” *World Acad. Sci. Eng. Technol.*, no. 69, pp. 386–390, 2012.

[61] C. B. Owen, F. Xiao, and P. Middlin, “What is the best fiducial?,” in *ART 2002 - 1st IEEE International Augmented Reality Toolkit Workshop, Proceedings*, 2002, p. 8.

[62] S. Garrido-Jurado, R. Muñoz-Salinas, F. J. Madrid-Cuevas, and M. J. Marín-Jiménez, “Automatic generation and detection of highly reliable fiducial markers under occlusion,” *Pattern Recognit.*, vol. 47, no. 6, pp. 2280–2292, 2014.

[63] R. Bencina, M. Kaltenbrunner, and S. Jorda, “Improved topological fiducial tracking in the reacTIVision System,” in *ieeexplore.ieee.org*, 2006, pp. 99–99.

[64] E. Costanza and J. Robinson, “A region adjacency tree approach to the detection and design of fiducials,” *Video Vis. Graph.*, pp. 63–69, 2003.

[65] A. Xu and G. Dudek, “Fourier tag: A smoothly degradable fiducial marker system with configurable payload capacity,” in *Proceedings - 2011 Canadian Conference on Computer and Robot Vision, CRV 2011*, 2011, pp. 40–47.

[66] F. Bergamasco, A. Albarelli, L. Cosmo, E. Rodola, and A. Torsello, “An accurate and robust artificial marker based on cyclic codes,” *IEEE Trans. Pattern Anal. Mach. Intell.*, vol. 38, no. 12, pp. 2359–2373, Dec. 2016.

[67] F. Bergamasco, A. Albarelli, and A. Torsello, “Pi-Tag: A fast image-space marker design based on projective invariants,” *Mach. Vis. Appl.*, vol. 24, no. 6, pp. 1295–1310, Aug. 2013.

[68] M. P. McEvoy and K. Grimmer, “Reliability of upright posture measurements in primary school children,” *BMC Musculoskelet. Disord.*, vol. 6, no. 1, p. 35, Dec. 2005.

[69] C. J. Goldberg, M. Kaliszer, D. P. Moore, E. E. Fogarty, and F. E. Dowling, “Surface topography, Cobb angles, and cosmetic change in scoliosis.,” *Spine (Phila. Pa. 1976).*, vol. 26, no. 4, pp. E55-63, 2001.

[70] P. Roussouly, S. Gollogly, E. Berthonnaud, and J. Dimnet, “Classification of the normal variation in the sagittal alignment of the human lumbar spine and pelvis in the standing position,” *Spine (Phila. Pa. 1976).*, vol. 30, no. 3, pp. 346–353, Feb. 2005.

[71] D. A. Krause, M. S. Boyd, A. N. Hager, E. C. Smoyer, A. T. Thompson, and J. H. Hollman, “Reliability and accuracy of a goniometer mobile device application for video measurement of the functional movement screen deep squat test.,” *Int. J. Sports Phys. Ther.*, vol. 10, no. 1, pp. 37–44, Feb. 2015.

[72] B. B. *et al.*, “Validity and reliability of the Kinect within functional assessment activities: Comparison with standard stereophotogrammetry,” *Gait Posture*, vol. 39, no. 1, pp. 593–598, 2014.

[73] C. E. Mgbemena, A. Tiwari, Y. Xu, J. Oyekan, and W. Hutabarat, “Ergonomic assessment tool for real-time risk assessment of seated work postures,” in *Advances in Intelligent Systems and Computing*, 2018, vol. 604, pp. 423–434.

[74] S. Basiratzadeh, E. D. Lemaire, M. Dorrikhteh, and N. Baddour, “Fiducial marker approach for biomechanical smartphone-based measurements,” in *2019 3rd International Conference on Bio-engineering for Smart Technologies (BioSMART)*, 2019, pp. 1–4.

[75] N. Shah, R. Aleong, and I. So, “Novel Use of a Smartphone to Measure Standing Balance,” *JMIR Rehabil. Assist. Technol.*, vol. 3, no. 1, p. e4, 2016.

[76] E. Lemaire, “Biomechanics Augmented Reality - Apps on Google Play.” [Online]. Available: https://play.google.com/store/apps/details?id=ca.irrd.bar&hl=en. [Accessed: 24-May-2019].

[77] J. Kim and H. Jun, “Implementation of image processing and augmented reality programs for smart mobile device,” in *Proceedings of the 6th International Forum on Strategic Technology, IFOST 2011*, 2011, vol. 2, pp. 1070–1073.

[78] E. Lemaire, “A shockwave approach for web-based clinical motion analysis,” *Telemed. J. e-Health*, vol. 10, no. 1, pp. 39–43, Mar. 2004.

[79] M. H. Schwartz, J. P. Trost, and R. A. Wervey, “Measurement and management of errors in quantitative gait data,” *Gait Posture*, vol. 20, no. 2, pp. 196–203, 2004.

[80] M. El-Gohary and J. McNames, “Shoulder and elbow joint angle tracking with inertial sensors,” *IEEE Trans. Biomed. Eng.*, vol. 59, no. 9, pp. 2635–2641, Sep. 2012.

[81] G. E. Hancock, T. Hepworth, and K. Wembridge, “Accuracy and reliability of knee goniometry methods,” *J. Exp. Orthop.*, vol. 5, no. 1, p. 46, Dec. 2018.

[82] A. M. Olsen, “Posture and body movement perception,” *Acta Psychol. (Amst).*, vol. 19, pp. 820–821, Mar. 2007.

[83] U. Della Croce, A. Leardini, L. Chiari, and A. Cappozzo, “Human movement analysis using stereophotogrammetry Part 4: Assessment of anatomical landmark misplacement and its effects on joint kinematics,” *Gait and Posture*, vol. 21, no. 2. Elsevier, pp. 226–237, 01-Feb-2005.

[84] A. Peters, B. Galna, M. Sangeux, M. Morris, and R. Baker, “Quantification of soft tissue artifact in lower limb human motion analysis: A systematic review,” *Gait and Posture*, vol. 31, no. 1. Elsevier, pp. 1–8, 01-Jan-2010.

[85] M. Krogius, A. Haggenmiller, and E. Olson, “Flexible layouts for fiducial tags,” 2019.

Appendix A

This section presents human evaluation stored data. The overall human evaluation included pelvis obliquity, shoulder angle and arm-abduction angle measurement for 15 healthy people (10 trials for suject) from Vicon system, mobile app, and prosthetist AR reading (pelvis and shoulder measurements). The connected lines between points show trends and patterns between trials.

Pelvis obliquity

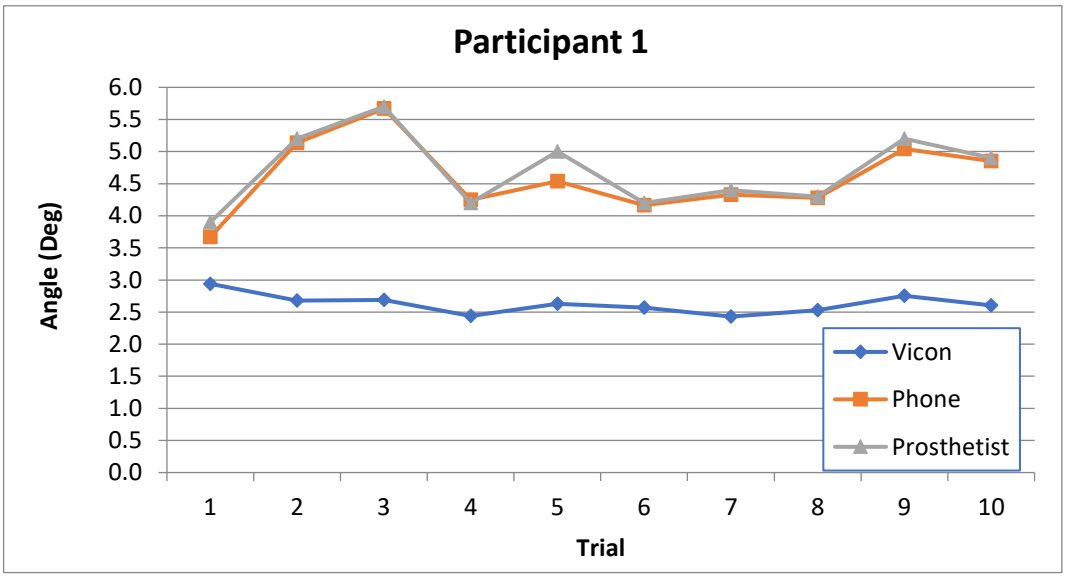

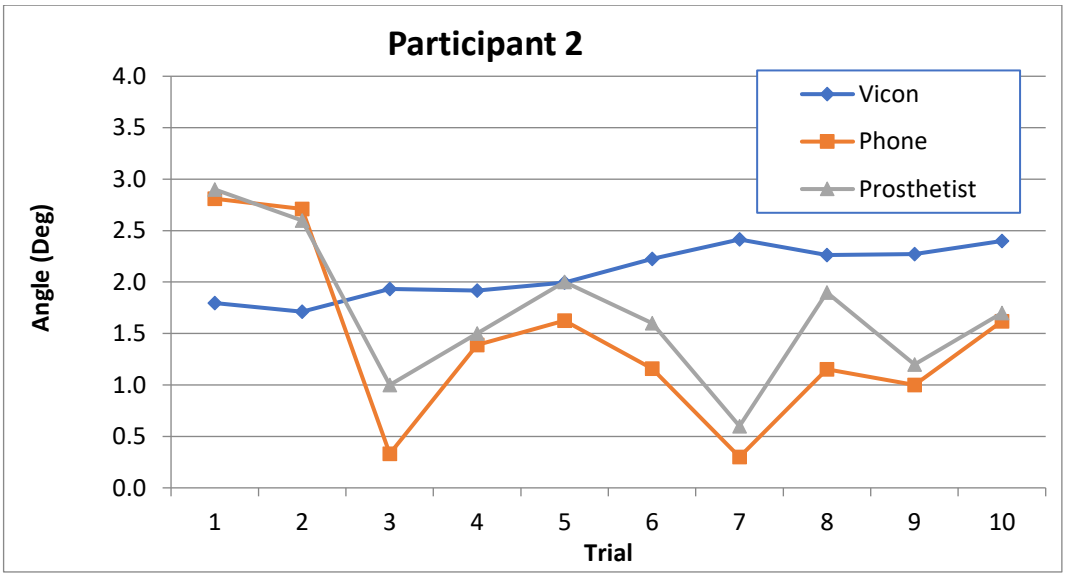

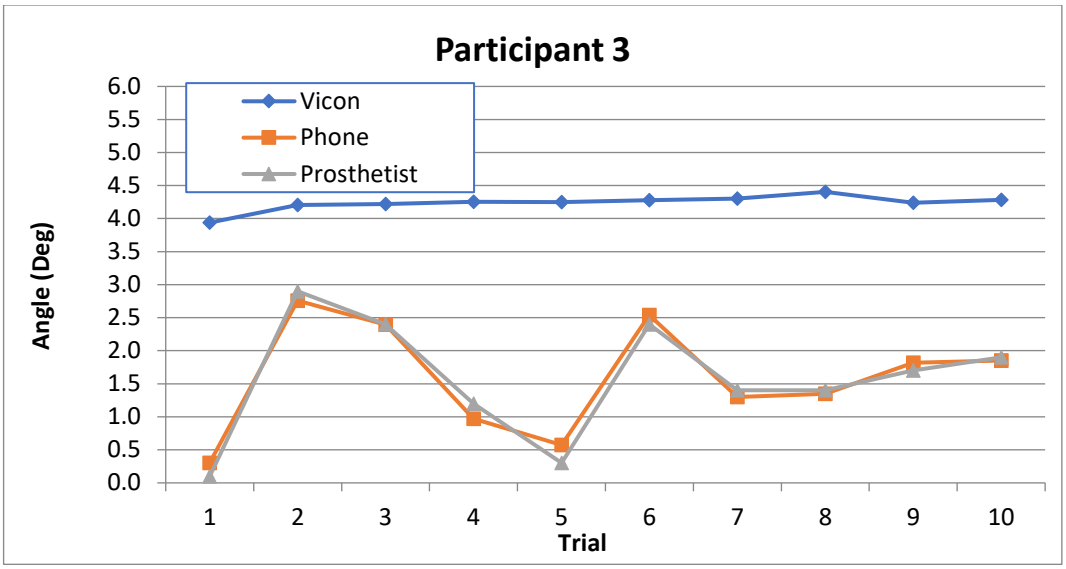
Participant 3
Vicon
Phone
Prosthetist
Angle (Deg)
6.0
5.5
5.0
4.5
4.0
3.5
3.0
2.5
2.0
1.5
1.0
0.5
0.0
1
2
3
4
5
6
7
8
9
10
Trial

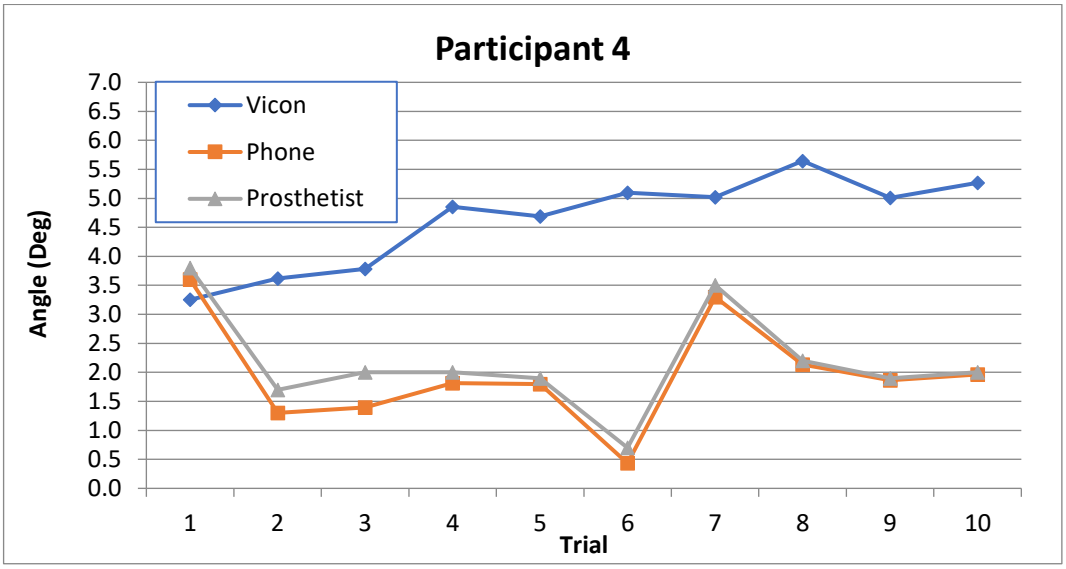
Participant 4
Vicon
Phone
Prosthetist
Angle (Deg)
7.0
6.5
6.0
5.5
5.0
4.5
4.0
3.5
3.0
2.5
2.0
1.5
1.0
0.5
0.0
1
2
3
4
5
6
7
8
9
10
Trial

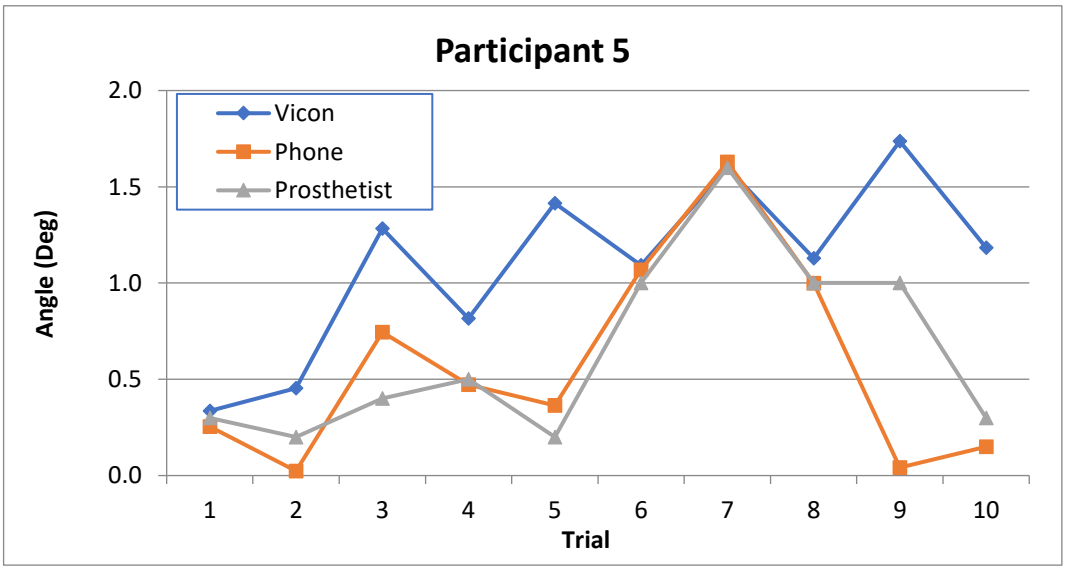
Participant 5
Vicon
Phone
Prosthetist
Angle (Deg)
2.0
1.5
1.0
0.5
0.0
1
2
3
4
5
6
7
8
9
10
Trial

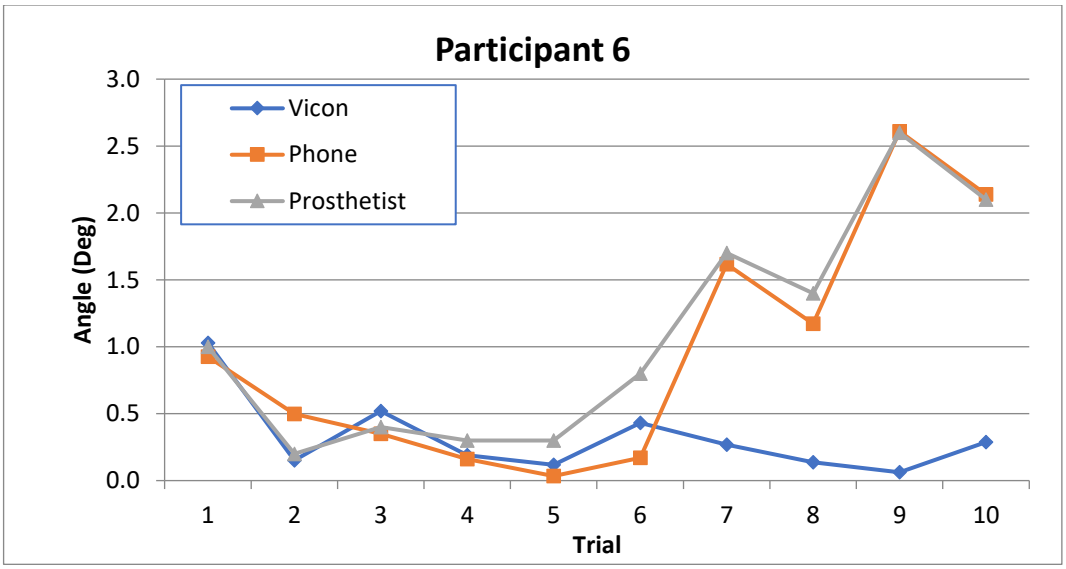
Participant 6
Vicon
Phone
Prosthetist
Angle (Deg)
3.0
2.5
2.0
1.5
1.0
0.5
0.0
1
2
3
4
5
6
7
8
9
10
Trial

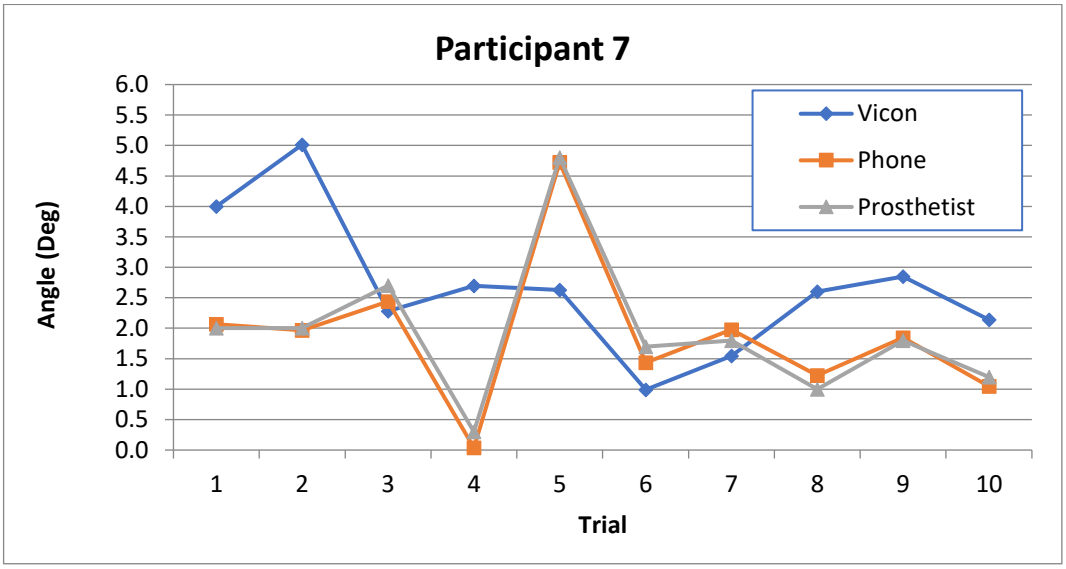
Participant 7
Vicon
Phone
Prosthetist
Angle (Deg)
6.0
5.5
5.0
4.5
4.0
3.5
3.0
2.5
2.0
1.5
1.0
0.5
0.0
1
2
3
4
5
6
7
8
9
10
Trial

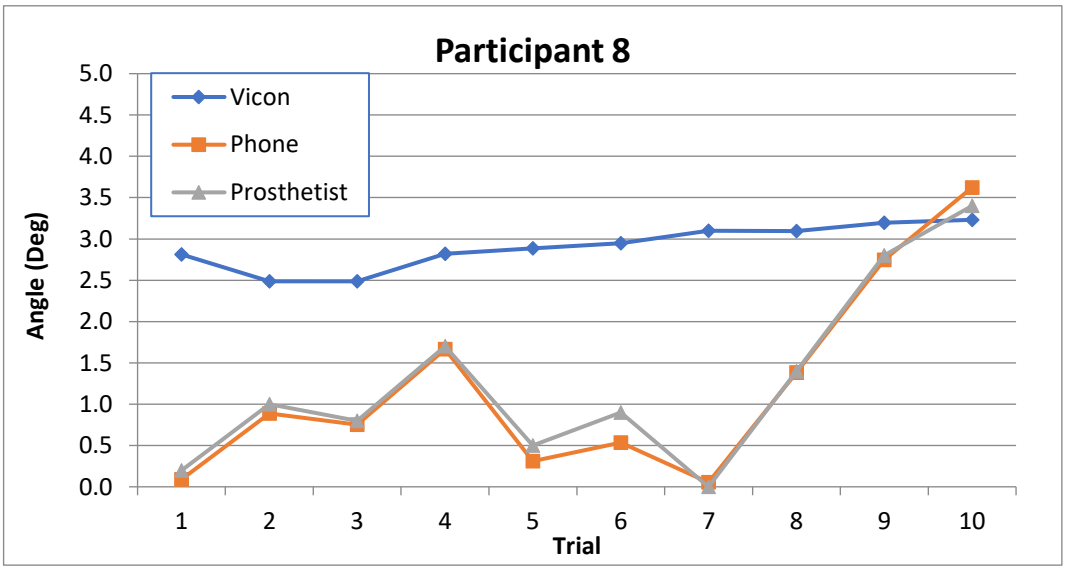
Participant 8
Vicon
Phone
Prosthetist
Angle (Deg)
5.0
4.5
4.0
3.5
3.0
2.5
2.0
1.5
1.0
0.5
0.0
1
2
3
4
5
6
7
8
9
10
Trial

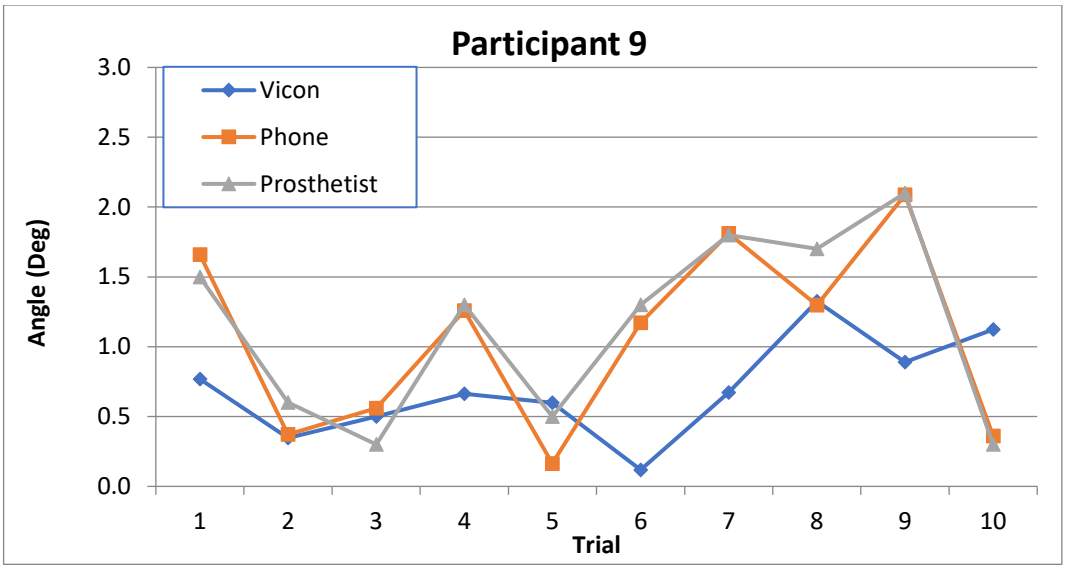
Participant 9
Vicon
Phone
Prosthetist
Angle (Deg)
3.0
2.5
2.0
1.5
1.0
0.5
0.0
1
2
3
4
5
6
7
8
9
10
Trial

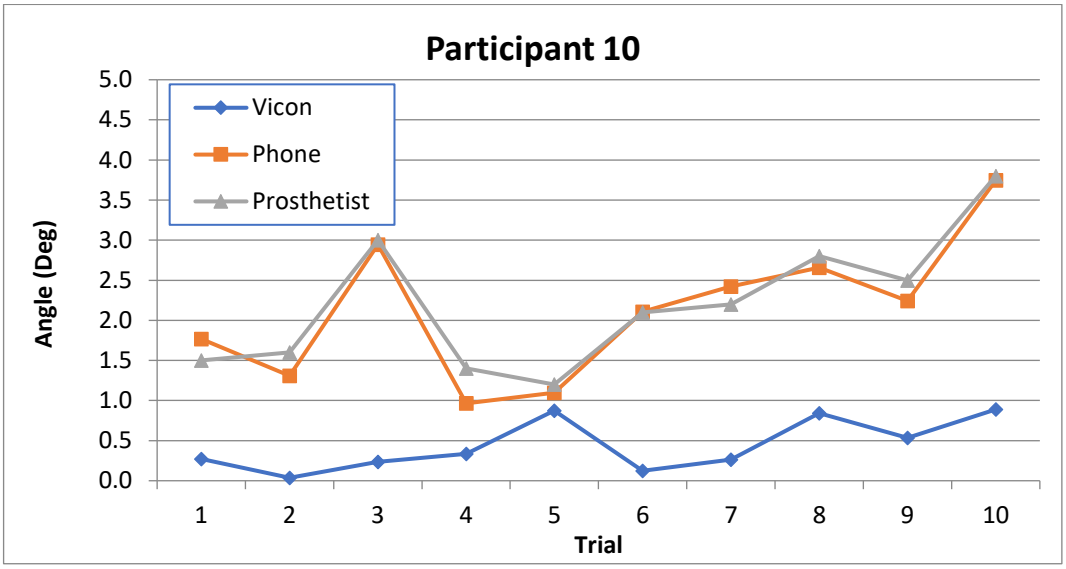
Participant 10
Vicon
Phone
Prosthetist
Angle (Deg)
5.0
4.5
4.0
3.5
3.0
2.5
2.0
1.5
1.0
0.5
0.0
1
2
3
4
5
6
7
8
9
10
Trial

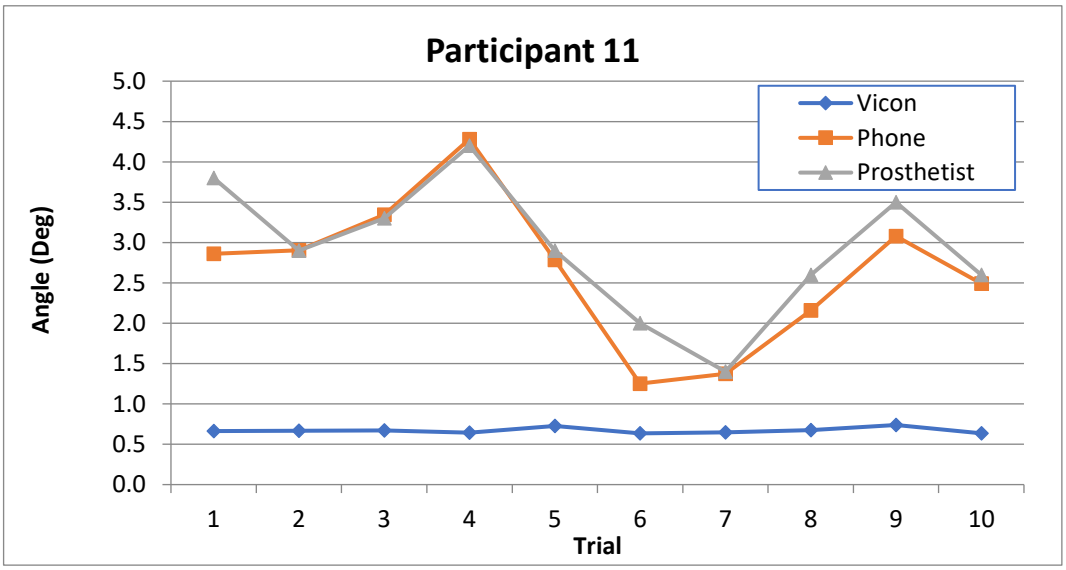
Participant 11
Vicon
Phone
Prosthetist
Angle (Deg)
5.0
4.5
4.0
3.5
3.0
2.5
2.0
1.5
1.0
0.5
0.0
1
2
3
4
5
6
7
8
9
10
Trial

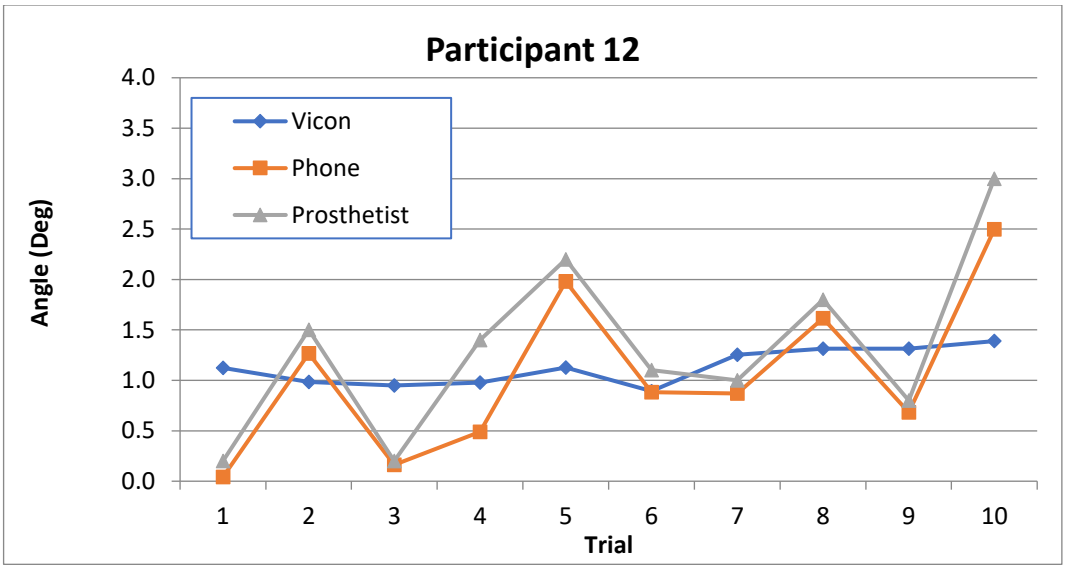
Participant 12
Angle (Deg)
4.0
3.5
3.0
2.5
2.0
1.5
1.0
0.5
0.0
Vicon
Phone
Prosthetist
1
2
3
4
5
6
7
8
9
10
Trial

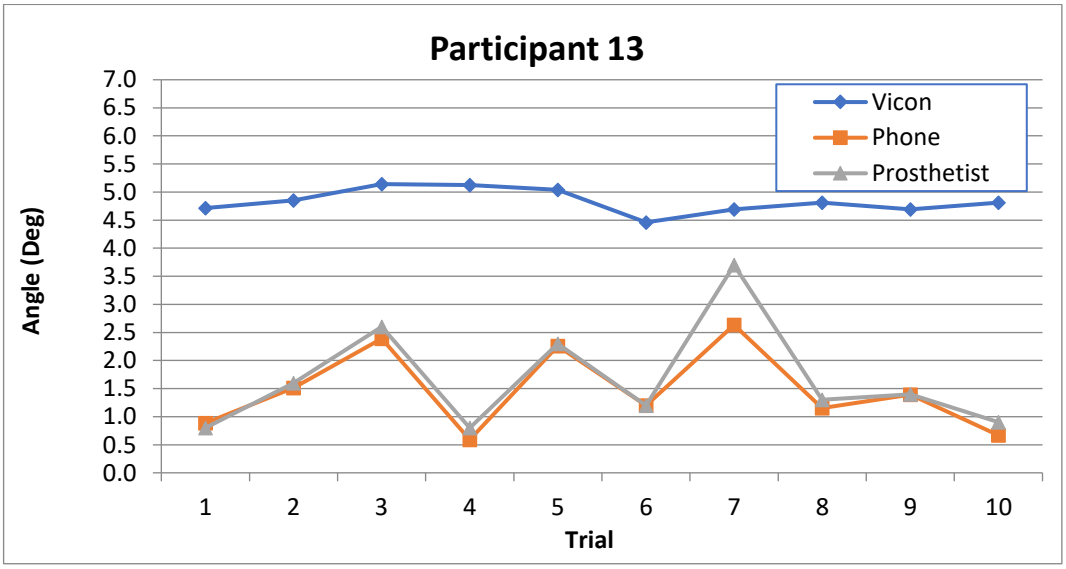
Participant 13
Angle (Deg)
7.0
6.5
6.0
5.5
5.0
4.5
4.0
3.5
3.0
2.5
2.0
1.5
1.0
0.5
0.0
Vicon
Phone
Prosthetist
1
2
3
4
5
6
7
8
9
10
Trial

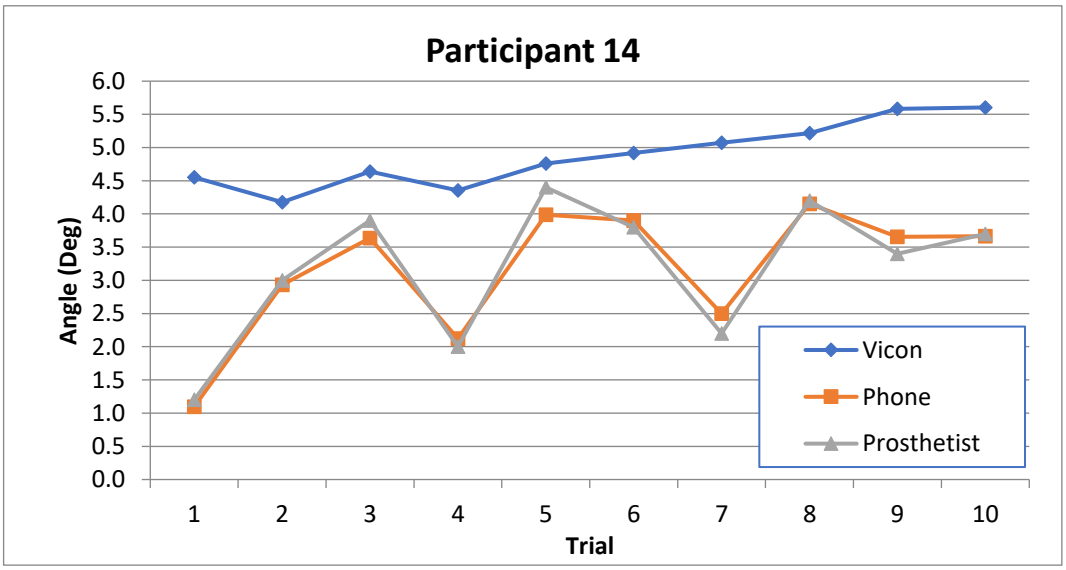
Participant 14
Angle (Deg)
6.0
5.5
5.0
4.5
4.0
3.5
3.0
2.5
2.0
1.5
1.0
0.5
0.0
Vicon
Phone
Prosthetist
1
2
3
4
5
6
7
8
9
10
Trial

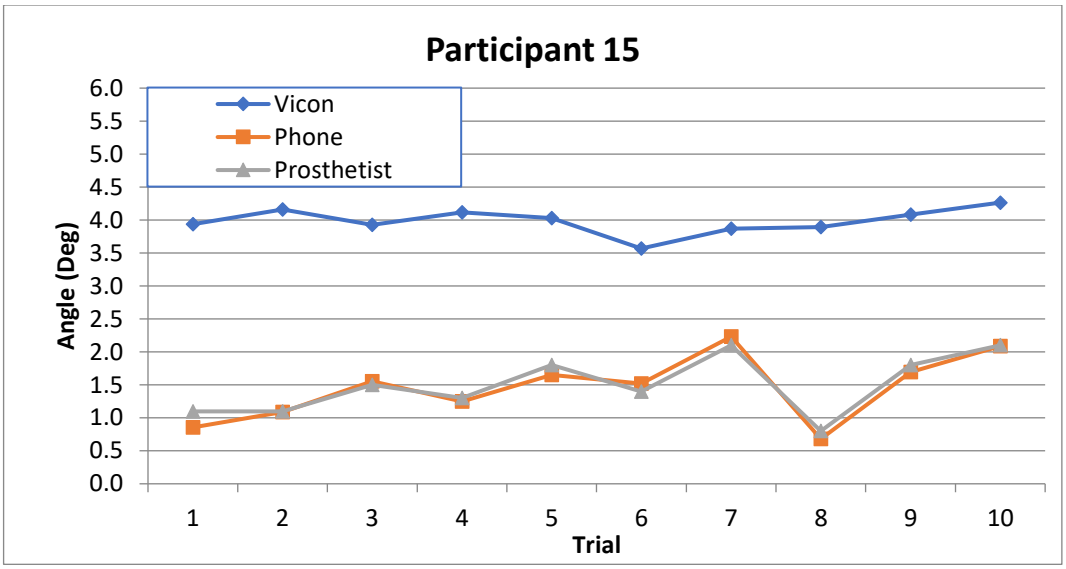
Participant 15
Vicon
Phone
Prosthetist
Angle (Deg)
6.0
5.5
5.0
4.5
4.0
3.5
3.0
2.5
2.0
1.5
1.0
0.5
0.0
1
2
3
4
5
6
7
8
9
10
Trial

Shoulder

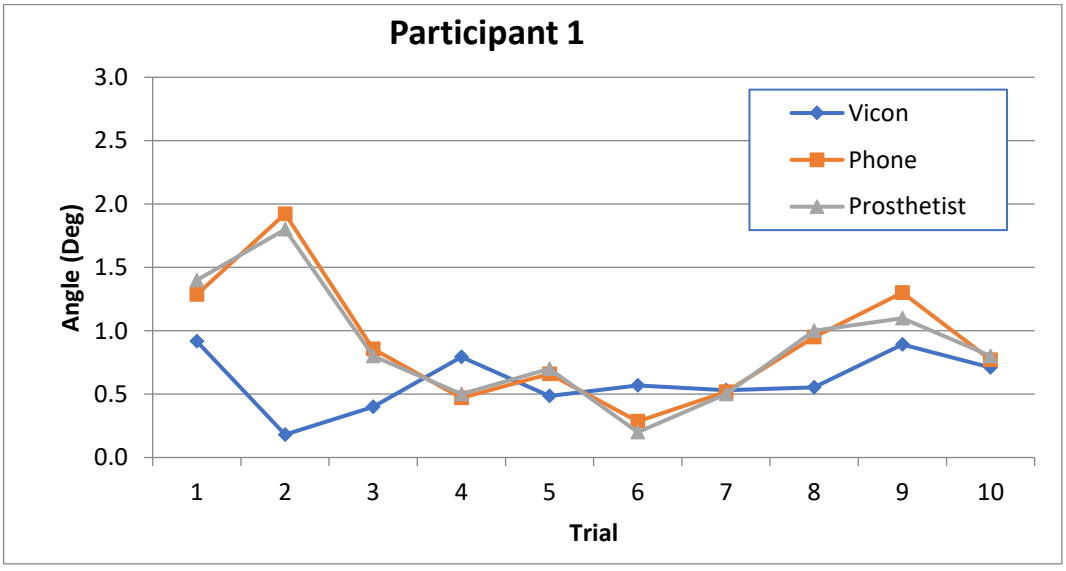
Participant 1
Vicon
Phone
Prosthetist
Angle (Deg)
3.0
2.5
2.0
1.5
1.0
0.5
0.0
1
2
3
4
5
6
7
8
9
10
Trial

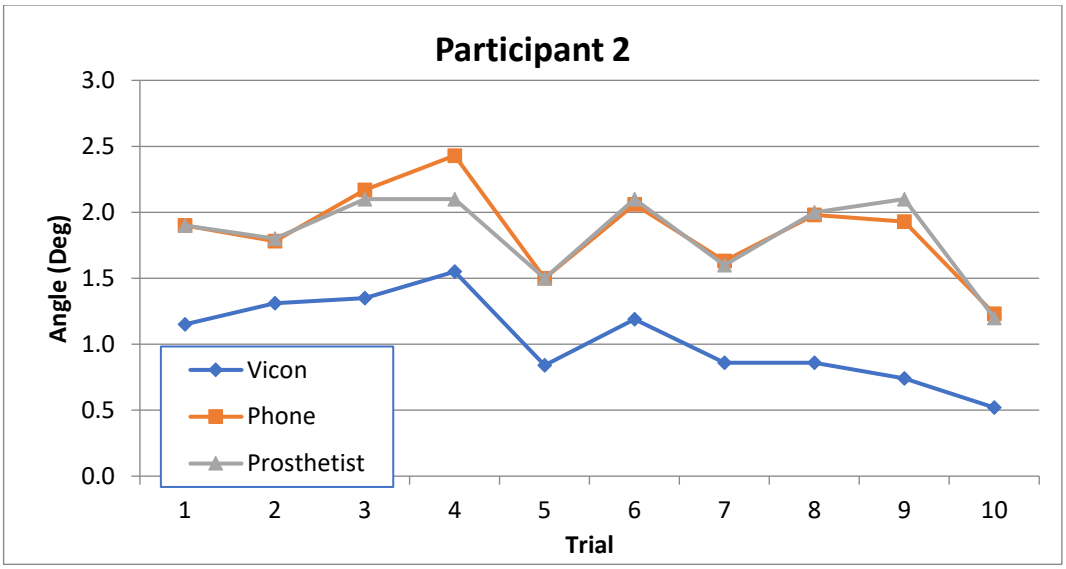
Participant 2
Angle (Deg)
3.0
2.5
2.0
1.5
1.0
0.5
0.0
Vicon
Phone
Prosthetist
1
2
3
4
5
6
7
8
9
10
Trial

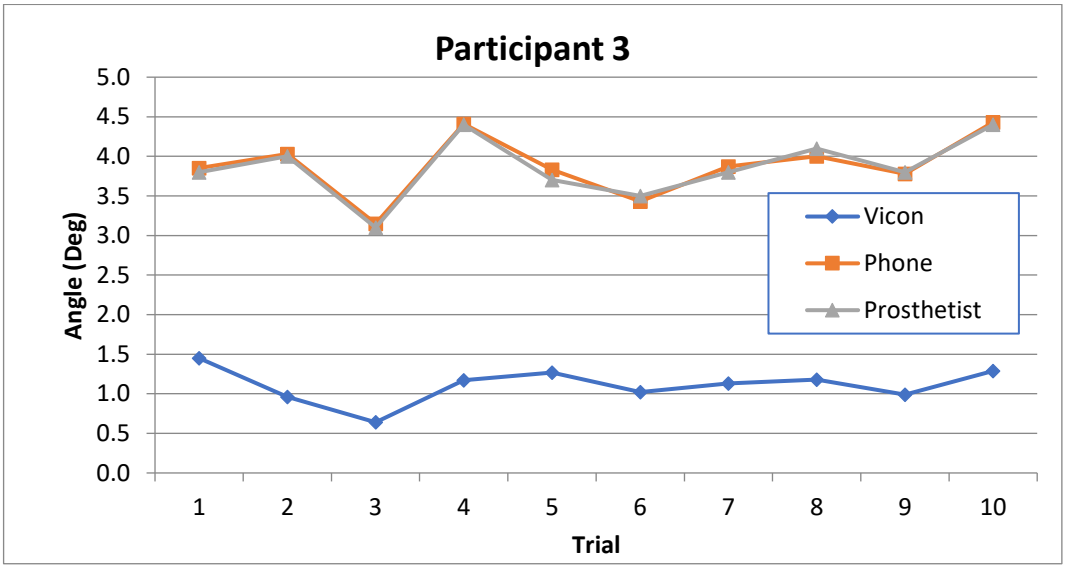
Participant 3
Angle (Deg)
5.0
4.5
4.0
3.5
3.0
2.5
2.0
1.5
1.0
0.5
0.0
Vicon
Phone
Prosthetist
1
2
3
4
5
6
7
8
9
10
Trial

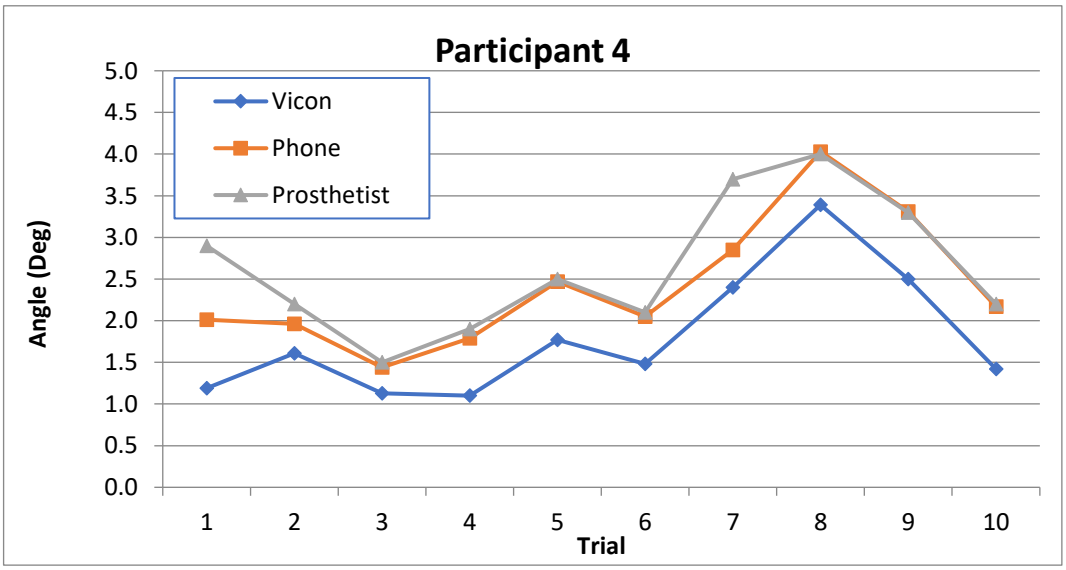
Participant 4
Angle (Deg)
5.0
4.5
4.0
3.5
3.0
2.5
2.0
1.5
1.0
0.5
0.0
Vicon
Phone
Prosthetist
1
2
3
4
5
6
7
8
9
10
Trial

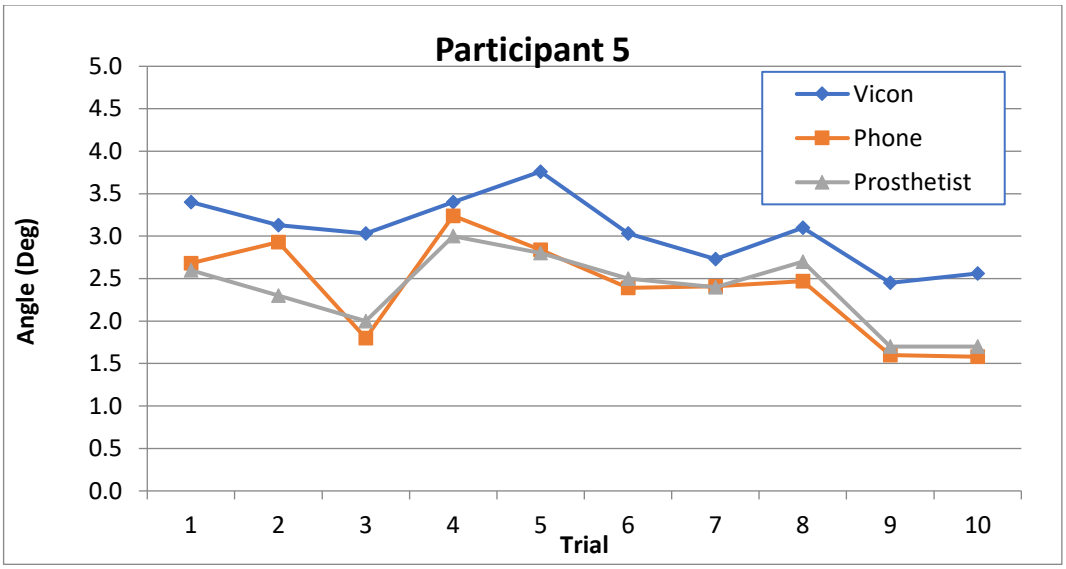
Participant 5
Angle (Deg)
5.0
4.5
4.0
3.5
3.0
2.5
2.0
1.5
1.0
0.5
0.0
1
2
3
4
5
6
7
8
9
10
Trial
Vicon
Phone
Prosthetist

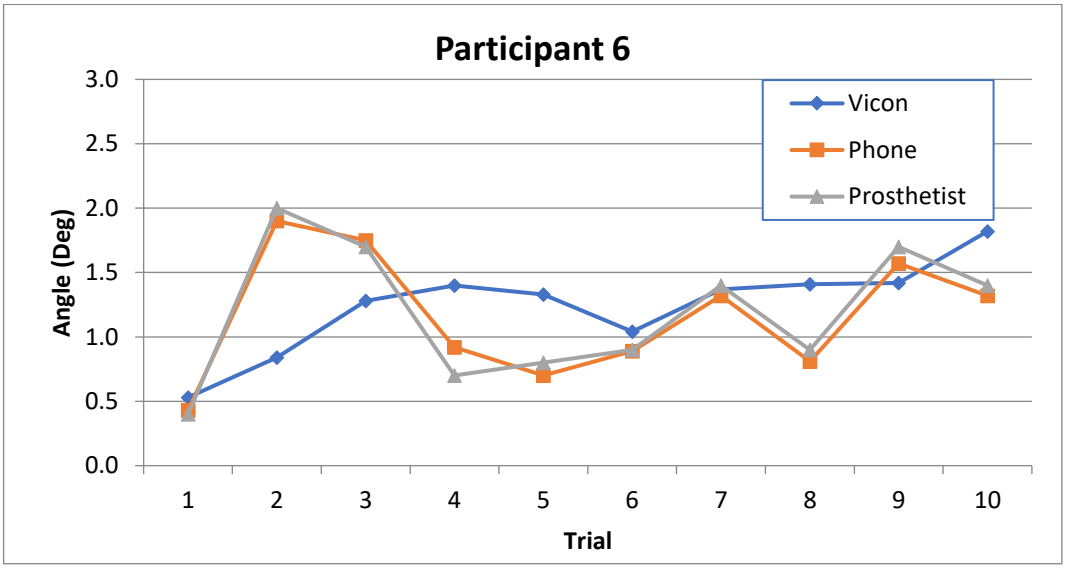
Participant 6
Angle (Deg)
3.0
2.5
2.0
1.5
1.0
0.5
0.0
1
2
3
4
5
6
7
8
9
10
Trial
Vicon
Phone
Prosthetist

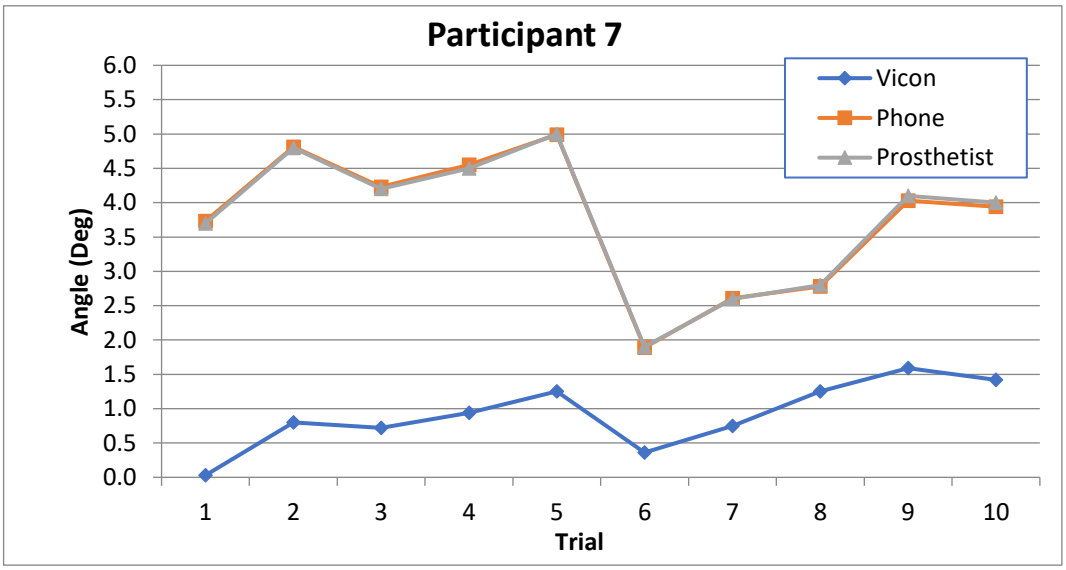
Participant 7
Angle (Deg)
6.0
5.5
5.0
4.5
4.0
3.5
3.0
2.5
2.0
1.5
1.0
0.5
0.0
1
2
3
4
5
6
7
8
9
10
Trial
Vicon
Phone
Prosthetist

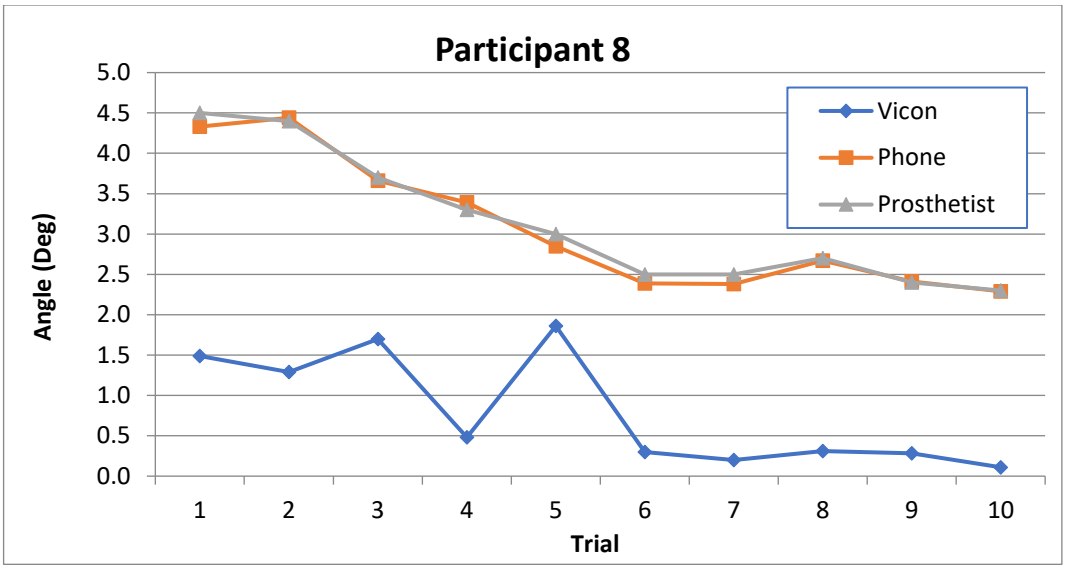
Participant 8
Angle (Deg)
5.0
4.5
4.0
3.5
3.0
2.5
2.0
1.5
1.0
0.5
0.0
1
2
3
4
5
6
7
8
9
10
Trial
Vicon
Phone
Prosthetist

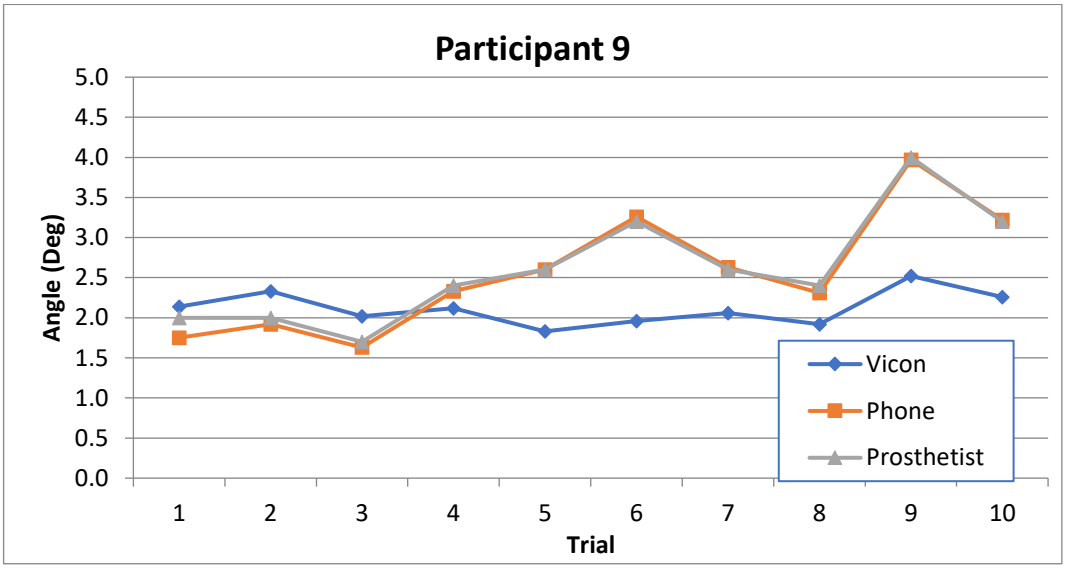
Participant 9
Angle (Deg)
5.0
4.5
4.0
3.5
3.0
2.5
2.0
1.5
1.0
0.5
0.0
1
2
3
4
5
6
7
8
9
10
Trial
Vicon
Phone
Prosthetist

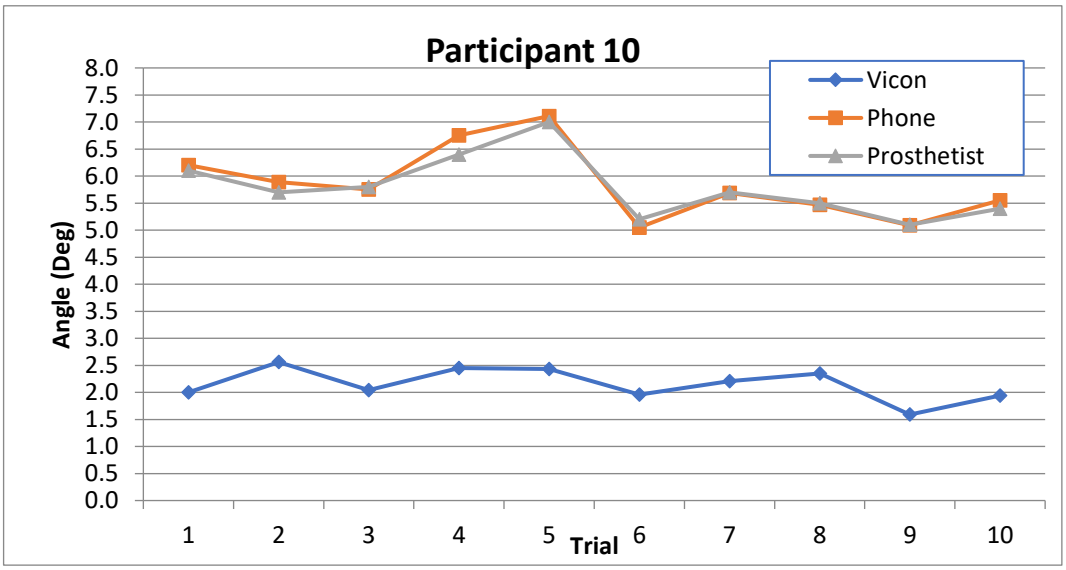
Participant 10
Angle (Deg)
8.0
7.5
7.0
6.5
6.0
5.5
5.0
4.5
4.0
3.5
3.0
2.5
2.0
1.5
1.0
0.5
0.0
1
2
3
4
5
6
7
8
9
10
Trial
Vicon
Phone
Prosthetist

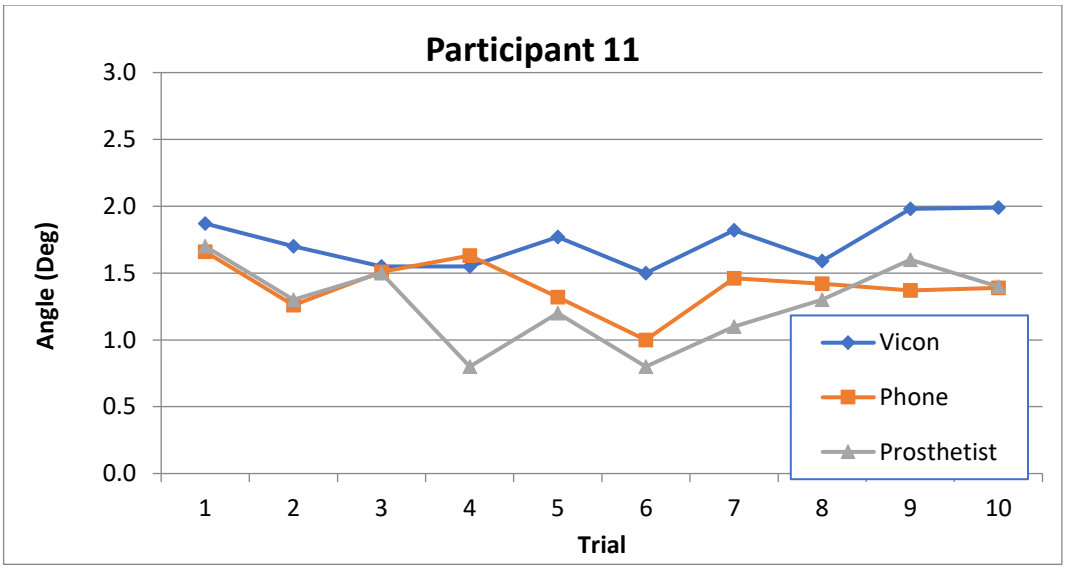
Participant 11
Angle (Deg)
3.0
2.5
2.0
1.5
1.0
0.5
0.0
1
2
3
4
5
6
7
8
9
10
Trial
Vicon
Phone
Prosthetist

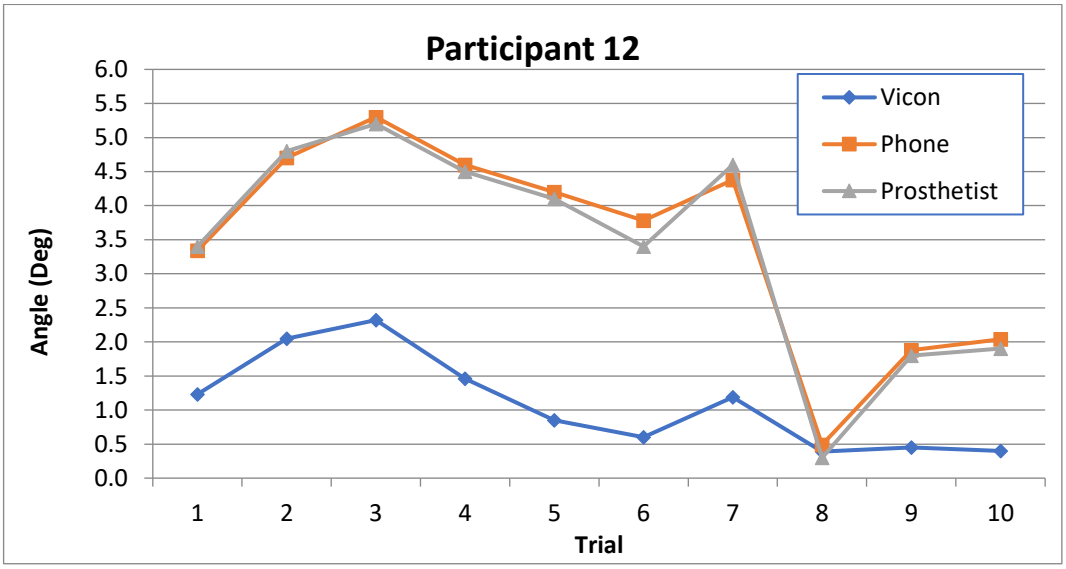
Participant 12
Angle (Deg)
6.0
5.5
5.0
4.5
4.0
3.5
3.0
2.5
2.0
1.5
1.0
0.5
0.0
1
2
3
4
5
6
7
8
9
10
Trial
Vicon
Phone
Prosthetist

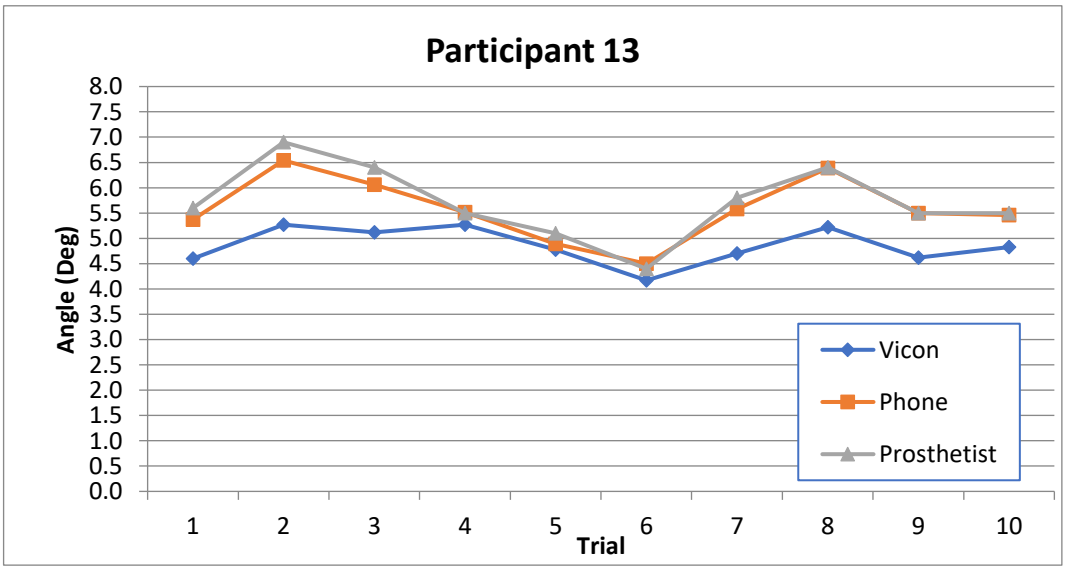
Participant 13
Angle (Deg)
8.0
7.5
7.0
6.5
6.0
5.5
5.0
4.5
4.0
3.5
3.0
2.5
2.0
1.5
1.0
0.5
0.0
1
2
3
4
5
6
7
8
9
10
Trial
Vicon
Phone
Prosthetist

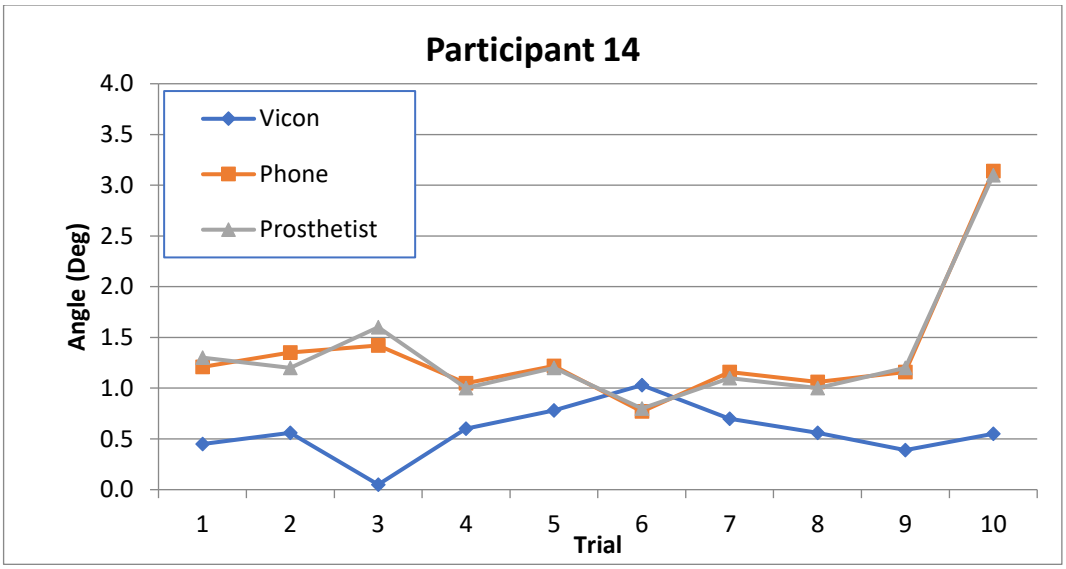

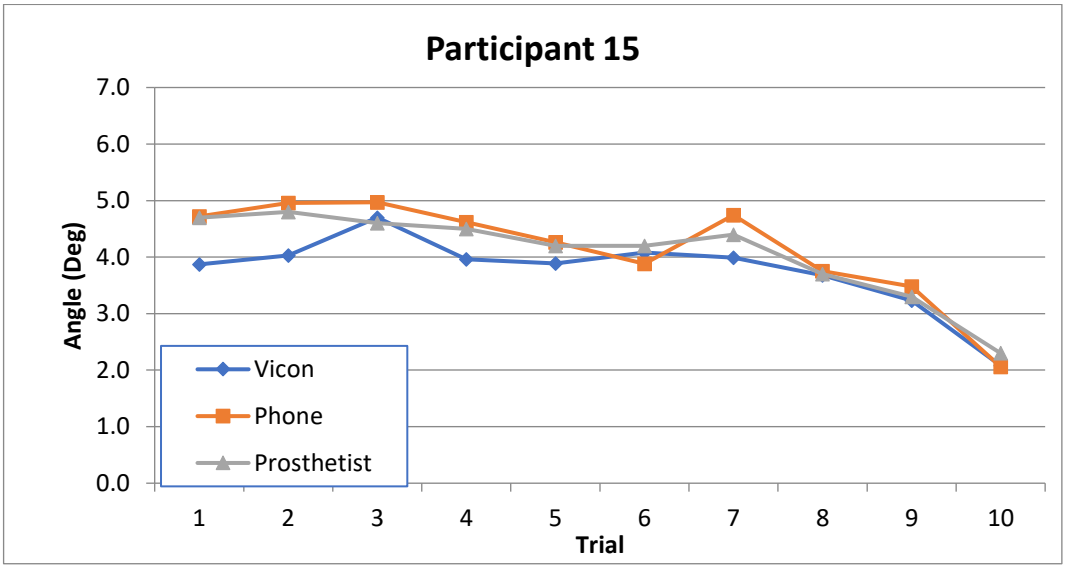

Arm abduction

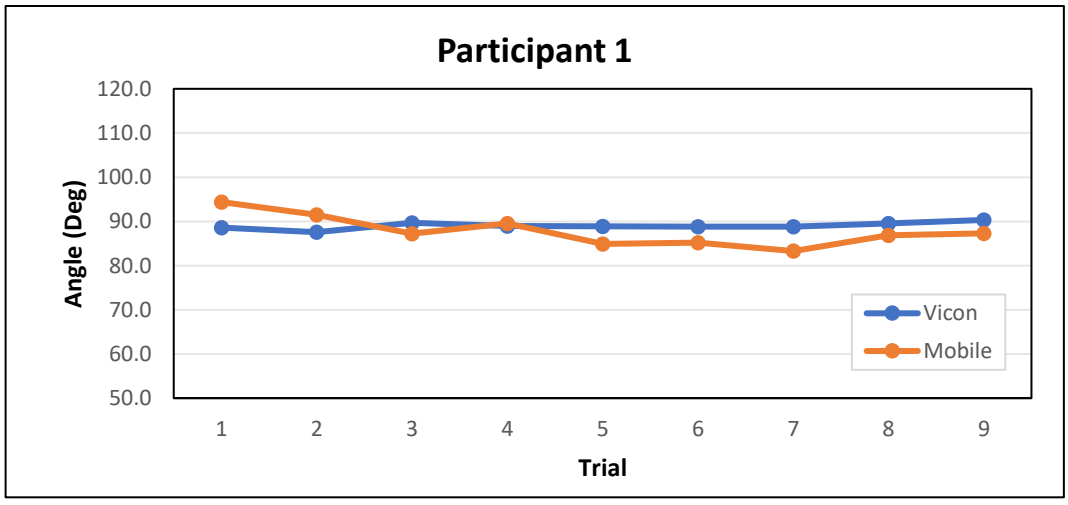

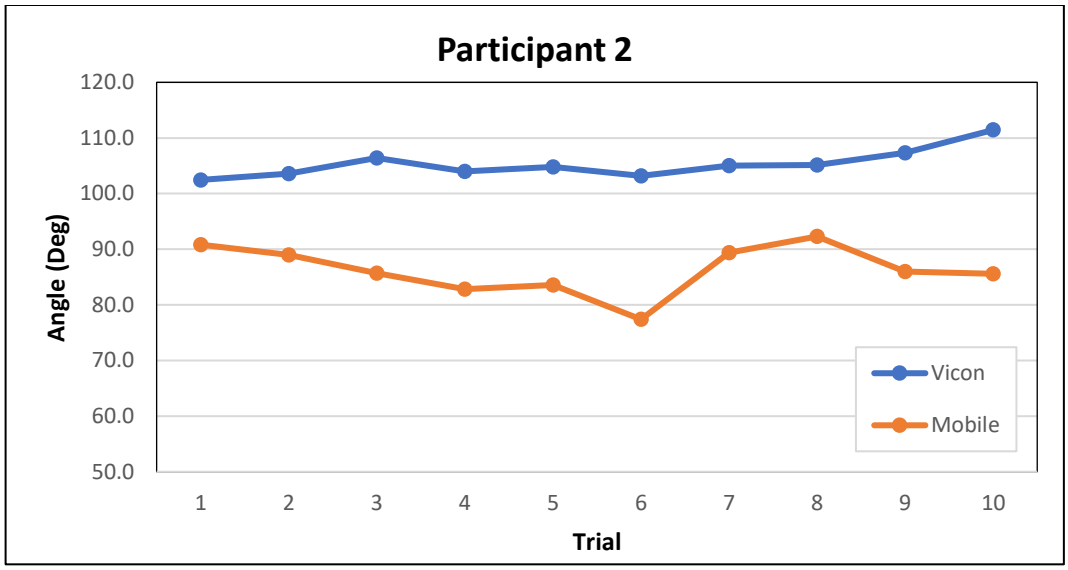
Participant 2
120.0
110.0
100.0
90.0
80.0
70.0
60.0
50.0
Angle (Deg)
1
2
3
4
5
6
7
8
9
10
Trial
Vicon
Mobile

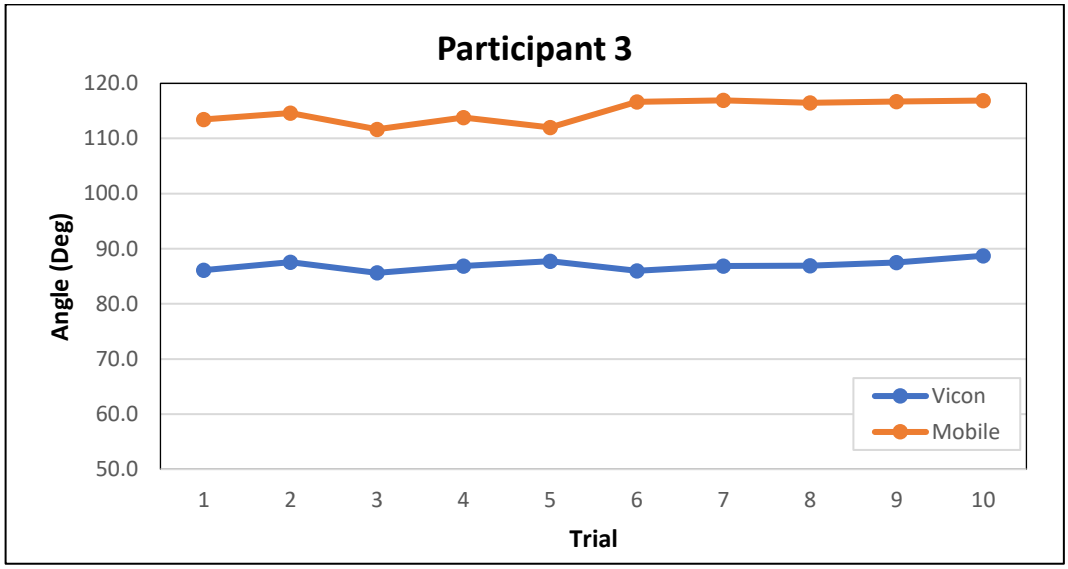
Participant 3
120.0
110.0
100.0
90.0
80.0
70.0
60.0
50.0
Angle (Deg)
1
2
3
4
5
6
7
8
9
10
Trial
Vicon
Mobile

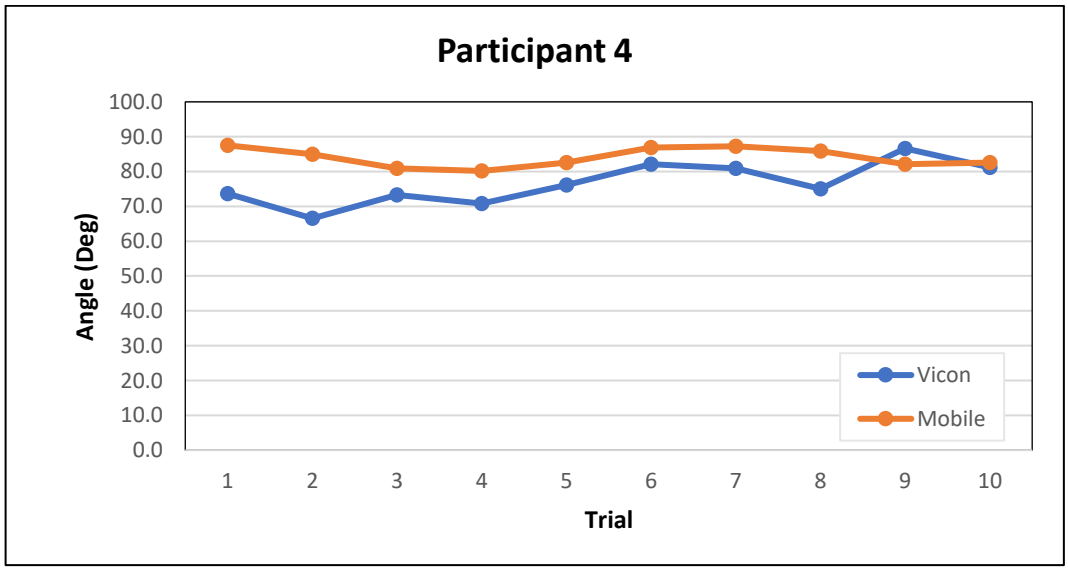
Participant 4
100.0
90.0
80.0
70.0
60.0
50.0
40.0
30.0
20.0
10.0
0.0
Angle (Deg)
1
2
3
4
5
6
7
8
9
10
Trial
Vicon
Mobile

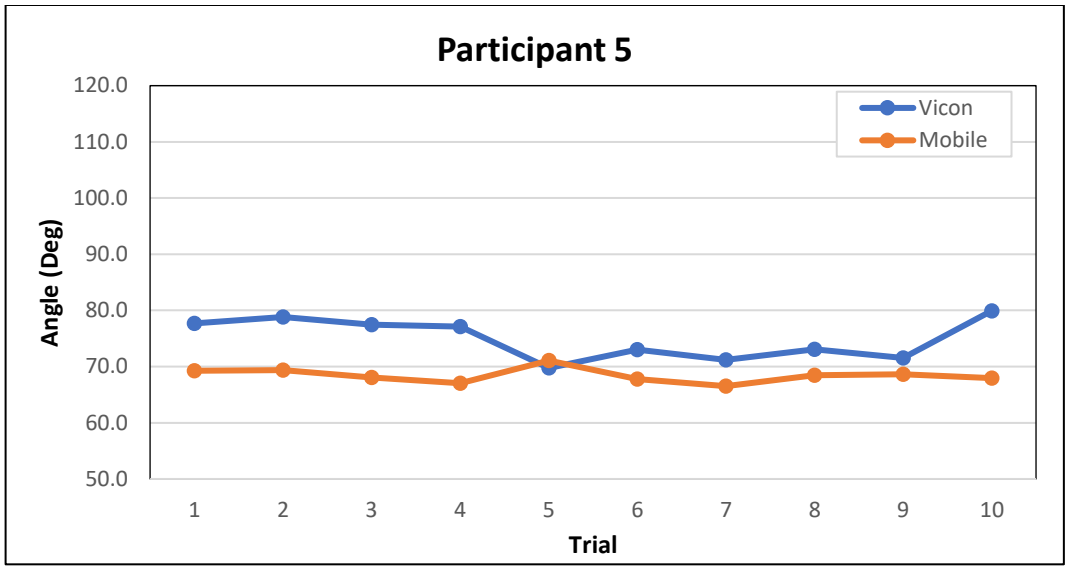
Participant 5
120.0
110.0
100.0
90.0
80.0
70.0
60.0
50.0
Angle (Deg)
Vicon
Mobile
1
2
3
4
5
6
7
8
9
10
Trial

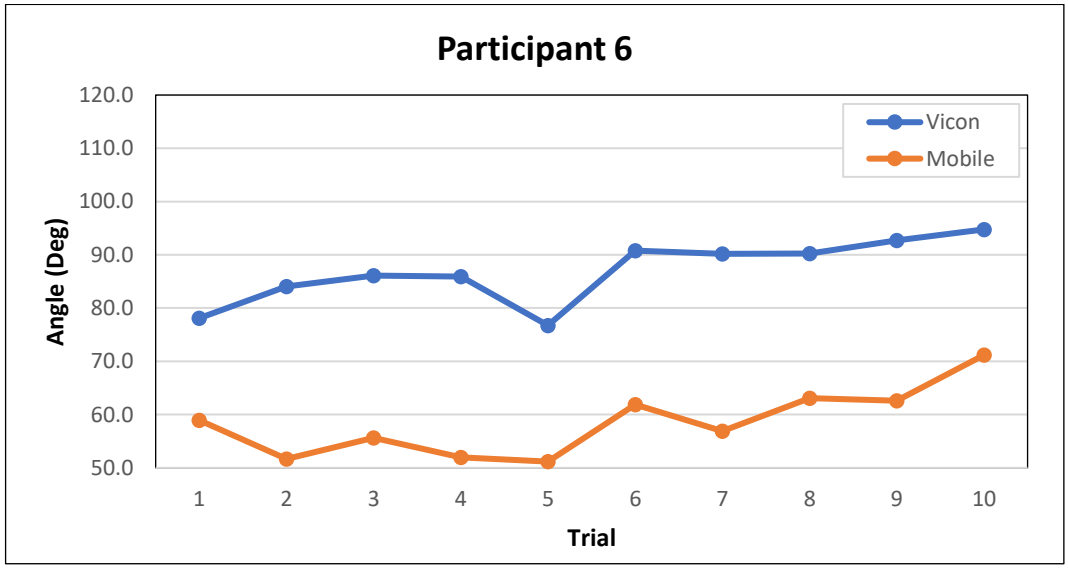
Participant 6
120.0
110.0
100.0
90.0
80.0
70.0
60.0
50.0
Angle (Deg)
Vicon
Mobile
1
2
3
4
5
6
7
8
9
10
Trial

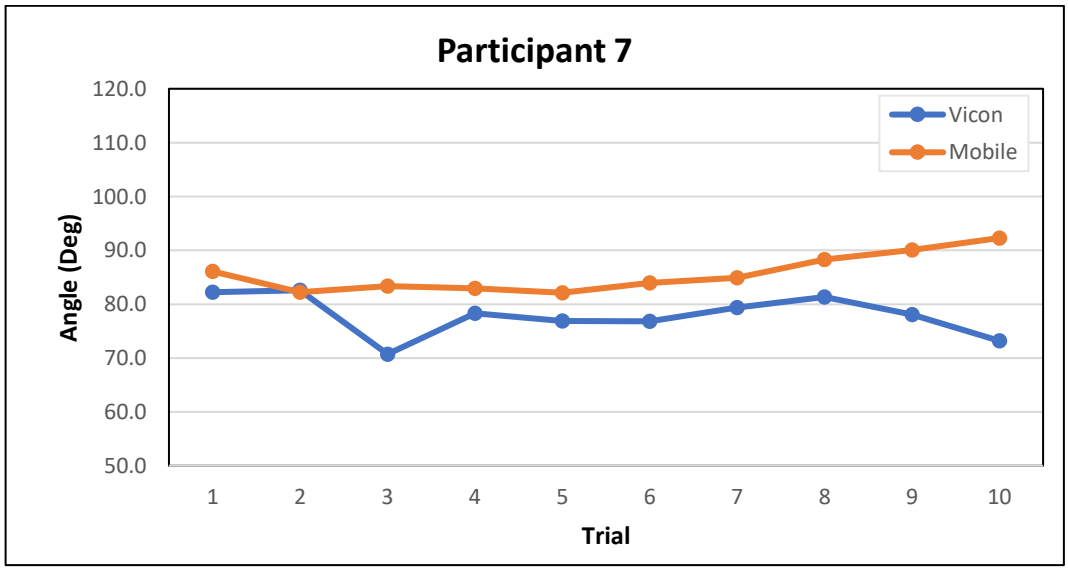
Participant 7
120.0
110.0
100.0
90.0
80.0
70.0
60.0
50.0
Angle (Deg)
Vicon
Mobile
1
2
3
4
5
6
7
8
9
10
Trial

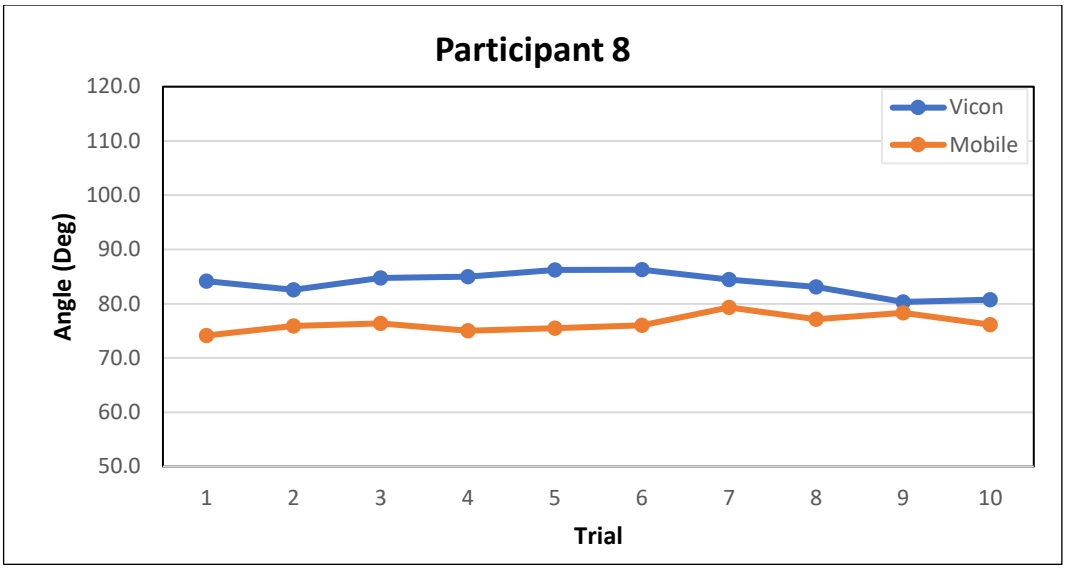
Participant 8
120.0
110.0
100.0
90.0
80.0
70.0
60.0
50.0
Angle (Deg)
1
2
3
4
5
6
7
8
9
10
Trial
Vicon
Mobile

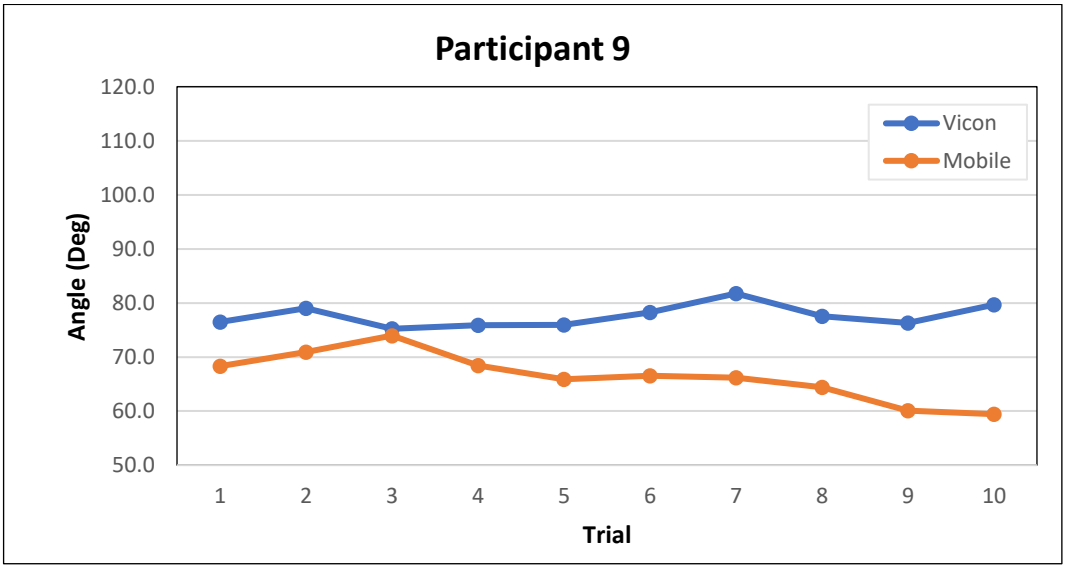
Participant 9
120.0
110.0
100.0
90.0
80.0
70.0
60.0
50.0
Angle (Deg)
1
2
3
4
5
6
7
8
9
10
Trial
Vicon
Mobile

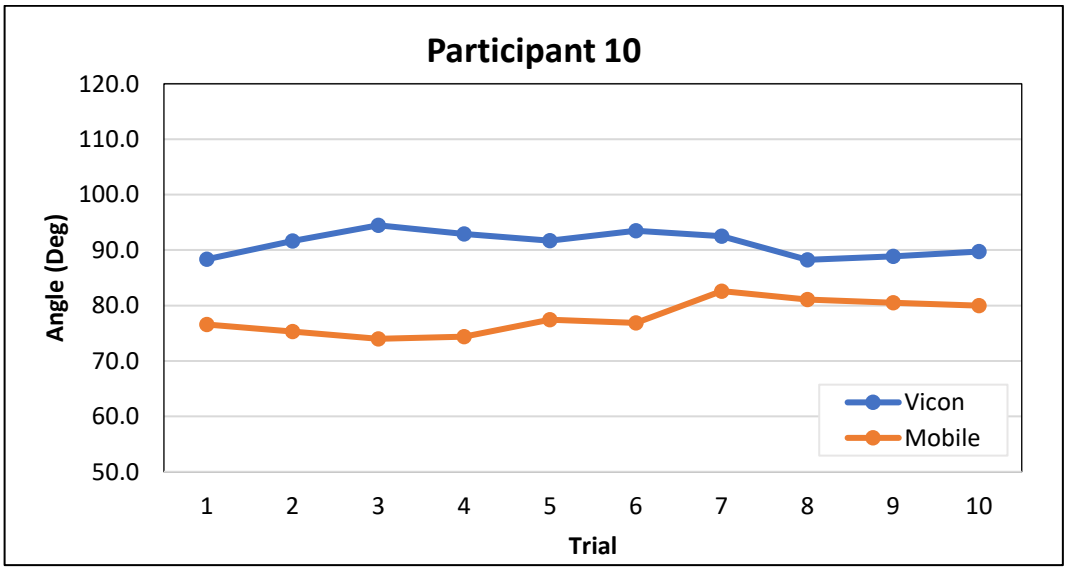
Participant 10
120.0
110.0
100.0
90.0
80.0
70.0
60.0
50.0
Angle (Deg)
1
2
3
4
5
6
7
8
9
10
Trial
Vicon
Mobile

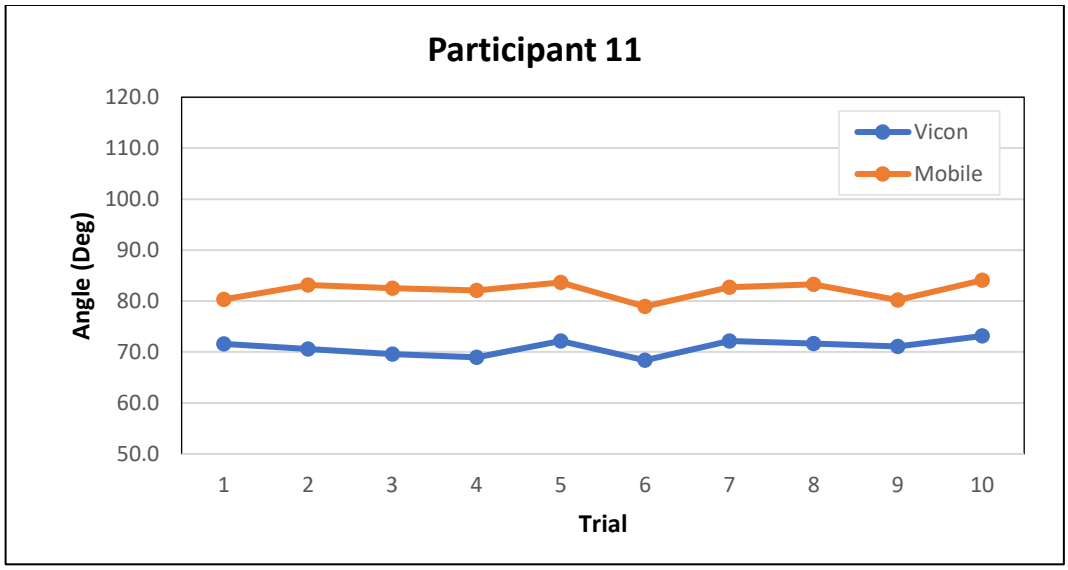
Participant 11
120.0
110.0
100.0
90.0
80.0
70.0
60.0
50.0
Angle (Deg)
Vicon
Mobile
1
2
3
4
5
6
7
8
9
10
Trial

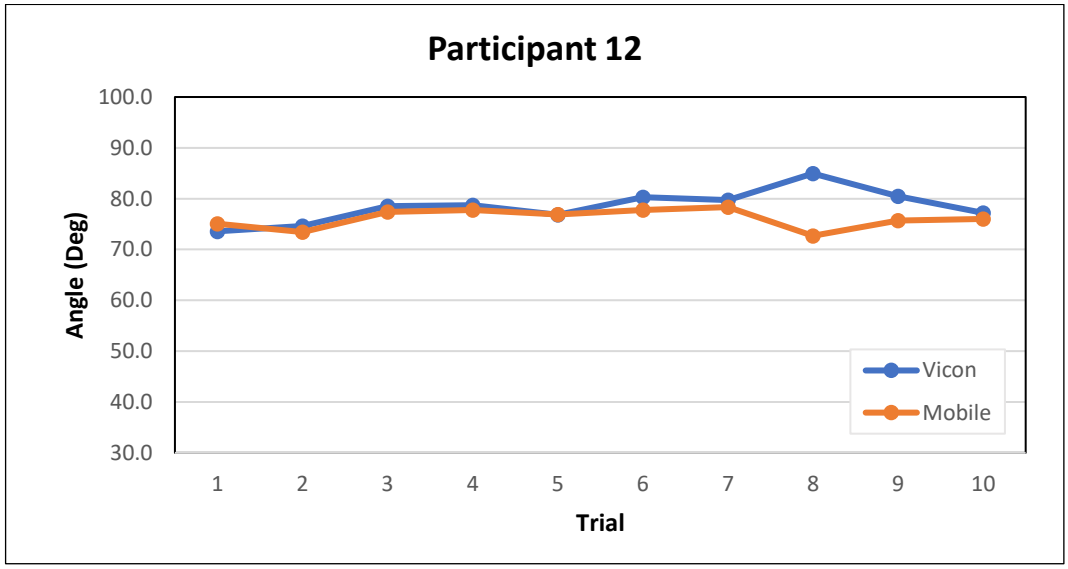
Participant 12
100.0
90.0
80.0
70.0
60.0
50.0
40.0
30.0
Angle (Deg)
Vicon
Mobile
1
2
3
4
5
6
7
8
9
10
Trial

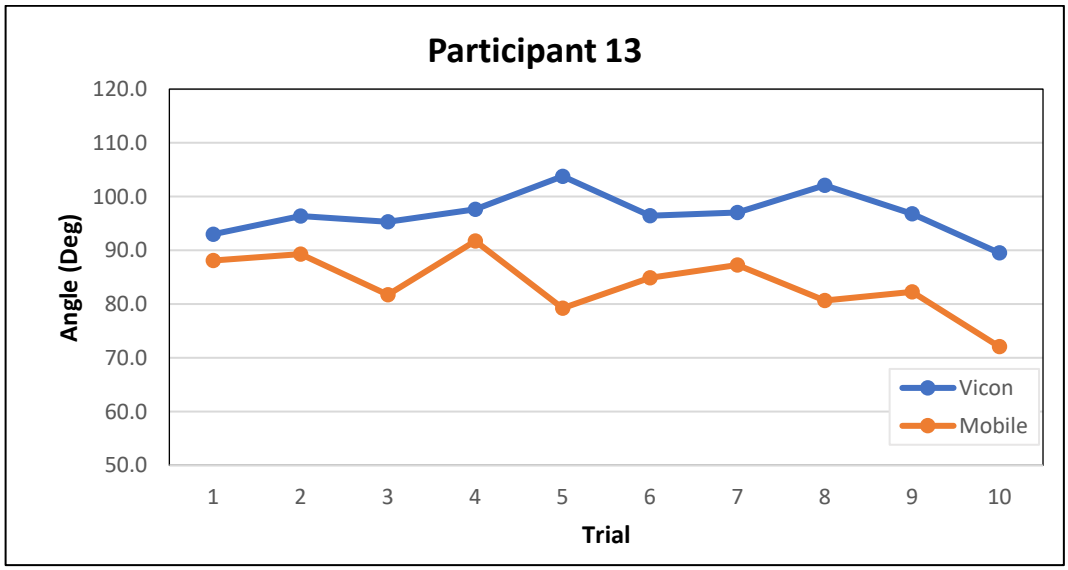
Participant 13
120.0
110.0
100.0
90.0
80.0
70.0
60.0
50.0
Angle (Deg)
Vicon
Mobile
1
2
3
4
5
6
7
8
9
10
Trial

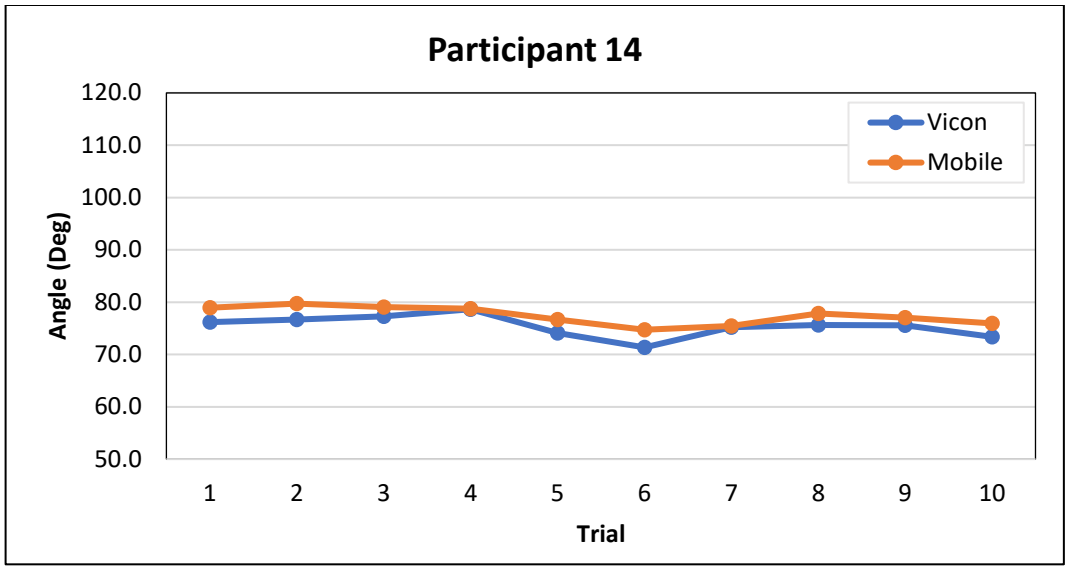
Participant 14
120.0
110.0
100.0
90.0
80.0
70.0
60.0
50.0
Angle (Deg)
1
2
3
4
5
6
7
8
9
10
Trial
Vicon
Mobile

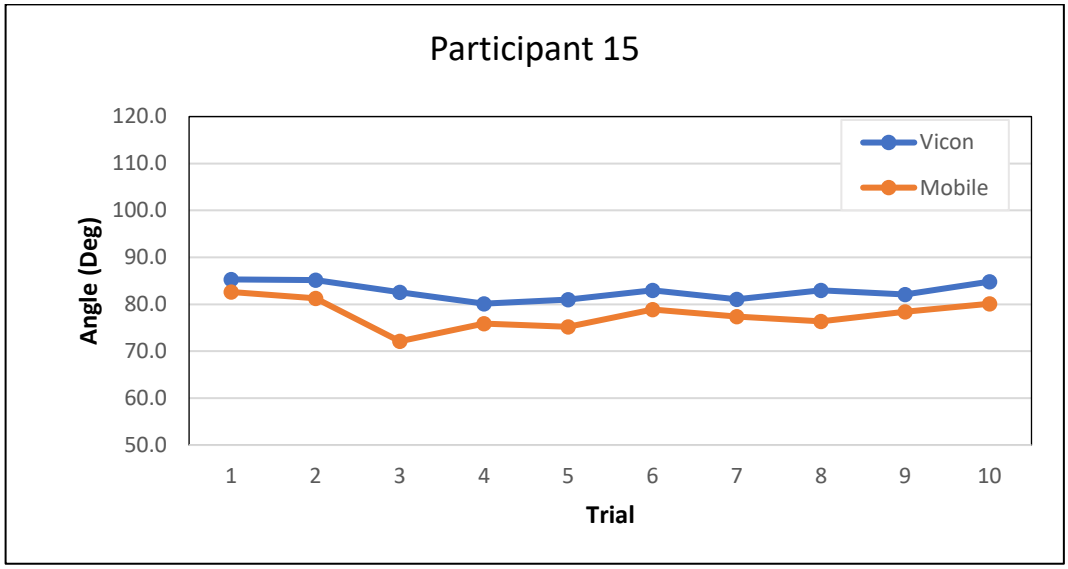
Participant 15
120.0
110.0
100.0
90.0
80.0
70.0
60.0
50.0
Angle (Deg)
1
2
3
4
5
6
7
8
9
10
Trial
Vicon
Mobile